



Published in final edited form as:

*Eur J Med Chem.* 2021 January 01; 209: 112866. doi:10.1016/j.ejmech.2020.112866.

## Design, synthesis and structure-activity relationship study of novel urea compounds as FGFR1 inhibitors to treat metastatic triple-negative breast cancer

Md Ashraf-Uz-Zaman<sup>1</sup>, Sadisna Shahi<sup>1</sup>, Racheal Akwii<sup>1</sup>, Md Sanullah Sajib<sup>1</sup>, Mohammad Jodeiri Farshbaf<sup>5</sup>, Raja Reddy Kallem<sup>3</sup>, William Putnam<sup>3</sup>, Wei Wang<sup>2</sup>, Ruiwen Zhang<sup>2</sup>, Karina Alvina<sup>4,5,6</sup>, Paul C. Trippier<sup>7,8,9</sup>, Constantinos M. Mikelis<sup>1</sup>, Nadezhda A. German<sup>1,4,\*</sup>

<sup>1</sup>Department of Pharmaceutical Sciences, Jerry H. Hodge School of Pharmacy, Texas Tech University Health Sciences Center, Amarillo, TX, USA.

<sup>2</sup>College of Pharmacy, University of Houston, Houston, TX, USA.

<sup>3</sup>Clinical Pharmacology & Experimental Therapeutics Center, Texas Tech University Health Sciences Center, Dallas, TX, USA.

<sup>4</sup>Center of Excellence for Translational Neuroscience and Therapeutics, Texas Tech University Health Sciences Center, Lubbock, TX, USA

<sup>5</sup>Department of Biological Sciences, Texas Tech University, Lubbock, TX, USA

<sup>6</sup>Department of Neuroscience, University of Florida, Gainesville, FL, USA

<sup>7</sup>Department of Pharmaceutical Sciences, College of Pharmacy, University of Nebraska Medical Center, Omaha, NE, USA

<sup>8</sup>Fred & Pamela Buffett Cancer Center, University of Nebraska Medical Center, Omaha, NE, USA.

<sup>9</sup>UNMC Center for Drug Discovery, University of Nebraska Medical Center, Omaha, NE, USA.

### Abstract

Triple-negative breast cancer (TNBC) is an aggressive type of cancer characterized by higher metastatic and reoccurrence rates, where approximately one-third of TNBC patients suffer from the metastasis in the brain. At the same time, TNBC shows good responses to chemotherapy, a feature that fuels the search for novel compounds with therapeutic potential in this area. Recently, we have identified novel urea-based compounds with cytotoxicity against selected cell lines and with the ability to cross the blood-brain barrier *in vivo*. We have synthesized and analyzed a library of more than 40 compounds to elucidate the key features responsible for the observed

\*Corresponding author, Tel: 806-414-9190, nadezhda.german@ttuhsc.edu.

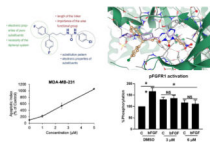
Declaration of interests

The authors declare that they have no known competing financial interests or personal relationships that could have appeared to influence the work reported in this paper.

**Publisher's Disclaimer:** This is a PDF file of an unedited manuscript that has been accepted for publication. As a service to our customers we are providing this early version of the manuscript. The manuscript will undergo copyediting, typesetting, and review of the resulting proof before it is published in its final form. Please note that during the production process errors may be discovered which could affect the content, and all legal disclaimers that apply to the journal pertain.

activity. We have also identified FGFR1 as a molecular target that is affected by the presence of these compounds, confirming our data using *in silico* model. Overall, we envision that these compounds can be further developed for the potential treatment of metastatic breast cancer.

## Graphical Abstract



## INTRODUCTION

Breast cancer is the second leading cause of cancer-related death in women. Despite the tremendous advances in cancer treatment in recent decades, over 42,000 women were expected to die of breast cancer in 2020.<sup>1</sup> Triple-negative breast cancer (TNBC) is the subset of breast cancer that is characterized by the absence of estrogen receptor (ER), progesterone receptor (PR) and human epidermal growth factor receptor 2 (HER2).<sup>2</sup> It accounts for approximately 15–20% of all breast cancer diagnoses,<sup>3</sup> and has been categorized as the most aggressive subtype, correlated with poor prognosis.<sup>4</sup> Triple-negative tumors possess a higher risk of developing distant metastases, recurrence, and lower five-year survival compared with other subtypes of breast cancer.<sup>5, 6</sup> TNBC has a unique propensity for metastasis to the lung and brain that contribute to its lower survival rates.<sup>7</sup>

In the absence of viable targets for the endocrine and HER-2 targeted therapies, chemotherapy is the mainstream treatment for TNBC.<sup>2</sup> Several retrospective studies have concluded that chemotherapy, in combination with whole-brain radiation therapy, gives the most prolonged median survival. At the same time, CALGB trial<sup>8</sup> and WSG AM-01 study<sup>9</sup> emphasized the benefits of dose-dense and dose-intensive chemotherapeutic regimens in the treatment of TNBC. A retrospective analysis of trastuzumab treatment has identified that this otherwise potent anticancer agent has increased brain metastasis incidents at a rate of 12.6% to 34%.<sup>10</sup> The reason for such an increase is seen as “driving” cancer cells to the brain as a sanctuary site, suggesting the treatment of TNBC would be more successful with the use of chemotherapeutic agents with the ability to cross the blood-brain-barrier (BBB). Most available chemotherapies are not able to cross the BBB, not even if the barrier is disrupted by tumor invasion.<sup>11, 12</sup> As a result, there is an ongoing drive to develop novel chemotherapeutic agents that are BBB-permeable for the treatment of TNBC patients.

We have targeted the optimization of penfluridol (PFL), an antipsychotic drug, for potential anticancer use. This compound demonstrates antitumor properties in various cancer cell lines such as breast, pancreatic, glioblastoma, and lung cancer cells.<sup>13–16</sup> The anticancer effects of PFL were further confirmed *in vivo* in a variety of models, including the metastatic heart to brain TNBC model.<sup>17</sup> Therefore, penfluridol has the potential to be repurposed as a novel antitumor agent.<sup>18, 19</sup> Moreover, the ability of PFL to cross the BBB, makes it an attractive candidate to develop anticancer therapeutics to treat brain metastasized cancers. However, this compound has extensive interactions with the majority of G-protein

coupled receptors (GPCRs) (Fig. 2A)<sup>20</sup> at levels that correspond to the proposed anticancer dosing (estimated as 50 mg of daily dosing in human<sup>14, 16, 17, 21</sup>). Thus, an off-target CNS activity of penfluridol as an anticancer agent will lead to intensified neurological side effects associated with this agent.<sup>22–25</sup>

Our group has previously reported the employment of PFL as the hit molecule that can be further optimized for its anticancer properties and the removal of GPCR-related activity.<sup>20</sup> We observed that the 4-hydroxypiperidine moiety that was previously shown to be important for its cytotoxicity<sup>26, 27</sup> is also essential for the interaction with GPCRs. Here, we report our next step in the optimization of the PFL structure, where a topology-based scaffold hopping approach<sup>28–31</sup> was used to identify the second generation of analogs with the retained anticancer activity and alleviated affinity to the GPCRs. To achieve this goal, a set of six diverse chemical fragments was designed to replace the substituted 4-hydroxy-piperidine moiety of PFL (hereafter referred to as the “head” moiety). Selected structural features of the original “head” moiety, such as the presence of a phenyl ring and abundance of heteroatoms, were incorporated in the design of new fragments. The diphenyl-butyl chain (hereafter referred to as the “tail” moiety) was kept unchanged due to its auxophoric character.<sup>20, 26</sup> All six molecules were evaluated for their anticancer properties using cytotoxicity assay (see supplemental materials) (Fig. 1), where compound **4a** (IC<sub>50</sub> = 7.7 μM) was identified as our new “hit” molecule for further evaluation.

In the next step, compound **4a** was assessed for the ability to interact with the GPCRs expressed in the brain (Fig. 2B). We found a significant reduction in the interaction of **4a** with the GPCRs, where only six receptors were inhibited at the level above 50%. Under the same test conditions, PFL was shown to inhibit 28 GPCRs at the level above 50%. Previously, it has been demonstrated that neurological side effects of PFL are associated with the inhibition of serotonin and dopamine receptors.<sup>24, 32, 33</sup> Our hit compound (**4a**) had no significant interaction with the dopamine receptors (subtypes D1-D5) at 10 μM concentration. Similarly, it has no activity at serotonin receptors, except for 5HT-2C, which is a subtype with low expression levels, and its potential role in CNS-induced toxicity can be considered insignificant.<sup>34</sup> Thus, for compound **4a**, only inhibition of the dopamine transporter (DAT) and histamine 1 receptor (H1R) was noted as sources of possible neurotoxicity.

Further, we evaluated compound **4a** for its ability to cross the BBB *in vivo*, where mice were injected with a dose of 10 mg/kg through intraperitoneal (i.p.) administration<sup>35</sup> and sacrificed at selected time points. We observed that **4a** reaches the peak values of approximately 1000 nM at 1-hour post-injection (Fig. 3), similarly to the data found for PFL, confirming its retained activity to cross the BBB.<sup>36</sup> In summary, our scaffold-hopping design identified compound **4a** with cytotoxicity against MDA-MB-231 cells retained the ability to cross the BBB *in vivo* and limited inhibitory activity on GPCRs. Hence, we envisioned that this compound can be further evaluated as an anticancer agent with the potential therapeutic application in the treatment of the metastatic TNBC. Our current report presents an analysis of the performed structure-activity relationship studies, where a library of 45 analogs was prepared and tested for the anticancer activity. In addition, we investigated

potential unwanted overlap in structural requirements for the cytotoxic activity of **4a** and its ability to interact with the DAT.

## CHEMISTRY

The synthesis of compounds designed for the scaffold-hopping study is depicted in scheme 1. We have coupled commercially available 4-fluorobenzaldehyde (**30**), and 4-chlorophenol (**31**) afforded aryl ether **32** (Scheme 1A) which was subsequently reduced in the presence of lithium aluminum hydride to yield intermediate alcohol **33** and was further coupled with diphenyl alkyl intermediate **27a** (scheme 2) to access compound **2**.<sup>37, 38</sup> Commercially available phenol **34** was protected by benzylation (**35**), followed by base-mediated hydrolysis of the ester functionality<sup>39</sup> to obtain carboxylic acid intermediate **36** (Scheme 1B). A Steglich esterification successfully afforded compound **3**.<sup>40</sup> Chloro-phenyl isocyanate **48a** was coupled with diphenyl alkyl intermediate **27a** to afford urea compound **4a** (Scheme 1C). A condensation reaction between glycerol (**37**) and benzaldehyde (**38**) under acidic conditions afforded 2-phenyl,1,3-dioxane-2-ol **39** (Scheme 1D),<sup>41</sup> that was coupled with **27a** to form compound **5**.<sup>42</sup> Synthesis of analog **6** (Scheme 1E) began with the Buchwald-Hartwig<sup>43</sup> coupling of aryl iodide **41** using 1,1'-bis(diphenylphosphino)ferrocene (DPPF) as a catalyst to afford diphenylamine intermediate **42**.<sup>44</sup> Next, coupling with **27a** afforded compound **6**. Finally, key intermediate **45** was obtained by sulfonylation of piperazine (**44**) with substituted arylsulfonyl chloride **43**,<sup>45</sup> and was further coupled with the tail moiety **27a** to form compound **7** (Scheme 1F).<sup>26</sup>

The preparation of diphenyl alkyl intermediates (“tail” moieties) that were used to synthesize the final compounds depicted in schemes 1 and 3–6 is outlined in scheme 2. Suitably substituted aryl bromides (**21a-e**) were converted to the corresponding Grignard reagents, which underwent a double addition reaction with the respective lactones **22a-c** to afford dihydroxyl intermediates **23a-g**. Acid-catalyzed dehydration of the tertiary alcohol afforded unsaturated aliphatic alcohols **24a-g**. Intermediates **26a-g** were obtained by subjecting alcohols **24a-g** to Appel conditions.<sup>46</sup> A palladium-carbon mediated hydrogenation reaction was utilized to obtain saturated intermediates **25a-c**, **27a-e**, and **27g-h**.<sup>26</sup> Compound **27f** was prepared from **27e** using modified nitration conditions to avoid unwanted *ortho*-substitutions.<sup>47, 48</sup> Aliphatic bromides **27a-h** were converted to primary amines **29a-h** by treatment with ammonia or by Staudinger reduction via the azide intermediates **28a, d-f**.<sup>49, 50</sup>

Synthesis of a subgroup of analogs with substitutions at the “head” moiety is depicted in Scheme 3. Diphenyl-alkyl amine **29a** (scheme 2) was coupled with freshly prepared isocyanates<sup>51</sup> **48a-q**, to obtain desired urea compounds **4a-d**, **4g-m**, and **4p-u**. Amino substituted derivatives **4e**, and **4n** were prepared using standard Raney-Ni-catalyzed reduction conditions from the respective nitro-precursors **4d** and **4m**. They were further acetylated to afford analogs **4f** and **4o**. Prior to being converted to isocyanates **51a,b** via exposure to triphosgene,<sup>52</sup> benzoic acid **49** was protected as the methyl,<sup>53</sup> or benzyl,<sup>54</sup> ester (Scheme 3B). Coupling of **51a,b** with **29a** afforded analogs **4v-w**.<sup>55</sup> The final compound in this scheme, acid **4x**, was obtained by reductive deprotection of the benzyl ester of **4w**.

Analogs with varied substitution at the diphenyl (“tail”) moiety were synthesized according to Scheme 4. The diphenyl-alkyl amine intermediates **29b-f** were coupled with the freshly prepared selected isocyanates **48a** and **48j-k** to produce desired urea compounds **8a-g**. Raney-Ni catalyzed reduction was utilized to make compound **8h**, which was converted to an acetylated analog **8i**. To prepare *N*-linked diphenyl analogs, **9a-e** diphenyl amine **42** was coupled with butyl bromide to obtain **52**, which was further converted to the primary alkylamine **53**. Final compounds **9a-e** were synthesized using **53** and freshly prepared isocyanates **48a**, **48b**, **48j**, **48n**, and **48q** (Scheme 4B). Synthesis of the last analog (Scheme 4C), compound **10**, began with the reduction of 4-fluorophenyl valeric acid (**54**) with LiAlH<sub>4</sub> using a modified literature procedure.<sup>56</sup> The resultant primary alcohol **55** was converted to the desired analog **10** in three subsequent steps involving Appel reaction, amination, and urea formation.

Several analogs bearing modifications of the linker chain were prepared using conditions outlined in Scheme 5. Alterations in the length of the linker were achieved by reacting intermediates **29g** or **29h** with isocyanide **48j**. The similar synthetic procedure was employed for the preparation of the thiourea analog **12** (Scheme 5B), where thioisocyanate **57** was used as starting material and for the introduction of the carbamate bioisostere **13** (Scheme 5C), where primary alcohol **25a** reacted with isocyanate **48j** under basic condition.<sup>57</sup>

Scheme 6 depicts reaction conditions for the preparation of mono- and dimethyl substituted urea analogs **14** (Scheme 6A) and **15** (Scheme 6B).<sup>58,57</sup> In addition, it describes final modifications of the linker performed in this study, such as the synthesis of *N*-phenyl and *C*-phenyl amides **16** (Scheme 6C) and **17** (Scheme 6D). To prepare **16**, primary alcohol **25c** was oxidized under metal-free conditions,<sup>59</sup> to afford acid **59**, which was subsequently activated as the acid chloride and coupled with substituted aniline **47j**.<sup>60</sup> Analog **17**, was accessed by the acid chloride of free acid **60**<sup>60</sup> reacting with diphenyl alkyl amine **29a**.

To evaluate the effect of a constrained linker on the anticancer activity of compounds, we prepared analogs **18** and **19a-b** following reported literature procedures.<sup>52, 61, 62</sup> As depicted in scheme 7, Grignard reaction of substituted *Boc*-protected piperidine **61a-b** with 4-fluorophenylmagnesium bromide afforded tertiary alcohol **62**. This compound underwent simultaneous dehydration and *Boc*-deprotection in the presence of HCl<sub>conc</sub> to obtain unsaturated intermediates **63a-b**. Palladium assisted hydrogenation conditions were used to convert **63b** to 4-substituted piperidine intermediate **64b**. Final compounds **18** and **19b** were synthesized by reacting an isocyanate with the respective piperidine intermediates **64a** and **64b**, whereas the preparation of **19a** required treatment of **62a** with trifluoroacetic acid and NaBH<sub>4</sub> to prepare piperidine **64a** prior to the coupling reaction.

## RESULTS AND DISCUSSION

### *In vitro* cytotoxic activity of synthesized analogs

In our SAR studies, we have used a fragment-based approach to design and synthesize a series of 49 analogs of the hit compound **4a** that were further evaluated for cytotoxic potential using the MDA-MB-231 triple-negative breast cancer line (see supplemental

materials). The structural modifications were performed in three areas of the hit compound: monophenyl (“head”) moiety, urea linker, and diphenyl (“tail”) moiety (Fig. 4). Thus, we have grouped our *in vitro* data according to the site of the performed modification.

**Modifications in the mono-phenyl “head” moiety and their effect on the cytotoxicity of analogs.**—As shown in table 1, a mono-substitution pattern favors the presence of an electron-withdrawing group located *meta*- to the urea moiety (compound **4g**, **4i-4k**) or strong electron-withdrawing functionality at the *para*-position (**4h**). Electron-donating groups in both *para*- (**4c**, **4e**) and *meta*- (**4k**) positions cause abrogation of cytotoxic activity. Interestingly, the presence of a hydrogen-bond acceptor is well tolerated in the *meta*-position (**4g** vs. **4j**), but causes increase in IC<sub>50</sub> values in compounds bearing mono *para*-substitution (**4d** vs. **4h**). We observed that increase in the size of the *para*-substituents leads to decreased (**4b**) or complete loss (**4f**) of cytotoxicity. Another factor that might lead to the observed changes is the loss in the electron-withdrawing properties of substituents when moving from **4d** to **4a** to **4b**, and, finally, to **4f**.

Given that electron-withdrawing groups at *para* and *meta* positions were favored, we next prepared a series of di-substituted analogs that possess similar electronic characteristics. As shown in Table 2, a combination of **4g** and **4a** yielded compound **4l** with an activity slightly better than **4g** but with a two-fold increase in activity when compared to our hit molecule **4a**. Substitution of the trifluoromethyl moiety (**4l**) with the hydrogen-bond acceptor nitro functionality (**4m**) led to a slight decrease in overall activity, which was restored in the positional isomer **4i**. This data suggests that the *meta* position prefers non-hydrogen bonding functional groups, a conclusion that was further confirmed by the observed change in the activity of **4o**. Although the *para* position tolerates the presence of H-bond acceptor groups (**4l**, **4q**, **4v**), the introduction of a carboxylic acid, an ionizable H-bond donor moiety (**4x**), led to the loss of cytotoxic activity. We also observed a possible inverse correlation between the size of the *meta*-substituent and the activity of compounds (**4l** vs. **4q**), suggesting potential size limitations in this part of the binding pocket. Di-substitution with electron-donating groups (**4r**) abolished the desired activity, whereas a combination of the *meta*-amino moiety and *para*-chloro group regained some activity. Finally, we have explored the possibility of *ortho*-, *para*- di-substitution pattern, but all of the compounds in this subgroup (**4s-4u**) were inactive, irrelevant to the electronic properties of substituents. Overall, we have concluded that di-substitution provides compounds with increased cytotoxicity if the *meta*-, *para*- pattern is preserved.

Our structure-activity relationship studies on the “tail” di-phenyl moiety allowed us to draw four main conclusions. First, we observed that the electronic properties of *para*-substituents do not play a defining role in the activity of the studied analogs, as seen by comparing compounds **4l**, **8a**, and **8c**. However, strong electron-withdrawing groups are favored (**8e** and **8g**). In the subgroup of analogs bearing electron-donating groups of similar size, **8a**, and **8h**, the ability to form H-bonds was disfavored, although not forbidden. Second, we noted that the size of the *para*-substitution might be inversely linked to the activity of compounds, as seen in pairs **8a** vs. **8c** and **8e** vs. **8i**. Finally, we observed that compounds containing an *N*-linker have less activity when compared to their carbon-containing bioisosteres (see pairs **9c**



vs. **4l**, **9a** vs. **4a**, **9b** vs. **4b**). Finally, compound **10** designed to determine the necessity of the diphenyl moiety showed just a slight decrease in the overall activity, indicating that the diphenyl moiety plays an auxiliary role in binding. However, it might affect the ability of a compound to penetrate the BBB, a hypothesis that is currently under investigation in our laboratory.

The result of structural modifications in the alkyl-urea linker is depicted in Table 4. First, we observed that increase in the length of the linker results in a slight increase in cytotoxicity (**4l** vs. **11b**). Limiting the flexibility of the linker chain by locking it into cyclic urea (**19b**) and by adding an olefin moiety (**18**) resulted in a minor decrease of activity, which became more prominent with the simultaneous reduction in the linker length (**19a**). It is known that substitution at the nitrogen atom of the urea functionality plays an important role in the conformational preferences of these compounds.<sup>63</sup> Thus, we have designed and evaluated a subgroup of analogs; the mono-methylated (**14**, corresponding to the *trans,cis* configuration) and di-methylated (**15**, corresponding to the *cis,cis* configuration) urea, where our results showed a clear preference for the *trans,trans* configuration of the unsubstituted functionality (**4l**). These results also show a potential involvement of the phenyl substituted nitrogen in the urea functionality in the hydrogen-bond interaction within the binding pocket. Finally, a substitution of the urea moiety to a thiourea functionality (**12**) or a carbamate (**13**) had no significant impact on the activity of the compound. In contrast, amide-containing linkers in **16** and **17** caused a reduction in the cytotoxicity of studied analogs.

Overall, our structure-activity relationship studies highlighted the importance of *para*-substitution of the “head” moiety with electron-withdrawing functionalities. Similar electronic properties were also favored for the *para*-substitution of the “tail” moiety. We observed that flexibility of the linker and *trans,trans* conformation of the urea moiety are preferred, as well as the presence of the three heteroatom-containing moiety. As a result of performed structural modifications, we were able to optimize the cytotoxicity of our “hit” molecule **4a** by 6-fold (**8g**).

***In vitro* activity of selected analogs against DAT.**—To evaluate the effect of performed structural modifications on the ability of compounds to inhibit DAT and estimate the possibility of separating this activity from cytotoxicity, we have selected 13 analogs with different anticancer profile. As shown in Table 5, for monosubstituted analogs **4a** and **4b**, the ability to inhibit DAT decreases as the size of *para*-substituent goes up. In a subgroup of disubstituted analogs **4l**, **4o**, and **4r**, there is no direct correlation between the electronic properties of substituents and the observed activity of compounds. We observe that either hydrogen bond acceptor character of meta-group in **4o** or slightly larger size may lead to a 100-fold decrease in affinity to DAT when compared to **4l**. Similar to the observed trend in anticancer activity, ortho-substitution is not favored here as well (**4s** and **4t**). Unlike in cytotoxicity-related SAR, modifications in the tail moiety (**8a-8c**) have a notable impact on the interaction with DAT, providing bases for separating pharmacophores responsible for transporter inhibition and anticancer activity. Unlike in other analogs (**4a** vs. **4l**, **9a** vs. **9c**), a di-substitution pattern in **8a**, bearing *para*-methyl groups at the tail moiety, is less active, than its mono-substituted counterpart **8b**. Finally, selected modifications in the linker moiety

affect the ability of compounds **9a-19b** to interact with the DAT. For example, introduction of a nitrogen atom causes a slight decrease in the inhibitory properties of compounds (**4a** vs **9a** and **4b** vs **9c**). Similar activity was observed in a series of analogs with the modified linker length (**4a** vs **11a** and **11b**). Conformational restrictions introduced by the piperidine moiety result in decreased activity in **19a** and abolished DAT activity in **19b**. Similarly, an unsubstituted urea moiety is required for DAT activity (**4a**), whereas the mono-methylated analog **14** loses some of this inhibitory activity, and di-methylated compound **15** is inactive as a DAT inhibitor. Substitution of the urea moiety with carbamate (**13**) or amide (**16**, **17**) functionalities causes significant loss of DAT activity as well. We have summarized the observed trend in the activity of this set of compounds in Figure 6.

**Evaluation of microsomal stability in vitro.**—As part of the pharmacokinetic assessment of urea analogs *in vitro*, we have evaluated the metabolic stability of selected analogs (**4l** and **4q**) using standard microsomal stability assay (see supplemental material). The compound's selection was based on two parameters: the IC<sub>50</sub> values and percent of the cell survival 48 hours post-treatment (Fig. S1). If both parameters were similar, we chose compounds with a more diverse substitution pattern. To validate our assay, we have used the clinically approved compound verapamil and PFL as the reference compounds. Both new analogs showed preferred metabolic stability over PFL when analyzed for up to 60 minutes (Fig. 7).

**Molecular target analysis.**—To elucidate the downstream molecular pathway of **4q**-induced antiproliferative effects observed in the cytotoxicity studies, we first explored whether apoptosis is induced. After 48 hours of **4q** treatment apoptosis was induced in MDA-MB-231 cells in a dose-dependent manner. Even at the 1  $\mu$ M concentration, significant induction of apoptosis was observed, whereas 5  $\mu$ M levels of compound **4q** increased the apoptotic index by 10.6-fold ( $P < 0.01$ ), compared to control cells (Figure 8A). Further, we observed that **4q** is capable of caspase-3 cleavage and activation (Supplemental material). At the same time, **4q** did not affect the cell cycle in MDA-MB-231 cell line (Figure 8B).

Fibroblast growth factor receptor (FGFR) pathways are significant driver pathways for breast cancer,<sup>64</sup> and FGFR overexpression has been proposed as a biomarker for TNBC.<sup>65</sup> TNBC presents with gene amplification and protein overexpression of FGFR1, FGFR2 and bFGF, with the latter being shown to have an autocrine effect on tumor growth. TNBCs, along with basal-like breast cancers, show sensitivity to FGFR inhibitors, such as PD173074, while upregulated FGFR signaling is a known resistance mechanism to CDK inhibitors, highlighting the FGFR signaling as a potential therapeutic target for breast cancer, among others.<sup>66-68</sup> We, therefore, explored the effect of compound **4q** on FGFR1 activation in the presence and absence of bFGF. As shown in Figure 9, compound **4q** completely abrogated phosphorylation of FGFR1 in the presence of its natural ligand bFGF at a concentration of 3  $\mu$ M and 6  $\mu$ M, indicating that inhibition of the FGFR1 signaling pathway is at least one of the molecular mechanisms responsible for the cytotoxic effects of compound **4q**.



**Molecular Modelling.**—Compound **4q** was selected for docking into the FGFR1 protein to gain insights into binding interactions. The crystal structure of FGFR1 in complex with the potent inhibitor AZD4547<sup>69</sup> (PDB code 4V05) was prepared for docking by removing the ligand and defining the binding site as the 35 amino acid residues surrounding the ligand and an additional 23 residues that account for unoccupied space around the ligand-binding site. Molecular docking simulations afforded binding poses that were scored by HYDE, as described in our previous publication.<sup>70</sup> Predicted protein-ligand interactions (Fig. 10) correlate well with experimental data obtained from SAR studies. The compound is predicted to occupy the ATP-binding cleft of FGFR1 in a similar position to the known inhibitor AZD4547.<sup>69</sup> The *p*-NO<sub>2</sub> moiety of **4q** is predicted to participate in hydrogen bonding interactions with an active site water molecule forming a bridging network that incorporates the LYS514, GLU531, and ASP641 residues. This is facilitated by the length of the linker allowing the bulky diphenyl tail moiety to remain outside the binding pocket and solvent-exposed. The urea moiety of **4q** occupies a similar position within the ATP-binding cleft to the pyrazole moiety of AZD4547 (Fig. 11). Calculation of hydrogen bonding distance results in potentially favorable proximity and orientation of a urea NH to the GLU562 residue (3.77 Å), whereas the second urea NH is positioned 4.78 Å away from the ALA564 residue precluding potential binding. This is supported by SAR data that shows a critical role for the hydrogen of the urea nitrogen alpha to the head group. The binding affinity of **4q** was predicted to be in the high nanomolar to a low micromolar range, which compares well to its experimentally derived value (IC<sub>50</sub> = 4.55 μM).

## CONCLUSION

We have described a novel series of cytotoxic compounds that possess cytotoxicity towards the MDA-MB-231 cell line. The first compound in this series, our “hit” molecule **4a**, was shown to cross the BBB *in vivo* and to have minimum interaction with CNS receptors when compared to the original penfluridol molecule. The first round of structure-activity relationship studies was designed to understand the structural requirements for the anticancer activity of these compounds. Observed results highlighted the importance of electron-withdrawing substitution with the hydrogen-bonding properties on both tail and head moieties of studied analogs, as well as the preferred length of a linker and its flexibility. Selected derivatives were subjected to a primary binding assay to investigate their affinity to the DAT. Based on the current data, we have concluded that the toluene-like structure of the tail-moiety will allow preserving the anticancer activity of urea analogs while eliminating unwanted interactions with the DAT. These results are in line with the reported SAR studies for DAT inhibitors,<sup>71</sup> and we will continue exploring the effect of electron-withdrawing groups in the tail moiety to clarify DAT-related pharmacophore of the urea compounds. Similarly, certain modification of the linker motif will allow preservation of the anticancer activity of compounds, while eliminating unwanted interactions with the DAT. Using a representative molecule, we have shown that this class of agents can induce apoptosis in MDA-MB-231 cell lines in a concentration-dependent manner while having no effect on cell cycle. Further, we observe that the tested analog was able to cleave caspase-3. Our initial mechanistic studies have identified FGFR1 as one of the potential targets modulated by this class of agents. Our molecular modeling studies confirmed the emphasized findings from the

SAR studies. We envision that these compounds can be further developed for the potential treatment of metastatic breast cancer. *In vivo* validation of the observed *in vitro* data, as well as further validation of FGFR1 as a potential target will be reported shortly.

## EXPERIMENTAL SECTION

### General chemistry procedures.

All reactions were carried out in oven- or flame-dried glassware under positive nitrogen/argon pressure unless otherwise noted. All solvents and chemicals were reagent grade. Unless otherwise noted, all reagents and solvents were purchased from commercial vendors and used as received. The purity and characterization of compounds were established by a combination of methods, including TLC, HPLC, mass spectrometry, NMR analysis.  $^1\text{H}$  and  $^{13}\text{C}$  NMR spectra were recorded on a Bruker 400 MHz Advance III HD spectrometer using chloroform-*d*, methanol-*d*, or DMSO-*d*<sub>6</sub> with tetramethyl (TMS) (0.00 ppm) or solvent peaks as the internal standard. Chemical shifts ( $\delta$ ) are recorded in ppm relative to the reference signal, and coupling constant (*J*) values are recorded in hertz (Hz). Multiplicates are indicated by s (singlet), d (doublet), dd (doublet of doublets), t (triplet), q (quartet), m (multiplet), br (broad). Thin-layer chromatography (TLC) was performed on EMD precoated silica gel 6-F254 plates, and spots were visualized with UV light or iodine staining. Flash column chromatography was performed with silica gel (40–63  $\mu\text{m}$ , 60  $\text{\AA}$ ) using the mobile phase indicated or on a Teledyne Isco (CombiFlash R<sub>f</sub> UV/Vis). High-resolution mass spectra were obtained using TripleTOF 5600 mass spectrometer. The purity of all final compounds was greater than 95%. The purity was determined by Waters Acquity UPLC using C18 column (Cortecs, 1.6 $\mu\text{m}$ , 2.1 $\times$ 50 mm): eluent A, 0.1 % aqueous CF<sub>3</sub>COOH and eluent B. CH<sub>3</sub>CN containing 0.1 % CF<sub>3</sub>COOH, gradient elution (0 min: 95% A, 5% B; 2 min: 50% A, 50% B; 4 min: 50% A, 50% B; 6 min: 10% A, 90% B; 9 min: 10% A, 90% B; 10 min: 95% A, 5%), with a flow rate of 0.2 ml/min.

### General procedure A.

A substituted phenyl isocyanate (0.50 mmol) dissolved in dichloromethane (2 mL) was added to a solution of selected alkyl amine (0.50 mmol) in dichloromethane (3 mL) at 0 °C under inert environment. After stirring for 6 hours at room temperature, the solvent was evaporated under reduced pressure, and the formed residue was purified by flash chromatography with ethyl acetate /hexane (1:9 to 1:1) to obtain the desired compound.

### General procedure B.

Hydrazine hydrate (0.50 mL) was added to a solution of a nitroaromatic compound (1.00 eq, 0.40 mmol) in methanol (10 mL). After stirring for 15 min at 50 °C, an excess of Raney®-Nickel was added (approx. 2.00 eq.). A reaction mixture was kept stirring at 50 °C for an hour then filtered using Celite® bed. The organic solvent was removed under reduced pressure, and formed residue was purified by flash chromatography with methanol/ dichloromethane (1:99 to 1:19) to obtain the reduced product.

### General procedure C.

An excess of acetic acid (0.03 mL) was added to a solution of an aniline derivative (1.00 equiv., 0.21 mmol) in dichloromethane (10 mL). After overnight stirring at room temperature, the reaction solvent was removed under reduced pressure and formed residue was purified by flash chromatography using methanol/ dichloromethane (1:99 to 1:19) to obtain desired *N*-phenylacetamide derivative.

#### 1-(5,5-bis(4-fluorophenyl)pentyl)-3-(4-chlorophenyl)urea (4a).

Compound **4a** was prepared in 56% yield from compound **29a** and **48a** using the general procedure A. <sup>1</sup>H NMR (400 MHz, CDCl<sub>3</sub>) δ<sub>H</sub> 1.12–1.27 (m, 2H), 1.46 (quin, 2H, *J* = 7.46 Hz), 1.87–2.01 (m, 2H), 3.11 (q, 2H, *J* = 6.85 Hz), 3.79 (t, 1H, *J* = 7.83 Hz), 5.00 (t, 1H, *J* = 5.62 Hz), 6.83 (s, 1H), 6.89–7.04 (m, 4H), 7.05–7.14 (m, 4H), 7.14–7.23 (m, 4H). <sup>13</sup>C NMR (100 MHz, CDCl<sub>3</sub>) δ<sub>C</sub> 25.18, 30.00, 35.47, 40.11, 49.67, 115.19, 115.40, 121.62, 128.99, 129.07, 129.14, 137.28, 140.36, 140.40, 160.12, 162.55. HRMS-ESI: (*m/z*) calculated for C<sub>24</sub>H<sub>23</sub>ClF<sub>2</sub>N<sub>2</sub>O, 429.1545 [M+H]<sup>+</sup>; found 429.1590. Purity: 98.67%

#### 1-(5,5-bis(4-fluorophenyl)pentyl)-3-(4-iodophenyl)urea (4b).

Compound **4b** was prepared in 31% yield from compounds **29a** and **48b** using the general procedure A. <sup>1</sup>H NMR (400 MHz, CDCl<sub>3</sub>) δ<sub>H</sub> 1.17–1.32 (m, 2H), 1.47–1.56 (m, 2H), 1.90–2.05 (m, 2H), 3.11–3.23 (m, 2H), 3.83 (t, 1H, *J* = 7.95 Hz), 4.64 (t, 1H, *J* = 5.62 Hz), 6.31 (s, 1H), 6.89–7.00 (m, 4H), 7.00–7.09 (m, 2H), 7.09–7.21 (m, 4H), 7.51–7.63 (m, 2H). <sup>13</sup>C NMR (100 MHz, CDCl<sub>3</sub>) δ<sub>C</sub> 25.19, 29.99, 35.48, 40.18, 49.68, 86.48, 115.21, 115.42, 122.27, 129.03, 129.11, 138.08, 138.47, 140.42, 160.13, 162.57. HRMS-ESI: (*m/z*) calculated for C<sub>24</sub>H<sub>23</sub>F<sub>2</sub>IN<sub>2</sub>O, 521.0901 [M+H]<sup>+</sup>; found 521.0897. Purity: 97.41%.

#### 1-(5,5-bis(4-fluorophenyl)pentyl)-3-(*p*-tolyl)urea (4c).

Compound **4c** was prepared in 84% yield from compounds **29a** and **48c** using the general procedure A. <sup>1</sup>H NMR (400 MHz, CDCl<sub>3</sub>) δ<sub>H</sub> 1.13–1.24 (m, 2H), 1.48 (quin, 2H, *J* = 7.40 Hz), 1.88–2.01 (m, 2H), 2.29 (s, 3 H), 3.06–3.20 (m, 2H), 3.80 (t, 1H, *J* = 7.83 Hz), 4.94 (t, 1H, *J* = 5.62 Hz), 6.59 (s, 1H), 6.88–7.01 (m, 4H), 7.03–7.19 (m, 8 H). <sup>13</sup>C NMR (100 MHz, CDCl<sub>3</sub>) δ<sub>C</sub> 20.80, 25.16, 30.02, 35.48, 40.05, 49.65, 115.16, 115.36, 122.01, 129.02, 129.10, 129.88, 133.96, 135.71, 140.45, 140.49, 156.31, 160.10, 162.53. HRMS-ESI: (*m/z*) calculated for C<sub>25</sub>H<sub>26</sub>F<sub>2</sub>N<sub>2</sub>O, 409.2091 [M+H]<sup>+</sup>; found 409.2127. Purity: >99%.

#### 1-(5,5-bis(4-fluorophenyl)pentyl)-3-(4-nitrophenyl)urea (4d).

Compound **4d** was prepared in 81% yield from compounds **29a** and **48d** using the general procedure A. <sup>1</sup>H NMR (400 MHz, CDCl<sub>3</sub>) δ<sub>H</sub> 1.21–1.31 (m, 2H), 1.55 (quin, 2H, *J* = 7.46 Hz), 1.93–2.03 (m, 2H), 3.22 (q, 2H, *J* = 6.85 Hz), 3.82 (t, 1H, *J* = 7.83 Hz), 5.13 (t, 1H, *J* = 5.50 Hz), 6.87–7.00 (m, 4H), 7.04–7.17 (m, 4H), 7.22 (s, 1H), 7.45–7.53 (m, 2H), 8.07–8.19 (m, 2H). <sup>13</sup>C NMR (100 MHz, CDCl<sub>3</sub>) δ<sub>C</sub> 25.19, 29.90, 35.47, 39.99, 49.69, 115.18, 115.39, 117.47, 117.52, 125.31, 128.99, 129.07, 140.35, 140.39, 141.73, 146.10, 160.10, 162.54. HRMS-ESI: (*m/z*) calculated for C<sub>24</sub>H<sub>23</sub>F<sub>2</sub>N<sub>3</sub>O<sub>3</sub>, 440.1785 [M+H]<sup>+</sup>; found 440.1830. Purity: 99.70%.

**1-(4-aminophenyl)-3-(5,5-bis(4-fluorophenyl)pentyl)urea (4e).**

Compound **4e** was prepared in 81% yield from compound **4d** using the general procedure B. <sup>1</sup>H NMR (400 MHz, CDCl<sub>3</sub>) δ<sub>H</sub> 1.12–1.27 (m, 2H), 1.48 (quin, 2H, *J* = 7.30 Hz), 1.90–2.04 (m, 2H), 3.16 (q, 2H, *J* = 6.85 Hz), 3.69 (br. s., 2H), 3.83 (t, 1H, *J* = 7.83 Hz), 4.52 (t, 1H, *J* = 5.50 Hz), 5.98 (s, 1H), 6.56–6.70 (m, 2H), 6.89–7.05 (m, 6H), 7.08–7.22 (m, 4H). <sup>13</sup>C NMR (100 MHz, CDCl<sub>3</sub>) δ<sub>C</sub> 25.13, 30.03, 35.52, 40.05, 49.65, 115.16, 115.37, 115.76, 126.69, 128.23, 129.05, 129.13, 140.51, 140.54, 144.74, 157.13, 160.12, 162.55. HRMS-ESI: (*m/z*) calculated for C<sub>24</sub>H<sub>25</sub>F<sub>2</sub>N<sub>3</sub>O, 410.2044 [M+H]<sup>+</sup>; found 410.2080. Purity: >99%.

**N-(4-(3-(5,5-bis(4-fluorophenyl)pentyl)ureido)phenyl)acetamide (4f).**

Compound **4f** was prepared in 81% yield from compound **4e** using the general procedure C. <sup>1</sup>H NMR (400 MHz, DMSO-*d*<sub>6</sub>) δ<sub>H</sub> 1.11–1.25 (m, 2H), 1.43–1.48 (m, 2H), 1.92–2.07 (m, 5H), 3.02 (q, 2H, *J* = 6.77 Hz), 3.97 (t, 1H, *J* = 7.83 Hz), 6.03 (t, 1H, *J* = 5.75 Hz), 7.08 (dd, 4H, *J* = 8.90, 8.90 Hz), 7.23–7.37 (m, 6H), 7.41 (d, 2H, *J* = 8.80 Hz), 8.25–8.40 (m, 1H), 9.77 (s, 1H). <sup>13</sup>C NMR (100 MHz, DMSO-*d*<sub>6</sub>) δ<sub>C</sub> 24.29, 25.29, 30.13, 35.15, 49.30, 115.43, 115.64, 118.35, 120.08, 129.70, 129.77, 133.44, 136.43, 141.72, 141.75, 155.73, 159.85, 162.26, 168.16. HRMS-ESI: (*m/z*) calculated for C<sub>26</sub>H<sub>27</sub>F<sub>2</sub>N<sub>3</sub>O<sub>2</sub>, 452.2149 [M+H]<sup>+</sup>; found 452.2186. Purity: >99%.

**1-(5,5-bis(4-fluorophenyl)pentyl)-3-(3-(trifluoromethyl)phenyl)urea (4g).**

Compound **4g** was prepared in 88% yield from compounds **29a** and **48e** using the general procedure A. <sup>1</sup>H NMR (400 MHz, CDCl<sub>3</sub>) δ<sub>H</sub> 1.08–1.21 (m, 2H), 1.42 (quin, 2H, *J* = 7.40 Hz), 1.82–1.95 (m, 2H), 3.02–3.16 (m, 2H), 3.74 (t, 1H, *J* = 7.70 Hz), 5.53 (t, 1H, *J* = 5.26 Hz), 6.84–6.97 (m, 4H), 7.00–7.12 (m, 4H), 7.13–7.20 (m, 1H), 7.20–7.28 (m, 1H), 7.37 (d, 1H, *J* = 8.31 Hz), 7.50 (s, 1H), 7.60 (s, 1H). <sup>13</sup>C NMR (100 MHz, CDCl<sub>3</sub>) δ<sub>C</sub> 25.17, 29.89, 35.43, 40.06, 49.64, 115.16, 115.37, 116.16, 116.20, 119.41, 122.60, 125.25, 128.95, 129.03, 129.49, 139.49, 140.35, 140.39, 156.00, 160.11, 162.54. HRMS-ESI: (*m/z*) calculated for C<sub>25</sub>H<sub>23</sub>F<sub>5</sub>N<sub>2</sub>O, 463.1809 [M+H]<sup>+</sup>; found 463.1845. Purity: >99%.

**1-(5,5-bis(4-fluorophenyl)pentyl)-3-(4-(trifluoromethyl)phenyl)urea (4h).**

Compound **4h** was prepared in 73% yield from compounds **29a** and **48f** using the general procedure A. <sup>1</sup>H NMR (400 MHz, CDCl<sub>3</sub>) δ<sub>H</sub> 1.15–1.24 (m, 2H), 1.47 (quin, 2H, *J* = 7.43 Hz), 1.87–1.99 (m, 2H), 3.13 (q, 2H, *J* = 6.85 Hz), 3.78 (t, 1H, *J* = 7.76 Hz), 5.18 (t, 1H, *J* = 5.50 Hz), 6.80–7.00 (m, 4H), 7.02–7.13 (m, 4H), 7.15 (s, 1H), 7.35 (m, 2H, *J* = 8.56 Hz), 7.46 (m, 2H, *J* = 8.56 Hz). <sup>13</sup>C NMR (100 MHz, CDCl<sub>3</sub>) δ<sub>C</sub> 25.18, 29.93, 35.45, 40.14, 49.68, 115.19, 115.40, 118.87, 126.26, 126.30, 126.33, 128.97, 129.05, 140.32, 140.35, 142.05, 155.33, 160.14, 162.56. HRMS-ESI: (*m/z*) calculated for C<sub>25</sub>H<sub>23</sub>F<sub>5</sub>N<sub>2</sub>O, 463.1809 [M+H]<sup>+</sup>; found 463.1764. Purity: 99.67%.

**1-(5,5-bis(4-fluorophenyl)pentyl)-3-(3-chlorophenyl)urea (4i).**

Compound **4i** was prepared in 66% yield from compounds **29a** and **48g** using the general procedure A. <sup>1</sup>H NMR (400 MHz, CDCl<sub>3</sub>) δ<sub>H</sub> 1.14–1.27 (m, 2H), 1.49 (t, 2H, *J* = 7.09 Hz), 1.95 (q, 2H, *J* = 7.62 Hz), 3.07–3.22 (m, 2H), 3.80 (t, 1H, *J* = 7.76 Hz), 4.99 (br. s., 1H), 6.78 (br. s., 1H), 6.89–7.02 (m, 5H), 7.02–7.21 (m, 6H), 7.33 (s, 1H). <sup>13</sup>C NMR (100 MHz,

CDCl<sub>3</sub>)  $\delta_C$  25.17, 29.96, 35.47, 40.16, 49.67, 115.18, 115.39, 118.07, 120.13, 123.36, 129.01, 129.09, 130.11, 134.75, 139.99, 140.40, 140.43, 155.42, 160.12, 162.55. HRMS-ESI: (*m/z*) calculated for C<sub>24</sub>H<sub>23</sub>ClF<sub>2</sub>N<sub>2</sub>O, 429.1545 [M+H]<sup>+</sup>; found 429.1505. Purity: 99.91%.

#### 1-(5,5-bis(4-fluorophenyl)pentyl)-3-(3-nitrophenyl)urea (4j).

Compound **4j** was prepared in 44% yield from compounds **29a** and **48h** using the general procedure A. <sup>1</sup>H NMR (400 MHz, CDCl<sub>3</sub>)  $\delta_H$  1.22–1.30 (m, 2H), 1.53 (quin, 2H, *J* = 7.40 Hz), 1.87–2.00 (m, 2H), 3.20 (q, 2H, *J* = 6.85 Hz), 3.81 (t, 1H, *J* = 7.76 Hz), 5.20 (t, 1H, *J* = 5.44 Hz), 6.86–6.98 (m, 4H), 7.05–7.16 (m, 4H), 7.35 (t, 1H, *J* = 8.13 Hz), 7.70 (dd, 1H, *J* = 8.19, 1.34 Hz), 7.78 (dt, 1H, *J* = 8.19, 1.10 Hz), 8.10 (t, 1H, *J* = 2.14 Hz). <sup>13</sup>C NMR (100 MHz, CDCl<sub>3</sub>)  $\delta_C$  25.19, 29.91, 35.47, 40.19, 49.67, 76.71, 113.65, 115.18, 115.39, 117.29, 124.90, 128.99, 129.07, 129.77, 140.32, 140.37, 140.40, 148.52, 155.28, 160.11, 162.55. HRMS-ESI: (*m/z*) calculated for C<sub>24</sub>H<sub>23</sub>F<sub>2</sub>N<sub>3</sub>O<sub>3</sub>, 440.1785 [M+H]<sup>+</sup>; found 440.1750. Purity: 99.65%.

#### 1-(5,5-bis(4-fluorophenyl)pentyl)-3-(*m*-tolyl)urea (4k).

Compound **4k** was prepared in 76% yield from compounds **29a** and **48i** using the general procedure A. <sup>1</sup>H NMR (400 MHz, CDCl<sub>3</sub>)  $\delta_H$  1.18–1.25 (m, 2H), 1.52 (quin, 2H, *J* = 7.40 Hz), 1.91–2.03 (m, 2H), 2.31 (s, 3H), 3.08–3.25 (m, 2H), 3.83 (t, 1H, *J* = 7.83 Hz), 4.75 (t, 1H, *J* = 5.62 Hz), 6.29 (s, 1H), 6.85–7.03 (m, 6H), 7.04–7.22 (m, 6H). <sup>13</sup>C NMR (100 MHz, CDCl<sub>3</sub>)  $\delta_C$  21.43, 25.17, 30.01, 35.50, 40.14, 49.68, 115.18, 115.39, 118.68, 122.38, 125.07, 129.03, 129.11, 129.18, 138.27, 139.41, 140.46, 155.83, 160.13. HRMS-ESI: (*m/z*) calculated for C<sub>25</sub>H<sub>26</sub>F<sub>2</sub>N<sub>2</sub>O, 409.2091 [M+H]<sup>+</sup>; found 409.2051. Purity: 98.34%.

#### 1-(5,5-bis(4-fluorophenyl)pentyl)-3-(4-chloro-3-(trifluoromethyl)phenyl)urea (4l).

Compound **4l** was prepared in 60% yield from compounds **29a** and **48j** using the general procedure A. <sup>1</sup>H NMR (400 MHz, CDCl<sub>3</sub>)  $\delta_H$  1.11–1.34 (m, 2H), 1.38–1.56 (m, 2H), 1.84–2.03 (m, 2H), 3.14 (q, 2H, *J* = 6.60 Hz), 3.79 (t, 1H, *J* = 7.70 Hz), 5.09 (br. s., 1H), 6.93 (t, 4H, *J* = 8.56 Hz), 7.10 (dd, 4H, *J* = 8.44, 5.26 Hz), 7.31 (d, 1H, *J* = 8.56 Hz), 7.42 (dd, 1H, *J* = 8.68, 2.32 Hz), 7.50–7.59 (m, 1H). <sup>13</sup>C NMR (100 MHz, CDCl<sub>3</sub>)  $\delta_C$  25.18, 29.91, 35.45, 40.21, 49.69, 115.21, 115.42, 123.33, 128.99, 129.06, 131.96, 137.74, 140.35, 155.13, 160.13, 162.56. HRMS-ESI: (*m/z*) calculated for C<sub>25</sub>H<sub>22</sub>ClF<sub>5</sub>N<sub>2</sub>O, 497.1419 [M+H]<sup>+</sup>; found 497.1455. Purity: 98.08%.

#### 1-(5,5-bis(4-fluorophenyl)pentyl)-3-(4-chloro-3-nitrophenyl)urea (4m).

Compound **4m** was prepared in 59% yield from compounds **29a** and **48k** using the general procedure A. <sup>1</sup>H NMR (400 MHz, CDCl<sub>3</sub>)  $\delta_H$  1.17–1.29 (m, 2H), 1.52 (quin, 2H, *J* = 7.46 Hz), 1.90–2.03 (m, 2H), 3.17 (q, 2H, *J* = 6.85 Hz), 3.81 (t, 1H, *J* = 7.83 Hz), 5.17 (t, 1H, *J* = 5.50 Hz), 6.85–6.99 (m, 4H), 7.05–7.19 (m, 4H), 7.28 (s, 1H), 7.34 (d, 1H, *J* = 8.80 Hz), 7.43 (dd, 1H, *J* = 8.93, 2.57 Hz), 7.90 (d, 1H, *J* = 2.69 Hz). <sup>13</sup>C NMR (100 MHz, CDCl<sub>3</sub>)  $\delta_C$  25.20, 29.86, 35.46, 40.25, 49.66, 115.20, 115.41, 115.53, 119.82, 123.33, 129.00, 129.08, 132.07, 138.72, 140.33, 140.36, 147.73, 154.92, 160.11, 162.55. HRMS-ESI: (*m/z*) calculated for C<sub>24</sub>H<sub>22</sub>ClF<sub>2</sub>N<sub>3</sub>O<sub>3</sub>, 474.1396 [M+H]<sup>+</sup>; found 474.1444. Purity: 100.00%.

**1-(3-amino-4-chlorophenyl)-3-(5,5-bis(4-fluorophenyl)pentyl)urea (4n).**

Compound **4n** was prepared in 97% yield from compound **4m** using the general procedure B.  $^1\text{H}$  NMR (400 MHz,  $\text{CDCl}_3$ )  $\delta_{\text{H}}$  1.15 (quin, 2H,  $J = 7.70$  Hz), 1.42 (quin, 2H,  $J = 7.40$  Hz), 1.82–1.97 (m, 2H), 3.06 (q, 2H,  $J = 6.85$  Hz), 3.76 (t, 1H,  $J = 7.70$  Hz), 3.95 (br. s., 1H), 5.26–5.38 (m, 1H), 6.44 (dd, 1H,  $J = 8.56, 2.20$  Hz), 6.79 (d, 1H,  $J = 2.20$  Hz), 6.85–7.00 (m, 4H), 7.00–7.18 (m, 6H).  $^{13}\text{C}$  NMR (100 MHz,  $\text{CDCl}_3$ )  $\delta_{\text{C}}$  25.19, 30.00, 35.46, 40.05, 49.65, 107.49, 110.99, 113.72, 115.17, 115.38, 129.01, 129.09, 129.64, 138.36, 140.43, 140.45, 143.51, 156.09, 160.09, 162.52. HRMS-ESI: ( $m/z$ ) calculated for  $\text{C}_{24}\text{H}_{24}\text{ClF}_2\text{N}_3\text{O}$ , 444.1654  $[\text{M}+\text{H}]^+$ ; found 444.1699. Purity: 99.74%.

**N-(5-(3-(5,5-bis(4-fluorophenyl)pentyl)ureido)-2-chlorophenyl)acetamide (4o).**

Compound **4o** was prepared in 78% yield from compound **4n** following the general procedure C.  $^1\text{H}$  NMR (400 MHz,  $\text{DMSO}-d_6$ )  $\delta_{\text{H}}$  1.08–1.25 (m, 2H), 1.45 (quin, 2H,  $J = 7.27$  Hz), 2.00 (q, 2H,  $J = 7.83$  Hz), 2.08 (s, 3H), 3.03 (q, 2H,  $J = 6.77$  Hz), 3.97 (t, 1H,  $J = 7.70$  Hz), 6.06 (t, 1H,  $J = 5.50$  Hz), 7.09 (t, 4H,  $J = 8.80$  Hz), 7.21–7.42 (m, 6H), 7.74 (s, 1H), 8.59 (s, 1H), 9.38 (s, 1H).  $^{13}\text{C}$  NMR (100 MHz,  $\text{DMSO}-d_6$ )  $\delta_{\text{C}}$  25.27, 30.02, 35.14, 49.29, 115.43, 115.64, 129.59, 129.69, 129.77, 135.43, 140.23, 141.74, 155.40, 159.86, 162.26. HRMS-ESI: ( $m/z$ ) calculated for  $\text{C}_{26}\text{H}_{26}\text{ClF}_2\text{N}_3\text{O}_2$ , 486.1760  $[\text{M}+\text{H}]^+$ ; found 486.1811. Purity: 99.86%.

**1-(5,5-bis(4-fluorophenyl)pentyl)-3-(3-chloro-4-nitrophenyl)urea (4p).**

Compound **4p** was prepared in 72% yield from compound **29a** and **48l** following the general procedure A.  $^1\text{H}$  NMR (400 MHz,  $\text{CDCl}_3$ )  $\delta_{\text{H}}$  1.19–1.30 (m, 2H), 1.54 (quin, 2H,  $J = 7.40$  Hz), 1.88–2.02 (m, 2H), 3.20 (q, 2H,  $J = 6.85$  Hz), 3.81 (t, 1H,  $J = 7.83$  Hz), 5.40 (t, 1H,  $J = 5.50$  Hz), 6.84–6.99 (m, 4H), 7.01–7.17 (m, 4H), 7.30 (dd, 1H,  $J = 9.05, 2.20$  Hz), 7.52–7.67 (m, 2H), 7.90 (d, 1H,  $J = 9.05$  Hz).  $^{13}\text{C}$  NMR (100 MHz,  $\text{CDCl}_3$ )  $\delta_{\text{C}}$  25.21, 29.81, 35.46, 40.23, 49.68, 115.20, 115.41, 116.25, 120.37, 127.65, 128.98, 129.06, 129.34, 140.30, 140.33, 140.76, 144.58, 154.46, 160.12, 162.55. HRMS-ESI: ( $m/z$ ) calculated for  $\text{C}_{24}\text{H}_{22}\text{ClF}_2\text{N}_3\text{O}_3$ , 474.1396  $[\text{M}+\text{H}]^+$ ; found 474.1446. Purity: 99.03%.

**1-(5,5-bis(4-fluorophenyl)pentyl)-3-(4-nitro-3-(trifluoromethyl)phenyl)urea (4q).**

Compound **4q** was prepared in 71% yield from compound **29a** and **48m** following the general procedure A.  $^1\text{H}$  NMR (400 MHz,  $\text{CDCl}_3$ )  $\delta_{\text{H}}$  1.28 (quin, 2H,  $J = 7.70$  Hz), 1.57 (quin, 2H,  $J = 7.46$  Hz), 2.01 (q, 2H,  $J = 7.82$  Hz), 3.24 (q, 2H,  $J = 6.77$  Hz), 3.84 (t, 1H,  $J = 7.83$  Hz), 4.90 (br. s., 1H), 6.87–7.05 (m, 5H), 7.14 (dd, 4H,  $J = 8.44, 5.50$  Hz), 7.70–7.85 (m, 2H), 7.95 (d, 1H,  $J = 8.80$  Hz).  $^{13}\text{C}$  NMR (100 MHz,  $\text{CDCl}_3$ )  $\delta_{\text{C}}$  25.15, 29.76, 35.44, 40.32, 49.69, 115.23, 115.43, 116.90, 120.45, 127.51, 129.01, 129.08, 140.30, 140.34, 160.14, 162.57. HRMS-ESI: ( $m/z$ ) calculated for  $\text{C}_{25}\text{H}_{22}\text{F}_5\text{N}_3\text{O}$ , 508.1659  $[\text{M}+\text{H}]^+$ ; found 508.1715. Purity: 97.34%.

**1-(5,5-bis(4-fluorophenyl)pentyl)-3-(3,4-dimethylphenyl)urea (4r).**

Compound **4r** was prepared in 73% yield from compound **29a** and **48n** following the general procedure A.  $^1\text{H}$  NMR (400 MHz,  $\text{CDCl}_3$ )  $\delta_{\text{H}}$  1.18–1.29 (m, 2H), 1.52 (dt, 2H,  $J = 14.67, 7.34$  Hz), 1.93–2.02 (m, 2H), 2.22 (s, 6H), 3.13–3.25 (m, 2H), 3.83 (t, 1H,  $J = 7.83$



Hz), 4.69 (t, 1H,  $J = 5.38$  Hz), 6.14 (s, 1H), 6.88–7.02 (m, 6H), 7.05 (d, 1H,  $J = 7.82$  Hz), 7.09–7.22 (m, 4H).  $^{13}\text{C}$  NMR (100 MHz,  $\text{CDCl}_3$ )  $\delta_{\text{C}}$  19.16, 19.85, 25.15, 30.01, 35.50, 40.11, 49.66, 115.16, 115.37, 124.09, 129.03, 129.11, 130.45, 135.72, 137.87, 156.14, 160.11. HRMS-ESI: ( $m/z$ ) calculated for  $\text{C}_{26}\text{H}_{28}\text{F}_2\text{N}_2\text{O}$ , 423.2248  $[\text{M}+\text{H}]^+$ ; found 423.2292. Purity: 96.99%.

#### 1-(5,5-bis(4-fluorophenyl)pentyl)-3-(4-chloro-2-(trifluoromethyl)phenyl)urea (4s).

Compound **4s** was prepared in 83% yield from compound **29a** and **48o** following the general procedure A.  $^1\text{H}$  NMR (400 MHz,  $\text{CDCl}_3$ )  $\delta_{\text{H}}$  1.18–1.28 (m, 2H), 1.50 (quin, 2H,  $J = 7.40$  Hz), 1.91–2.03 (m, 2H), 3.08–3.20 (m, 2H), 3.82 (t, 1H,  $J = 1.00$  Hz), 5.11 (t, 1H,  $J = 5.14$  Hz), 6.62 (s, 1H), 6.88–7.05 (m, 4H), 7.05–7.20 (m, 4H), 7.41 (dd, 1H,  $J = 8.93, 2.32$  Hz), 7.51 (d, 1H,  $J = 2.20$  Hz), 7.89 (d, 1H,  $J = 9.05$  Hz).  $^{13}\text{C}$  NMR (100 MHz,  $\text{CDCl}_3$ )  $\delta_{\text{C}}$  25.13, 29.83, 35.48, 40.31, 49.67, 115.20, 115.41, 125.91, 126.12, 126.18, 128.79, 129.00, 129.08, 132.72, 135.14, 140.38, 140.40, 154.80, 160.14, 162.57. HRMS-ESI: ( $m/z$ ) calculated for  $\text{C}_{25}\text{H}_{22}\text{ClF}_5\text{N}_2\text{O}$ , 497.1419  $[\text{M}+\text{H}]^+$ ; found 497.1480. Purity: 99.04%.

#### 1-(5,5-bis(4-fluorophenyl)pentyl)-3-(4-chloro-2-methylphenyl)urea (4t).

Compound **4t** was prepared in 94% yield from compound **29a** and **48p** following the general procedure A.  $^1\text{H}$  NMR (400 MHz,  $\text{CDCl}_3$ )  $\delta_{\text{H}}$  ppm 1.13–1.29 (m, 2H), 1.50 (quin, 2H,  $J = 7.34$  Hz), 1.90–2.05 (m, 2H), 3.17 (d, 2H,  $J = 5.26$  Hz), 3.83 (t, 1H,  $J = 7.76$  Hz), 4.49 (br. s., 1H), 5.94 (s, 1H), 6.95 (t, 4H,  $J = 8.68$  Hz), 7.13 (dd, 5H,  $J = 8.38, 5.56$  Hz), 7.18–7.22 (m, 1H), 7.28 (s, 1H).  $^{13}\text{C}$  NMR (100 MHz,  $\text{CDCl}_3$ )  $\delta_{\text{C}}$  17.76, 25.14, 30.04, 35.50, 40.18, 49.66, 115.18, 115.39, 126.68, 127.12, 129.01, 129.09, 130.83, 131.22, 134.46, 134.56, 140.41, 140.44, 160.12, 162.55. HRMS-ESI: ( $m/z$ ) calculated for  $\text{C}_{25}\text{H}_{25}\text{ClF}_2\text{N}_2\text{O}$ , 443.1701  $[\text{M}+\text{H}]^+$ ; found 443.1705. Purity: >99%.

#### 1-(5,5-bis(4-fluorophenyl)pentyl)-3-(4-bromo-2-iodophenyl)urea (4u).

Compound **4u** was prepared in 64% yield from compound **29a** and **48q** following the general procedure A.  $^1\text{H}$  NMR (400 MHz,  $\text{CDCl}_3$ )  $\delta_{\text{H}}$  1.19–1.33 (m, 2H), 1.55 (quin, 2H,  $J = 7.40$  Hz), 1.93–2.04 (m, 2H), 3.12–3.26 (m, 2H), 3.83 (t, 1H,  $J = 7.70$  Hz), 4.93 (t, 1H,  $J = 5.38$  Hz), 6.51 (s, 1H), 6.84–7.03 (m, 4H), 7.03–7.21 (m, 4H), 7.26 (s, 1H), 7.38 (dd, 1H,  $J = 8.68, 2.32$  Hz), 7.74–7.90 (m, 2H).  $^{13}\text{C}$  NMR (100 MHz,  $\text{CDCl}_3$ )  $\delta_{\text{C}}$  25.20, 29.92, 35.50, 40.43, 49.67, 90.75, 115.22, 115.42, 116.30, 122.83, 129.01, 129.09, 132.16, 138.57, 140.37, 140.41, 140.50, 154.66, 160.12, 162.55. HRMS-ESI: ( $m/z$ ) calculated for  $\text{C}_{24}\text{H}_{22}\text{BrF}_2\text{IN}_2\text{O}$ , 599.9959  $[\text{M}+\text{H}]^+$ ; found 599.9942. Purity: 99.07%.

#### methyl 4-(3-(5,5-bis(4-fluorophenyl)pentyl)ureido)-2-(trifluoromethyl)benzoate (4v).

Compound **4v** was prepared in 63% yield from compound **51a** and **29a** following the general procedure A.  $^1\text{H}$  NMR (400 MHz,  $\text{CDCl}_3$ )  $\delta_{\text{H}}$  1.09–1.25 (m, 2H), 1.46 (quin, 2H,  $J = 7.40$  Hz), 1.90 (q, 2H,  $J = 7.83$  Hz), 3.13 (q, 2H,  $J = 6.60$  Hz), 3.75 (t, 1H,  $J = 7.83$  Hz), 3.83 (s, 3H), 5.78 (d, 1H,  $J = 5.38$  Hz), 6.82–6.99 (m, 4H), 6.99–7.17 (m, 4H), 7.50 (d, 1H,  $J = 8.56$  Hz), 7.63 (s, 1H), 7.71 (d, 1H,  $J = 8.56$  Hz), 8.00–8.15 (m, 1H).  $^{13}\text{C}$  NMR (100 MHz,  $\text{CDCl}_3$ )  $\delta_{\text{C}}$  25.20, 29.85, 35.42, 40.08, 49.65, 52.63, 115.15, 115.36, 120.40, 128.95,

129.03, 132.41, 140.33, 140.38, 142.64, 155.61, 160.10, 162.53, 166.64. HRMS-ESI: (*m/z*) calculated for C<sub>27</sub>H<sub>25</sub>F<sub>5</sub>N<sub>2</sub>O<sub>3</sub>, 521.1863 [M+H]<sup>+</sup>; found 521.1867. Purity: 98.84%.

#### 4-(3-(5,5-bis(4-fluorophenyl)pentyl)ureido)-2-(trifluoromethyl)benzoic acid (4x).

NaBH<sub>4</sub> (0.02 g, 0.52 mmol) was added portion wise to a suspension of compound **4w** (0.15 g, 0.39 mmol) and Pd/C (0.02g, cat.) in methanol (15 mL). The reaction mixture was stirred for 20 min, filtered using Celite® bed, and washed with methanol. Organic solvent was removed under reduced pressure and formed residue was re-dissolved in methanol (5 mL). Precipitation by dropwise addition of dichloromethane afforded compound **4x** (0.08 g, 61%) as a white solid. <sup>1</sup>H NMR (400 MHz, DMSO-*d*<sub>6</sub>) δ<sub>H</sub> 1.10–1.26 (m, 2H), 1.47 (quin, 2H, *J* = 7.06 Hz), 2.00 (q, 2H, *J* = 7.78 Hz), 3.03 (q, 2H, *J* = 6.44 Hz), 3.97 (t, 1H, *J* = 7.89 Hz), 4.13 (d, 1H, *J* = 4.89 Hz), 7.00 (br. s., 1H), 7.07 (t, 4H, *J* = 8.86 Hz), 7.21–7.50 (m, 6H), 7.81 (d, 1H, *J* = 1.83 Hz), 9.47 (br. s., 1H). <sup>13</sup>C NMR (100 MHz, DMSO-*d*<sub>6</sub>) δ<sub>C</sub> 25.29, 30.02, 35.16, 49.05, 49.30, 115.39, 115.60, 120.14, 125.96, 129.69, 129.77, 129.92, 140.12, 141.73, 155.92, 159.84, 162.24, 171.05. HRMS-ESI: (*m/z*) calculated for C<sub>26</sub>H<sub>23</sub>F<sub>5</sub>N<sub>2</sub>O<sub>3</sub>, 507.1707 [M+H]<sup>+</sup>; found 507.1715. Purity: 98.34%.

#### 1-(4-chloro-3-(trifluoromethyl)phenyl)-3-(5,5-di-p-tolylpentyl)urea (8a).

Compound **8a** was prepared in 41% yield from compounds **29b** and **48j** following the general procedure A. <sup>1</sup>H NMR (400 MHz, CDCl<sub>3</sub>) δ<sub>H</sub> 1.17–1.29 (m, 2H), 1.47 (quin, 2H, *J* = 7.37 Hz), 1.97 (q, 2H, *J* = 7.78 Hz), 2.26 (s, 6H), 3.11 (q, 2H, *J* = 6.85 Hz), 3.75 (t, 1H, *J* = 7.76 Hz), 5.11 (t, 1H, *J* = 5.44 Hz), 6.95–7.10 (m, 8H), 7.15 (s, 1H), 7.20–7.32 (m, 1H), 7.37 (dd, 1H, *J* = 8.74, 2.51 Hz), 7.54 (d, 1H, *J* = 2.57 Hz). <sup>13</sup>C NMR (100 MHz, CDCl<sub>3</sub>) δ<sub>C</sub> 20.93, 25.30, 29.88, 35.27, 40.19, 50.43, 118.25, 118.31, 123.26, 125.36, 127.55, 129.14, 131.87, 135.56, 137.79, 142.12, 155.39. HRMS-ESI: (*m/z*) calculated for C<sub>27</sub>H<sub>28</sub>ClF<sub>3</sub>N<sub>2</sub>O, 489.1920 [M+H]<sup>+</sup>; found 489.1923. Purity: 99.80%.

#### 1-(4-chlorophenyl)-3-(5,5-di-p-tolylpentyl)urea (8b).

Compound **8b** was prepared in 39% yield from compounds **29b** and **48a** following the general procedure A. <sup>1</sup>H NMR (400 MHz, CDCl<sub>3</sub>) δ<sub>H</sub> 1.23–1.32 (m, 2H), 1.48 (quin, 2H, *J* = 7.40 Hz), 1.92–2.02 (m, 2H), 2.27 (s, 6H), 3.12 (q, 2H, *J* = 6.85 Hz), 3.77 (t, 1H, *J* = 7.76 Hz), 4.85 (t, 1H, *J* = 5.56 Hz), 6.64 (s, 1H), 7.01–7.12 (m, 8H), 7.12–7.22 (m, 4H). <sup>13</sup>C NMR (100 MHz, CDCl<sub>3</sub>) δ<sub>C</sub> 20.96, 25.33, 29.97, 35.33, 40.20, 50.43, 121.67, 127.58, 128.51, 129.14, 135.52, 137.30, 142.17, 155.55. HRMS-ESI: (*m/z*) calculated for C<sub>26</sub>H<sub>29</sub>ClN<sub>2</sub>O, 420.1968 [M+H]<sup>+</sup>; found 421.2037. Purity: 99.08%.

#### 1-(5,5-bis(4-methoxyphenyl)pentyl)-3-(4-chloro-3-(trifluoromethyl)phenyl)urea (8c).

Compound **8c** was prepared in 65% yield from compounds **29c** and **48j** following the general procedure A. <sup>1</sup>H NMR (400 MHz, CDCl<sub>3</sub>) δ<sub>H</sub> 1.16–1.27 (m, 2H), 1.40–1.51 (m, 2H), 1.93 (q, 2H, *J* = 7.78 Hz), 3.11 (q, 2H, *J* = 6.72 Hz), 3.65–3.79 (m, 7H), 5.24 (t, 1H, *J* = 5.32 Hz), 6.72–6.84 (m, 4H), 7.07 (d, 4H, *J* = 8.68 Hz), 7.26 (d, 1H, *J* = 8.68 Hz), 7.31–7.41 (m, 2H), 7.54 (d, 1H, *J* = 2.45 Hz). <sup>13</sup>C NMR (100 MHz, CDCl<sub>3</sub>) δ<sub>C</sub> 25.23, 29.79, 35.49, 40.12, 49.48, 55.21, 113.83, 118.14, 118.19, 123.15, 123.96, 125.21, 128.41, 128.57,

128.71, 131.86, 137.44, 137.89, 155.49, 157.81. HRMS-ESI: ( $m/z$ ) calculated for  $C_{27}H_{28}ClF_3N_2O_3$ , 521.1819 [M+H]<sup>+</sup>; found 521.1909. Purity: >99%.

#### 1-(5,5-bis(4-methoxyphenyl)pentyl)-3-(4-chloro-3-nitrophenyl)urea (8d).

Compound **8d** was prepared in 25% yield from compounds **29c** and **48k** following the general procedure A. <sup>1</sup>H NMR (400 MHz, CDCl<sub>3</sub>) δ<sub>H</sub> 1.23–1.30 (m, 2H), 1.51 (quin, 2H,  $J = 7.31$  Hz), 1.96 (q, 2H,  $J = 7.83$  Hz), 3.16 (q, 2H,  $J = 6.72$  Hz), 3.68–3.80 (m, 7H), 5.03 (t, 1H,  $J = 5.44$  Hz), 6.79 (d, 4H,  $J = 8.68$  Hz), 7.00–7.19 (m, 5H), 7.32 (d, 1H,  $J = 8.80$  Hz), 7.46 (dd, 1H,  $J = 8.80, 2.57$  Hz), 7.85 (d, 1H,  $J = 2.57$  Hz). <sup>13</sup>C NMR (100 MHz, CDCl<sub>3</sub>) δ<sub>C</sub> 25.19, 29.70, 35.45, 40.19, 49.46, 55.25, 113.85, 115.43, 119.64, 123.24, 128.61, 132.01, 137.46, 138.82, 147.74, 154.84, 157.82. Purity: HRMS-ESI: ( $m/z$ ) calculated for  $C_{26}H_{28}ClN_3O_5$ , 498.1795 [M+H]<sup>+</sup>; found 498.1782. Purity: 99.93%.

#### 1-(5,5-bis(4-(trifluoromethoxy)phenyl)pentyl)-3-(4-chloro-3-(trifluoromethyl)phenyl)urea (8e).

Compound **8e** was prepared in 62% yield from compounds **29d** and **48j** following the general procedure A. <sup>1</sup>H NMR (400 MHz, CDCl<sub>3</sub>) δ<sub>H</sub> 1.17–1.25 (m, 2H), 1.49 (quin, 2H,  $J = 7.40$  Hz), 1.97 (q, 2H,  $J = 7.91$  Hz), 3.15 (q, 2H,  $J = 6.72$  Hz), 3.85 (t, 1H,  $J = 7.76$  Hz), 5.04 (t, 1H,  $J = 5.50$  Hz), 7.05 (s, 1H), 7.10 (d, 4H,  $J = 8.31$  Hz), 7.17 (d, 4H,  $J = 8.68$  Hz), 7.32 (d, 1H,  $J = 8.80$  Hz), 7.44 (dd, 1H,  $J = 8.68, 2.45$  Hz), 7.56 (d, 1H,  $J = 2.45$  Hz). <sup>13</sup>C NMR (100 MHz, CDCl<sub>3</sub>) δ<sub>C</sub> 25.12, 29.72, 29.93, 35.25, 40.13, 49.97, 121.08, 123.33, 128.93, 131.97, 137.73, 142.87, 147.70, 147.72, 155.19. HRMS-ESI: ( $m/z$ ) calculated for  $C_{27}H_{22}ClF_9N_2O_3$ , 629.1253 [M+H]<sup>+</sup>; found 629.1231. Purity: 98.40%.

#### 1-(4-chloro-3-(trifluoromethyl)phenyl)-3-(5,5-diphenylpentyl)urea (8f).

Compound **8f** was prepared in 25% yield from compounds **29e** and **48j** following the general procedure A. <sup>1</sup>H NMR (400 MHz, CDCl<sub>3</sub>) δ<sub>H</sub> 1.25–1.32 (m, 2H), 1.46–1.56 (m, 2H), 1.99–2.10 (m, 2H), 3.09–3.23 (m, 2H), 3.86 (t, 1H,  $J = 7.76$  Hz), 4.73 (t, 1H,  $J = 5.56$  Hz), 6.63 (s, 1H), 7.16–7.29 (m, 10H), 7.34 (d, 1H,  $J = 8.68$  Hz), 7.46 (dd, 1H,  $J = 8.68, 2.57$  Hz), 7.58 (d, 1H,  $J = 2.45$  Hz). <sup>13</sup>C NMR (100 MHz, CDCl<sub>3</sub>) δ<sub>C</sub> 25.22, 29.81, 35.17, 40.21, 51.26, 118.25, 118.30, 123.31, 123.95, 126.19, 127.80, 128.48, 131.95, 137.77, 144.87, 154.83. HRMS-ESI: ( $m/z$ ) calculated for  $C_{25}H_{24}ClF_3N_2O$ , 461.1607 [M+H]<sup>+</sup>; found 461.1594. Purity: 99.35%.

#### 1-(5,5-bis(4-nitrophenyl)pentyl)-3-(4-chloro-3-(trifluoromethyl)phenyl)urea (8g).

Compound **8g** was prepared in 29% yield from compounds **29f** and **48j** following the general procedure A. <sup>1</sup>H NMR (400 MHz, CDCl<sub>3</sub>) δ<sub>H</sub> 1.27–1.33 (m, 2H), 1.56 (d, 2H,  $J = 7.21$  Hz), 2.12 (q, 2H,  $J = 7.74$  Hz), 3.21 (q, 2H,  $J = 6.81$  Hz), 4.11 (t, 1H,  $J = 7.70$  Hz), 4.79 (t, 1H,  $J = 5.56$  Hz), 6.65 (s, 1H), 7.31–7.42 (m, 5H), 7.50 (dd, 1H,  $J = 8.74, 2.38$  Hz), 7.62 (d, 1H,  $J = 2.45$  Hz), 8.14 (d, 4H,  $J = 8.80$  Hz). <sup>13</sup>C NMR (100 MHz, CDCl<sub>3</sub>) δ<sub>C</sub> 24.95, 29.71, 29.93, 34.59, 39.98, 50.96, 118.19, 118.24, 123.27, 124.10, 128.65, 132.03, 137.73, 146.84, 150.56, 154.78. HRMS-ESI: ( $m/z$ ) calculated for  $C_{25}H_{22}ClF_3N_4O_5$ , 551.1309 [M+H]<sup>+</sup>; found 551.1303. Purity: >99%.

**1-(5,5-bis(4-aminophenyl)pentyl)-3-(4-chloro-3-(trifluoromethyl)phenyl)urea (8h).**

Compound **8h** was prepared in 85% yield from compound **8g** following the general procedure B. <sup>1</sup>H NMR (400 MHz, CDCl<sub>3</sub>) δ<sub>H</sub> 1.13–1.23 (m, 2H), 1.34–1.45 (m, 2H), 1.81–1.94 (m, 2H), 3.05 (q, 2H, *J* = 6.56 Hz), 3.53 (br. s., 4H), 3.61 (t, 1H, *J* = 7.76 Hz), 5.16 (t, 1H, *J* = 5.38 Hz), 6.55 (d, 4H, *J* = 8.44 Hz), 6.95 (d, 4H, *J* = 8.44 Hz), 7.19–7.29 (m, 1H), 7.31–7.41 (m, 2H), 7.55 (d, 1H, *J* = 2.32 Hz). <sup>13</sup>C NMR (100 MHz, CDCl<sub>3</sub>) δ<sub>C</sub> 25.30, 28.55, 35.38, 45.31, 49.37, 115.23, 123.86, 123.91, 128.52, 128.98, 130.06, 132.98, 135.65, 144.34, 180.69. HRMS-ESI: (*m/z*) calculated for C<sub>25</sub>H<sub>26</sub>ClF<sub>3</sub>N<sub>4</sub>O, 491.1825 [M+H]<sup>+</sup>; found 491.1842. Purity: 96.38%.

**N,N'-((5-(3-(4-chloro-3-(trifluoromethyl)phenyl)ureido)pentane-1,1-diyl)bis(4,1 phenylene)) diacetamide (8i).**

Compound **8i** was prepared in 51% yield from compound **8h** following the general procedure C. <sup>1</sup>H NMR (400 MHz, DMSO-*d*<sub>6</sub>) δ<sub>H</sub> 1.11–1.25 (m, 2H), 1.40–1.52 (m, 2H), 1.89–2.05 (m, 8H) 3.03, (q, 2H, *J* = 6.60 Hz), 3.79 (t, 1H, *J* = 7.83 Hz), 6.29 (t, 1H, *J* = 5.62 Hz), 7.18 (d, 4H, *J* = 8.56 Hz), 7.45 (d, 4H, *J* = 8.56 Hz), 7.49–7.61 (m, 2H), 8.05 (d, 1H, *J* = 1.96 Hz), 8.92 (s, 1H), 9.84 (s, 2H). <sup>13</sup>C NMR (100 MHz, DMSO-*d*<sub>6</sub>) δ<sub>C</sub> 20.91, 24.35, 25.43, 30.01, 35.21, 49.94, 119.58, 121.65, 122.69, 128.08, 132.26, 137.66, 140.47, 140.67, 155.29, 168.49. HRMS-ESI: (*m/z*) calculated for C<sub>29</sub>H<sub>30</sub>ClF<sub>3</sub>N<sub>4</sub>O<sub>3</sub>, 575.2037 [M+H]<sup>+</sup>; found 575.2048. Purity: 99.79%.

**1-(4-(bis(4-fluorophenyl)amino)butyl)-3-(4-chlorophenyl)urea (9a).**

Compound **9a** was prepared in 51% yield from compounds **53** and **48a** following the general procedure A. <sup>1</sup>H NMR (400 MHz, DMSO-*d*<sub>6</sub>) δ<sub>H</sub> 1.40–1.50 (m, 2H) 1.50–1.60 (m, 2H), 3.08 (q, 2H, *J* = 6.36 Hz), 3.63 (t, 2H, *J* = 7.21 Hz), 6.21 (t, 1H, *J* = 5.50 Hz), 6.89–7.02 (m, 4H), 7.02–7.15 (m, 4H), 7.21–7.29 (m, 2H), 7.36–7.48 (m, 2H), 8.60 (s, 1H). <sup>13</sup>C NMR (100 MHz, DMSO-*d*<sub>6</sub>) δ<sub>C</sub> 24.71, 27.61, 52.17, 116.27, 116.48, 119.52, 122.59, 122.67, 124.82, 128.89, 140.04, 144.80, 144.83, 155.54, 156.35, 158.72. HRMS-ESI: (*m/z*) calculated for C<sub>23</sub>H<sub>22</sub>ClF<sub>2</sub>N<sub>3</sub>O, 430.1497 [M+H]<sup>+</sup>; found 430.1508. Purity: >99%.

**1-(4-(bis(4-fluorophenyl)amino)butyl)-3-(4-iodophenyl)urea (9b).**

Compound **9b** was prepared in 29% yield from compounds **53** and **48b** following the general procedure A. <sup>1</sup>H NMR (400 MHz, DMSO-*d*<sub>6</sub>) δ<sub>H</sub> 1.39–1.50 (m, 2H) 1.50–1.59 (m, 2H), 3.07 (q, 2H, *J* = 6.32 Hz), 3.63 (t, 2H, *J* = 7.27 Hz) 6.18 (t, 1H, *J* = 5.62 Hz), 6.87–7.00 (m, 4H), 7.02–7.14 (m, 4H), 7.24 (m, 2H, *J* = 8.80 Hz), 7.52 (m, 2H, *J* = 8.80 Hz), 8.54 (s, 1H). <sup>13</sup>C NMR (100 MHz, DMSO-*d*<sub>6</sub>) δ<sub>C</sub> 24.72, 27.61, 52.17, 83.87, 116.27, 116.49, 120.36, 121.01, 122.59, 122.67, 137.59, 137.78, 140.97, 144.83, 155.45 HRMS-ESI: (*m/z*) calculated for C<sub>23</sub>H<sub>22</sub>F<sub>2</sub>IN<sub>3</sub>O, 522.0854 [M+H]<sup>+</sup>; found 522.0864.

**1-(4-(bis(4-fluorophenyl)amino)butyl)-3-(4-chloro-3-(trifluoromethyl)phenyl)urea (9c).**

Compound **9c** was prepared in 65% yield from compounds **53** and **48j** following the general procedure A. <sup>1</sup>H NMR (400 MHz, DMSO-*d*<sub>6</sub>) δ<sub>H</sub> <sup>1</sup>H NMR (400 MHz, CDCl<sub>3</sub>) δ<sub>H</sub> 1.50–1.58 (m, 2H), 1.59–1.65 (m, 2H), 3.22 (q, *J* = 6.56 Hz, 2H), 3.59, (t, *J* = 7.09 Hz, 2H), 4.93 (t, *J* = 5.56 Hz, 1H), 6.77 (s, 1H), 6.80–6.88 (m, 4H), 6.88–6.99 (m, 4H), 7.34 (d, *J* = 8.68

Hz, 1H), 7.44 (dd,  $J = 8.68, 2.57$  Hz, 1H), 7.58 (d,  $J = 2.45$  Hz, 1H).  $^{13}\text{C}$  NMR (100 MHz,  $\text{CDCl}_3$ )  $\delta_{\text{C}}$  24.79, 27.56, 40.19, 52.36, 115.89, 116.11, 118.36, 118.41, 122.28, 122.35, 123.40, 132.00, 137.59, 144.46, 144.48, 155.02, 156.77, 159.17. HRMS-ESI: ( $m/z$ ) calculated for  $\text{C}_{24}\text{H}_{21}\text{ClF}_5\text{N}_3\text{O}$ , 498.1371  $[\text{M}+\text{H}]^+$ ; found 498.1373. Purity: 97.52%.

#### 1-(4-(bis(4-fluorophenyl)amino)butyl)-3-(3,4-dimethylphenyl)urea (9d).

Compound **9d** was prepared in 57% yield from compound **53** and **48n** following the general procedure A.  $^1\text{H}$  NMR (400 MHz,  $\text{CDCl}_3$ )  $\delta_{\text{H}}$  1.47–1.57 (m, 2H), 1.58–1.66 (m, 2H), 2.12–2.27 (m, 6H), 3.21 (q, 2H,  $J = 6.68$  Hz), 3.58 (t, 2H,  $J = 7.21$  Hz), 4.82 (t, 1H,  $J = 5.62$  Hz), 6.27 (s, 1H), 6.79–6.89 (m, 4H), 6.89–6.98 (m, 5H), 6.98–7.02 (m, 1H), 7.04 (d, 1H,  $J = 8.07$  Hz).  $^{13}\text{C}$  NMR (100 MHz,  $\text{CDCl}_3$ )  $\delta_{\text{C}}$  19.14, 19.84, 24.74, 27.75, 40.02, 52.46, 115.83, 116.05, 119.98, 122.23, 122.31, 123.96, 130.44, 133.18, 135.72, 137.84, 144.49, 144.52, 156.25, 156.72, 159.11. HRMS-ESI: ( $m/z$ ) calculated for  $\text{C}_{25}\text{H}_{27}\text{F}_2\text{N}_3\text{O}$ , 424.2200  $[\text{M}+\text{H}]^+$ ; found 424.2189. Purity: >99%.

#### 1-(4-(bis(4-fluorophenyl)amino)butyl)-3-(4-bromo-2-iodophenyl)urea (9e).

Compound **9e** was prepared in 51% yield from compounds **53** and **48q** following the general procedure A.  $^1\text{H}$  NMR (400 MHz,  $\text{DMSO}-d_6$ )  $\delta_{\text{H}}$  1.43–1.53 (m, 2H), 1.53–1.62 (m, 2H), 3.09 (q, 2H,  $J = 6.32$  Hz), 3.64 (t, 2H,  $J = 7.21$  Hz), 6.90–7.02 (m, 4H), 7.02–7.18 (m, 5H), 7.47 (dd, 1H,  $J = 8.93, 2.32$  Hz), 7.80, (d, 1H,  $J = 8.93$  Hz), 7.94 (d, 1H,  $J = 2.32$  Hz).  $^{13}\text{C}$  NMR (100 MHz,  $\text{DMSO}-d_6$ )  $\delta_{\text{C}}$  24.81, 27.45, 52.16, 114.62, 116.28, 116.51, 122.60, 122.68, 123.46, 131.62, 140.47, 140.76, 144.81, 144.83, 155.18, 156.38, 158.74. HRMS-ESI: ( $m/z$ ) calculated for  $\text{C}_{23}\text{H}_{21}\text{BrF}_2\text{IN}_3\text{O}$ , 599.9959  $[\text{M}+\text{H}]^+$ ; found 599.9942. Purity: 99.07%.

#### 1-(4-chloro-3-(trifluoromethyl)phenyl)-3-(5-(4-fluorophenyl)pentyl)urea (10).

Compound **10** was prepared in 58% yield from compounds **56** and **48j** following the general procedure A.  $^1\text{H}$  NMR (400 MHz,  $\text{CDCl}_3$ )  $\delta_{\text{H}}$  1.24–1.30 (m, 2H), 1.45 (quin, 2H,  $J = 7.46$  Hz), 1.53 (quin, 2H,  $J = 7.64$  Hz), 2.50 (t, 2H,  $J = 7.64$  Hz), 3.07–3.22 (m, 2H), 5.56 (t, 1H,  $J = 5.01$  Hz), 6.79–6.98 (m, 2H), 7.04 (dd, 2H,  $J = 8.38, 5.56$  Hz), 7.20–7.31 (m, 1H), 7.31–7.38 (m, 1H), 7.59 (d, 1H,  $J = 2.45$  Hz), 7.70 (s, 1H).  $^{13}\text{C}$  NMR (100 MHz,  $\text{CDCl}_3$ )  $\delta_{\text{C}}$  26.35, 29.85, 31.11, 34.88, 40.28, 114.89, 115.10, 118.37, 118.43, 123.34, 125.46, 129.54, 129.61, 131.87, 137.75, 137.79, 137.81, 155.90, 159.99, 162.42. HRMS-ESI: ( $m/z$ ) calculated for  $\text{C}_{19}\text{H}_{19}\text{ClF}_4\text{N}_2\text{O}$ , 403.1200  $[\text{M}+\text{H}]^+$ ; found 403.1203. Purity: 99.35%.

#### 1-(4,4-bis(4-fluorophenyl)butyl)-3-(4-chloro-3-(trifluoromethyl)phenyl)urea (11a).

Compound **11a** was prepared in 83% yield from compounds **29g** and **48j** following the general procedure A.  $^1\text{H}$  NMR (400 MHz,  $\text{CDCl}_3$ )  $\delta_{\text{H}}$  1.34 (dt, 2H,  $J = 14.92, 7.46$  Hz), 1.82–1.96 (m, 2H), 3.14 (q, 2H,  $J = 6.85$  Hz), 3.74 (t, 1H,  $J = 7.70$  Hz), 5.52 (t, 1H,  $J = 5.38$  Hz), 6.90 (t, 4H,  $J = 8.56$  Hz), 7.05 (dd, 4H,  $J = 8.56, 5.38$  Hz), 7.23 (d, 1H,  $J = 8.80$  Hz), 7.29 (dd, 1H,  $J = 8.68, 2.32$  Hz), 7.55 (d, 1H,  $J = 2.20$  Hz), 7.66 (s, 1H).  $^{13}\text{C}$  NMR (100 MHz,  $\text{CDCl}_3$ )  $\delta_{\text{C}}$  28.44, 33.00, 40.11, 49.40, 115.26, 115.47, 118.30, 118.35, 123.29, 125.52, 128.77, 128.90, 128.98, 131.90, 137.70, 140.03, 155.83, 160.17, 162.61. HRMS-

ESI: ( $m/z$ ) calculated for  $C_{24}H_{20}ClF_5N_2O$ , 483.1262  $[M+H]^+$ ; found 483.1294. HRMS-ESI: ( $m/z$ ) calculated for  $C_{24}H_{20}ClF_5N_2O$ , 483.1262  $[M+H]^+$ ; found 483.1294. Purity: >99%.

### 1-(6,6-bis(4-fluorophenyl)hexyl)-3-(4-chloro-3-(trifluoromethyl)phenyl)urea (11b).

Compound **11b** was prepared in 42.86% yield from compounds **29h** and **48j** following the general procedure A.  $^1H$  NMR (400 MHz,  $CDCl_3$ )  $\delta_H$  1.20–1.29 (m, 2H), 1.29–1.41 (m, 2H) 1.48 (quin, 2H,  $J = 7.24$  Hz), 1.96 (q, 2H,  $J = 7.74$  Hz), 3.20 (q, 2H,  $J = 6.85$  Hz), 3.83 (t, 1H,  $J = 7.83$  Hz), 4.67 (t, 1H,  $J = 5.50$  Hz), 6.49 (s, 1H), 6.96 (t, 4H,  $J = 8.62$  Hz), 7.13 (dd, 4H,  $J = 8.44, 5.50$  Hz), 7.33–7.42 (m, 1H), 7.51 (dd, 1H,  $J = 8.74, 2.26$  Hz), 7.63 (d, 1H,  $J = 2.32$  Hz).  $^{13}C$  NMR (100 MHz,  $CDCl_3$ )  $\delta_C$  26.79, 27.62, 29.92, 35.79, 40.41, 49.70, 115.16, 115.36, 118.36, 118.42, 123.41, 125.62, 128.99, 129.07, 131.97, 137.69, 140.52, 140.55, 155.08, 160.11, 162.54. HRMS-ESI: ( $m/z$ ) calculated for  $C_{26}H_{24}ClF_5N_2O$ , 511.1575  $[M+H]^+$ ; found 511.1566. Purity: 96.81%.

### 1-(5,5-bis(4-fluorophenyl)pentyl)-3-(4-chloro-3-(trifluoromethyl)phenyl)thiourea (12).

Compound **12** was prepared in 51% yield from compounds **29a** and **57** following the general procedure A.  $^1H$  NMR (400 MHz,  $CDCl_3$ )  $\delta_H$  1.20–1.32 (m, 2H), 1.64 (quin, 2H,  $J = 7.52$  Hz), 1.95–2.08 (m, 2H), 3.59 (d, 2H,  $J = 5.38$  Hz), 3.86 (t, 1H,  $J = 7.83$  Hz), 5.86 (br. s., 1H), 6.87–7.02 (m, 4H), 7.07–7.21 (m, 4H), 7.30 (d, 1H,  $J = 7.34$  Hz), 7.47–7.56 (m, 2H), 7.74 (br. s., 1H).  $^{13}C$  NMR (100 MHz,  $CDCl_3$ )  $\delta_C$  25.16, 28.64, 35.35, 45.25, 49.57, 115.24, 115.45, 123.88, 123.93, 129.02, 129.10, 133.10, 140.25, 140.30, 160.16, 162.59, 180.62. HRMS-ESI: ( $m/z$ ) calculated for  $C_{25}H_{22}ClF_5N_2S$ , 513.1190  $[M+H]^+$ ; found 513.1199. Purity: >99%.

### 5,5-bis(4-fluorophenyl)pentyl (4-chloro-3-(trifluoromethyl)phenyl)carbamate (13).

A substituted isocyanate **48j** (0.12 g, 0.54 mmol) was added drop wise to a solution of intermediate **25a** (0.15 g, 0.54 mmol) in chloroform (5 mL), followed by addition of TEA (113  $\mu$ L, 0.81 mmol). The reaction mixture was stirred for 9 hours. Upon completion, organic solvent was removed under reduced pressure and obtained residue was purified using column chromatography with ethyl acetate/ hexanes (1:19 to 1:3) to obtain desired compound **13** (0.11 g, 40%) as colorless liquid.  $^1H$  NMR (400 MHz,  $CDCl_3$ )  $\delta_H$  1.26–1.38 (m, 2H), 1.70 (quin, 2H,  $J = 7.15$  Hz), 1.95–2.07 (m, 2H), 3.86 (t, 1H,  $J = 7.83$  Hz), 4.14, (t, 2H,  $J = 6.60$  Hz), 6.62 (s, 1H), 6.88–7.03 (m, 4H), 7.06–7.21 (m, 4H), 7.41 (d, 1H,  $J = 8.80$  Hz), 7.52 (d, 1H,  $J = 8.07$  Hz), 7.71 (d, 1H,  $J = 2.20$  Hz).  $^{13}C$  NMR (100 MHz,  $CDCl_3$ )  $\delta_C$  24.20, 28.69, 35.45, 49.69, 65.49, 115.22, 115.43, 129.02, 129.10, 132.05, 136.80, 140.34, 140.38, 153.16, 160.16, 162.59. HRMS-ESI: ( $m/z$ ) calculated for  $C_{25}H_{21}ClF_5NO_2$ , 498.1259  $[M+H]^+$ ; found 498.1247. Purity: 97.51%.

### 1-(5,5-bis(4-fluorophenyl)pentyl)-3-(4-chloro-3-(trifluoromethyl)phenyl)-1-methylurea (14).

Compound **14** was prepared in 36% yield from compounds **58** and **48j** following the general procedure A.  $^1H$  NMR (400 MHz,  $CDCl_3$ )  $\delta_H$  1.20–1.30 (m, 2H), 1.60 (quin, 2H,  $J = 7.55$  Hz), 1.94–2.09 (m, 2H), 2.95 (s, 3H), 3.30 (t, 2H,  $J = 7.46$  Hz), 3.84 (t, 1H,  $J = 7.76$  Hz), 6.42 (s, 1H), 6.86–6.99 (m, 4H), 7.07–7.19 (m, 4H), 7.37 (d, 1H,  $J = 8.68$  Hz), 7.54 (dd, 1H,  $J = 8.80, 2.57$  Hz), 7.68 (d, 1H,  $J = 2.57$  Hz).  $^{13}C$  NMR (100 MHz,  $CDCl_3$ )  $\delta_C$  25.17, 27.84,



34.57, 35.59, 48.86, 49.75, 115.19, 115.40, 118.56, 118.62, 123.65, 129.02, 129.10, 131.72, 138.13, 140.36, 140.39, 154.64, 160.14, 162.58. HRMS-ESI: (*m/z*) calculated for C<sub>26</sub>H<sub>24</sub>ClF<sub>5</sub>N<sub>2</sub>O, 511.1575 [M+H]<sup>+</sup>; found 511.1571. Purity: 100 %.

#### **1-(5,5-bis(4-fluorophenyl)pentyl)-3-(4-chloro-3-(trifluoromethyl)phenyl)-1,3-dimethylurea (15).**

Sodium hydride (0.07 g, 1.70 mmol) was added portion wise to a solution of compound **4l** (0.20 g, 0.42 mmol) in dimethylformamide (5 mL) at 0 °C under inert environment and reaction mixture was stirred for 10 min. Methyl iodide (0.20 g, 1.70 mmol) dissolved in dimethylformamide (1 mL) was added to the reaction mixture dropwise and stirring continued for 3 hours at room temperature. Upon reaction completion, dimethylformamide was removed by air flow, formed residue was re-suspended in dichloromethane (50 mL) and filtered. Filtrate was washed with aqueous solution of LiCl (5%) (5 × 50 mL), dried over Na<sub>2</sub>SO<sub>4</sub> and concentrated in vacuum. The obtained residue was purified by column chromatography with ethyl acetate/ hexanes (1:19 to 1:2) to afford **15** (0.12 g, 56%) as colorless semi-solid. <sup>1</sup>H NMR (400 MHz, CDCl<sub>3</sub>) δ<sub>H</sub> 1.17 (quin, 2H, *J* = 7.76 Hz), 1.51 (quin, 2H, *J* = 7.64 Hz), 1.90–2.04 (m, 2H), 2.59 (s, 3H), 3.07–3.22 (m, 5H), 3.83 (t, 1H, *J* = 7.70 Hz), 6.91–7.01 (m, 4H), 7.07 (dd, 1H, *J* = 8.68, 2.57 Hz), 7.10–7.23 (m, 4H), 7.31 (d, 1H, *J* = 2.69 Hz), 7.38 (d, 1H, *J* = 8.56 Hz). <sup>13</sup>C NMR (100 MHz, CDCl<sub>3</sub>) δ<sub>C</sub> 25.23, 27.06, 35.59, 36.14, 38.93, 49.75, 60.40, 115.21, 115.42, 121.17, 121.22, 123.90, 126.25, 126.39, 129.02, 129.11, 132.38, 140.40, 140.44, 145.53, 160.17, 160.87, 162.60. HRMS-ESI: (*m/z*) calculated for C<sub>27</sub>H<sub>26</sub>ClF<sub>5</sub>N<sub>2</sub>O, 525.1732 [M+H]<sup>+</sup>; found 525.1739. Purity: 95.31%.

#### **N-(4-chloro-3-(trifluoromethyl)phenyl)-6,6-bis(4-fluorophenyl)hexanamide (16).**

Carboxylic acid **59** (0.20 g, 0.66 mmol) and aromatic amine **81f** (0.15 g, 0.77 mmol) were dissolved in dimethylformamide (9 ml), followed by addition of DIEA (0.51 g, 3.94 mmol) and BOP (0.87 g, 1.97 mmol). The reaction mixture was stirred overnight at room temperature, diluted with ethyl acetate (40 mL), washed with brine (5 × 25 mL), and dried over MgSO<sub>4</sub>. Organic solvent was removed under reduced pressure and formed residue was purified with column chromatography using ethyl acetate/ hexanes (1:19 to 1:1) to afford compound **16** (0.14 g, 43.08%) as yellow semi solid. <sup>1</sup>H NMR (400 MHz, CDCl<sub>3</sub>) δ<sub>H</sub> 1.27–1.35 (m, 2H), 1.75 (quin, 2H, *J* = 7.61 Hz), 1.96–2.08 (m, 2H), 2.31 (t, 2H, *J* = 7.46 Hz), 3.86 (t, 1H, *J* = 7.83 Hz), 6.87–7.03 (m, 4H), 7.06–7.19 (m, 4H), 7.20–7.26 (m, 1H), 7.42 (d, 1H, *J* = 8.68 Hz), 7.67 (dd, 1H, *J* = 8.68, 2.20 Hz), 7.79 (d, 1H, *J* = 2.32 Hz). <sup>13</sup>C NMR (100 MHz, CDCl<sub>3</sub>) δ<sub>C</sub> 25.16, 27.48, 35.63, 37.38, 49.52, 115.21, 115.42, 118.62, 118.67, 123.65, 129.02, 129.09, 132.00, 136.61, 140.37, 140.40, 160.15, 162.58, 171.21. HRMS-ESI: (*m/z*) calculated for C<sub>25</sub>H<sub>21</sub>ClF<sub>5</sub>NO, 482.1310 [M+H]<sup>+</sup>; found 482.1306. Purity: 96.14%.

#### **N-(5,5-bis(4-fluorophenyl)pentyl)-4-chloro-3-(trifluoromethyl)benzamide (17).**

To a solution of substituted benzoic acid **60** (0.10 g, 0.45 mmol) in dichloromethane (2 mL), oxalyl chloride (77.00 μL, 0.95 mmol) was added drop wise. A catalytic amount of dimethylformamide was added and reaction mixture was stirred at room temperature for an hour. Upon reaction completion, the reaction mixture was concentrated under reduced pressure and formed residue was re-dissolved in dichloromethane (2 mL). Compound **29a**

(0.12 g, 0.45 mmol) was added to the reaction mixture and solution was stirred overnight. Upon completion of the reaction, reaction mixture was washed with water ( $5 \times 10$  mL), and dried over  $\text{MgSO}_4$ . Organic solvent was removed under reduced pressure and formed residue was purified with column chromatography using ethyl acetate/hexanes (1:19 to 1:3) to obtain compound **17** (0.05 g, 22.35%) as white semi solid.  $^1\text{H}$  NMR (400 MHz,  $\text{CDCl}_3$ )  $\delta_{\text{H}}$  1.28–1.37 (m, 2H), 1.66 (quin, 2H,  $J = 7.46$  Hz), 1.99–2.09 (m, 2H), 3.43 (q, 2H,  $J = 6.93$  Hz), 3.86 (t, 1H,  $J = 7.83$  Hz), 6.22 (br. s., 1H), 6.90–7.03 (m, 4H), 7.10–7.23 (m, 4H), 7.58 (d, 1H,  $J = 8.31$  Hz), 7.79 (dd, 1H,  $J = 8.31, 1.96$  Hz), 8.00 (d, 1H,  $J = 1.71$  Hz).  $^{13}\text{C}$  NMR (100 MHz,  $\text{CDCl}_3$ )  $\delta_{\text{C}}$  25.15, 29.25, 35.35, 40.28, 49.61, 115.23, 115.44, 126.10, 126.16, 129.01, 129.09, 131.20, 131.97, 132.96, 135.98, 140.28, 140.32, 160.16, 162.59, 165.91. HRMS-ESI: ( $m/z$ ) calculated for  $\text{C}_{25}\text{H}_{21}\text{ClF}_5\text{NO}$ , 482.1310  $[\text{M}+\text{H}]^+$ ; found 482.1318. Purity: 99.98%.

#### 4-(bis(4-fluorophenyl)methylene)-N-(4-chloro-3-(trifluoromethyl)phenyl) piperidine-1-carboxamide (**18**).

Compound **18** was prepared in 46% yield from compounds **63a** and **48j** following the general procedure A.  $^1\text{H}$  NMR (400 MHz,  $\text{DMSO}-d_6$ )  $\delta$  ppm 2.30 (t, 4H,  $J = 5.50$  Hz), 3.54 (t, 4H,  $J = 5.50$  Hz), 7.10–7.24 (m, 8H) 7.57 (d, 1H,  $J = 1.00$  Hz), 7.79 (d, 1H,  $J = 1.00$  Hz), 8.06 (s, 1H), 8.97 (s, 1H).  $^{13}\text{C}$  NMR (100 MHz,  $\text{CDCl}_3$ )  $\delta_{\text{C}}$  31.19, 45.10, 115.14, 115.35, 118.63, 118.68, 123.71, 131.09, 131.17, 131.81, 133.46, 136.26, 137.50, 137.53, 138.00, 154.12, 160.52, 162.97. HRMS-ESI: ( $m/z$ ) calculated for  $\text{C}_{26}\text{H}_{20}\text{ClF}_5\text{N}_2\text{O}$ , 507.1262  $[\text{M}+\text{H}]^+$ ; found 507.1260. Purity: 97.98%.

#### 4-(bis(4-fluorophenyl)methyl)-N-(4-chloro-3-(trifluoromethyl)phenyl)piperidine-1-carboxamide (**19a**).

Compound **19a** was prepared 17.97% yield from compounds **64a** and **48j** following the general procedure A in.  $^1\text{H}$  NMR (400 MHz,  $\text{CDCl}_3$ )  $\delta_{\text{H}}$  1.15 (q, 2H,  $J = 11.00$  Hz), 1.62 (q, 2H,  $J = 12.00$  Hz), 2.23 (m, 1H,  $J = 9.50$  Hz), 2.86 (t, 2H,  $J = 12.23$  Hz), 3.49 (d, 1H,  $J = 9.80$  Hz), 4.02 (t, 2H,  $J = 12.00$  Hz), 6.50 (d, 1H,  $J = 1.00$  Hz), 6.87–7.10 (m, 4H), 7.11–7.24 (m, 4H), 7.37 (d, 1H,  $J = 7.34$  Hz), 7.52 (s, 1H), 7.64 (s, 1H).  $^{13}\text{C}$  NMR (100 MHz,  $\text{CDCl}_3$ )  $\delta_{\text{C}}$  30.97, 39.96, 44.54, 57.03, 115.52, 115.74, 118.59, 118.64, 123.68, 129.15, 129.23, 131.76, 138.07, 138.57, 138.60, 154.12, 160.29, 162.73. HRMS-ESI: ( $m/z$ ) calculated for  $\text{C}_{26}\text{H}_{22}\text{ClF}_5\text{N}_2\text{O}$ , 509.1419  $[\text{M}+\text{H}]^+$ ; found 509.1418. Purity: 98.87%.

#### 4-(2,2-bis(4-fluorophenyl)ethyl)-N-(4-chloro-3-(trifluoromethyl)phenyl) piperidine-1-carboxamide (**19b**).

Compound **19b** was prepared in 35% yield from compounds **64b** and **48j** following the general procedure A.  $^1\text{H}$  NMR (400 MHz,  $\text{CDCl}_3$ )  $\delta_{\text{H}}$  1.25 (td, 2H,  $J = 12.26, 3.73$  Hz), 1.36 (m, 1H), 1.76 (d, 2H,  $J = 10.76$  Hz), 1.95 (dd, 2H,  $J = 7.58, 6.97$  Hz), 2.68–2.84 (m, 2H), 3.92–4.08 (m, 3H), 6.55 (s, 1H), 6.89–7.06 (m, 4H), 7.09–7.22 (m, 4H), 7.36 (d, 1H,  $J = 8.80$  Hz), 7.53 (dd, 1H,  $J = 8.68, 2.57$  Hz), 7.65 (d, 1H,  $J = 2.57$  Hz).  $^{13}\text{C}$  NMR (100 MHz,  $\text{CDCl}_3$ )  $\delta_{\text{C}}$  32.00, 33.37, 42.63, 44.45, 46.36, 115.36, 115.58, 118.57, 118.63, 123.68, 125.30, 128.31, 128.96, 129.04, 131.73, 138.17, 140.10, 140.14, 154.10, 160.21, 162.64.

HRMS-ESI: ( $m/z$ ) calculated for  $C_{27}H_{24}ClF_5N_2O$ , 523.9518  $[M+H]^+$ ; found 523.1563.  
Purity: 98.86%.

### Biological evaluation. Cell lines and culture condition.

The human breast cancer cells MDA-MB-231 were used for cytotoxicity studies. Cells were cultured at 37 °C, 95% humidity, and 5% (v/v) CO<sub>2</sub> in a Napco series 8000 WJ CO<sub>2</sub> incubator (ThermoScientific). MDA-MB-231 cells were maintained in Dulbecco's Modified Eagle Media (DMEM) supplemented with 10% heat-inactivated FBS and 1% antibiotic-antimycotic. Adherent cells were passaged via the addition of trypsin/0.05% EDTA solution (GIBCO), followed by centrifugation and resuspension in fresh media. All cell lines were routinely tested for the presence of mycoplasma infection.

### Cytotoxicity assay of analogs on MDA-MB-231 cells.

Cytotoxicity of synthesized compounds was determined by MTT (3-(4,5-dimethyl-2-thiazolyl)-2,5-diphenyl-2H-tetrazolium bromide) assay. MDA-MB-231 (8000 cells per well) were seeded into 96-well plates in 100  $\mu$ L of 10% FBS containing DMEM media and incubated for 24 hours. The percentage of cell viability at 20  $\mu$ M concentration of synthesized analogs was assessed initially. The compounds showed more than 50% growth inhibition at 20  $\mu$ M concentration were subjected to IC<sub>50</sub> determination. DMSO stocks synthesized analogs were diluted in culture media (2% FBS containing DMEM) to obtain a series of concentrations (25, 20, 15, 10, 7.5, 5, 2.5, and 0  $\mu$ M). The final concentration of DMSO in the treatment medium was 0.1% for all wells. After 48 hours of treatment, MTT solution was added to each well (0.5 mg/mL) and incubated at 37 °C for 2 hours. The media was removed from each well, and the formed blue formazan crystals were dissolved in 100  $\mu$ L of DMSO. The optical density was determined at the wavelength of 570 nm. For each time point, we have performed triplicate data, and mean cell viability was calculated. IC<sub>50</sub> values ( $\pm$  SEM) were calculated using GraphPad Prism 8 Software.

### Evaluation of microsomal stability in vitro.

Liver microsomal stability of selected compounds was determined by following modified literature procedures<sup>72, 73</sup> and a protocol provided by Waters<sup>74</sup>. Instead of 96-well plates, microcentrifuge tubes were used as reaction pot/vessel. In brief, 0.5 mM stock solutions of the compounds in DMSO were prepared and then diluted to 5  $\mu$ M with dilution buffer. Microsomes (The Pooled Male Rat Liver Microsomes, Sprague-Dawley, Cat. # 452501, Corning®) were rapidly thawed, then diluted with warm potassium-phosphate buffer to prepare a 6.2% microsomal mixture. This mixture was maintained at 37°C (for <30 minutes) while NADPH solution (NADPH Regenerating System - Solution A, Cat. # 451220, Corning® and Solution B, Cat. # 451200, Corning®) in potassium-phosphate buffer was prepared and kept in 4°C. 100  $\mu$ L of NADPH solution was transferred to each microcentrifuge tube arranged in a tray. 50  $\mu$ L of each of the 5  $\mu$ M samples were added to the respective microcentrifuge tube and warmed to 37 °C in a shaker (100 rpm) for approximately 10 minutes. After warming to 37 °C, 100  $\mu$ L of liver microsome solution was added to each tube and incubated at 37 °C on the shaker (100 rpm) for an hour. 20  $\mu$ L samples from each tube were collected at 5, 15, 30, and 60 min time points, and 200  $\mu$ L ice-cold acetonitrile was added to quench the reaction. For the 0 min time point (baseline), 12

$\mu\text{L}$  of the compound-NADPH solution, and 8  $\mu\text{L}$  of liver microsome solution was added to 200  $\mu\text{L}$  ice-cold acetonitrile. Samples were centrifuged for 15 minutes at 4°C, and collected supernatant solutions were analyzed using the LC-MS/MS according to in-house developed LC-MS/MS method. The percent remaining of a compound was calculated relative to the amount of compound found at time point T= 0 using peak area ratios.

### ***In vivo* BBB permeability.**

All animal studies were carried out according to the Texas Tech University Health Sciences Center Institutional Animal Care and Use Committee (IACUC)-approved protocols. Eight weeks old C57 mice, male and female mice weighing ~20 grams, were used for the experiments. Compound **4a** was administered intraperitoneally at a dose 10 mg/kg (vehicle: ethanol 2.5%, DMSO 2.5%, Tween 80 5.0%, PEG 400 25% and PBS 65%). At different time points (0, 0.5, 1, 6, 24, and 48 hours), mice were anesthetized, and blood samples were collected. Brains were collected after performing cardiac perfusion. Plasma and brain were stored at -80 °C until the following LC-MS/MS analysis.

### **LC-MS/MS method development.**

Briefly, an AB SCIEX QTRAP® 5500 tandem mass spectrometer (Framingham, MA), attached to the UHPLC system and electrospray ionization (ESI) interface, maintained in positive ionization mode, was used. All chemicals and solvents (liquid chromatography-mass spectrometry grade) were obtained from Fisher Scientific. The analytes were quantified by multiple-reaction monitoring (MRM) method with the transitions of the parent ions to the product ions of m/z 524.1→149.1 for penfluridol, 455.0→165.3 for verapamil, 429.1→180.3 for **4a**, 497.2→180.3 for **4i**, 508.0→412.1 for **4q** and m/z 395.1→213.0 for rotenone (internal standard) respectively. Standard calibration curves were constructed by analyzing a series of the blank matrix of corresponding organs from untreated mice spiked with a known amount of tested compounds and internal standard.

The organs and plasma samples collected in animal studies were stored at -80°C prior to protein precipitation and LC-MS/MS analysis. The samples were homogenized in phosphate buffer saline (1:3, w/v). The standards and study samples (30  $\mu\text{l}$ ) were extracted using 200  $\mu\text{l}$  acetonitrile containing a mixture of 100 ng/ml of the internal standard. Upon protein precipitation by centrifugation at 14,000 rpm for 10 min, 150  $\mu\text{l}$  of clear supernatant from the top was subjected to analysis. Compounds were eluted using a Kinetex C18 column (50 × 2.1 mm, 1.3  $\mu\text{m}$ ; Phenomenex) with a mobile phase consisting of 0.1% formic acid in water-acetonitrile (gradient flow, 5 min) at a flow rate of 0.5 ml/min. The concentration of test compounds in each unknown sample was determined using the linear calibration curve equation for each corresponding drug/internal standard ratio. The peaks of analytes were integrated and quantified using Analyst 1.6.2 software (AB Sciex).

### **Immunoblot analysis.**

The immunoblot analysis was performed according to reported literature.<sup>75</sup> The cells were treated for 48 hours and then lysed on ice in RIPA buffer (10 mmol/L Tris-HCl, 1 mmol/L EDTA, 0.5 mmol/L EGTA, 1% Triton X-100, 0.1% sodium deoxycholate, 0.1% SDS and 140 mmol/L NaCl), supplemented with protease and phosphatase inhibitors (Halt Protease

and Phosphatase Inhibitor Cocktail; Thermo Scientific). Cell lysates were centrifuged at 13,000 rpm for 10 min at 4 °C, and each supernatant was mixed with the appropriate volume of 5x SDS loading buffer, heated to 95–100 °C for 5 min and briefly centrifuged. Equal amounts of proteins were subjected to SDS-PAGE and transferred onto an Immobilon P, polyvinylidene difluoride membrane (Millipore, Billerica, MA). The membranes were then incubated with the appropriate primary antibodies: The membranes were then incubated with the appropriate primary antibodies: pFGFR1 (Cat# 3471; 1:1000), Cleaved Caspase-3 (Cat# 9664; 1:1000), Caspase-3 (Cat# 9668; 1:1000) and  $\beta$ -tubulin (1:2000) (all from Cell Signaling Technology, Beverly, MA). As a secondary antibody, goat anti-rabbit was used (1:50000). The antigens were visualized using the Immobilon Western Chemiluminescent HRP substrate (Millipore), according to the manufacturer's instructions. The protein levels that corresponded to immunoreactive bands were quantified using the Image PC image analysis software (Scion Corp., Frederick, MD) and ImageJ image analysis software (National Institutes of Health).

### Docking study.

The docking study was performed with SeeSAR version 10.0; BioSolveIT GmbH, Sankt Augustin, Germany, 2020, [www.biosolveit.de/SeeSAR](http://www.biosolveit.de/SeeSAR), using the FGFR1 protein structure from the RCSB protein data bank (PDB code: 4V05).

### Supplementary Material

Refer to Web version on PubMed Central for supplementary material.

### ACKNOWLEDGMENTS

K<sub>i</sub> determinations and receptor binding profiles were generously provided by the National Institute of Mental Health's Psychoactive Drug Screening Program, Contract # HHSN-271-2013-00017-C (NIMH PDSP). The NIMH PDSP is Directed by Bryan L. Roth MD, Ph.D. at the University of North Carolina at Chapel Hill and Project Officer Jamie Driscoll at NIMH, Bethesda MD, USA.

This work is supported by the NIH 1R15CA231339-0 to N.G. and C.M., CPRIT RP170003 to T.P. and N.G, NIH R01 CA186662 and R01CA214019 to R.Z., and American Cancer Society (ACS) grant RSG-15-009-01-CDD to W.W.

### ABBREVIATIONS USED

<b>BBB</b>	blood brain barrier
<b>bFGF</b>	basic fibroblast growth factor
<b>Boc</b>	tertbutoxycarbonyl
<b>CALGB</b>	Cancer and Leukemia Group B
<b>CNS</b>	central nervous system
<b>D1-5</b>	dopamine receptor subtypes
<b>DAT</b>	dopamine transporter

<b>DCM</b>	dichloromethane
<b>DMEM</b>	Dulbecco's Modified Eagle Medium
<b>DMSO</b>	dimethyl sulfoxide
<b>DPPH</b>	1,1'-bis(diphenylphosphino)ferrocene
<b>EMEM</b>	Eagle's Minimum Essential Medium
<b>ER</b>	estrogen receptor
<b>EtOH</b>	ethanol
<b>FGFR</b>	fibroblast growth factor receptor
<b>GPCR</b>	G-protein coupled receptor
<b>HER2</b>	human epidermal growth factor receptor 2
<b>H1R</b>	histamine 1 receptor
<b>5HT</b>	serotonin receptors
<b>HYDE</b>	hydrogen bond and dehydration energies
<b>IC<sub>50</sub></b>	half-maximum inhibitory concentration
<b>i.p.</b>	intraperitoneal injection
<b>K<sub>i</sub></b>	inhibition constant
<b>LC</b>	liquid chromatography
<b>LC-MS</b>	liquid chromatography-mass spectrometry
<b>MDA-MB-231</b>	human triple-negative breast cancer cell line
<b>MTT</b>	3-[4,5-dimethylthiazol-2-yl]-2,5-dimethyltetrazolium bromide
<b>NADPH</b>	Nicotinamide adenine dinucleotide phosphate-H
<b>NIMH</b>	National Institute of Mental Health
<b>NMR</b>	nuclear magnetic resonance
<b>PDB</b>	protein data bank
<b>PDSP</b>	Psychoactive Drug Screening Program
<b>PFL</b>	penfluridol
<b>PR</b>	progesterone receptor
<b>rt</b>	room temperature



<b>SAR</b>	structure-activity relationship
<b>SEM</b>	standard error of the mean
<b>THF</b>	tetrahydrofuran
<b>TLC</b>	thin-layer chromatography
<b>TNBC</b>	triple-negative breast cancer
<b>WSG</b>	West German Study Group

## REFERENCES

1. Siegel RL; Miller KD; Jemal A, Cancer statistics, 2020. *CA: A Cancer Journal for Clinicians* 2020, 70 (1), 7–30. [PubMed: 31912902]
2. Oualla K; El-Zawahry HM; Arun B; Reuben JM; Woodward WA; Gamal El-Din H; Lim B; Mellas N; Ueno NT; Fouad TM, Novel therapeutic strategies in the treatment of triple-negative breast cancer. *Therapeutic Advances in Medical Oncology* 2017, 9 (7), 493–511. [PubMed: 28717401]
3. Lehmann BD; Bauer JA; Chen X; Sanders ME; Chakravarthy AB; Shyr Y; Pietenpol JA, Identification of human triple-negative breast cancer subtypes and preclinical models for selection of targeted therapies. *Journal of Clinical Investigation* 2011, 121 (7), 2750–2767.
4. Dent R; Trudeau M; Pritchard KI; Hanna WM; Kahn HK; Sawka CA; Lickley LA; Rawlinson E; Sun P; Narod SA, Triple-Negative Breast Cancer: Clinical Features and Patterns of Recurrence. *Clinical Cancer Research* 2007, 13 (15), 4429–4434. [PubMed: 17671126]
5. Freedman GM; Anderson PR; Li T; Nicolaou N, Locoregional recurrence of triple-negative breast cancer after breast-conserving surgery and radiation. *Cancer* 2009, 115 (5), 946–951. [PubMed: 19156929]
6. Voduc KD; Cheang MCU; Tyldesley S; Gelmon K; Nielsen TO; Kennecke H, Breast Cancer Subtypes and the Risk of Local and Regional Relapse. *Journal of Clinical Oncology* 2010, 28 (10), 1684–1691. [PubMed: 20194857]
7. Kennecke H; Yerushalmi R; Woods R; Cheang MCU; Voduc D; Speers CH; Nielsen TO; Gelmon K, Metastatic Behavior of Breast Cancer Subtypes. *Journal of Clinical Oncology* 2010, 28 (20), 3271–3277. [PubMed: 20498394]
8. Liedtke C; Mazouni C; Hess KR; Andre F; Tordai A; Mejia JA; Symmans WF; Gonzalez-Angulo AM; Hennessy B; Green M; Cristofanilli M; Hortobagyi GN; Pusztai L, Response to neoadjuvant therapy and long-term survival in patients with triple-negative breast cancer. *J Clin Oncol* 2008, 26 (8), 1275–81. [PubMed: 18250347]
9. Gluz O; Nitz UA; Harbeck N; Ting E; Kates R; Herr A; Lindemann W; Jackisch C; Berdel WE; Kirchner H; Metzner B; Werner F; Schutt G; Frick M; Poremba C; Diallo-Danebrock R; Mohrmann S; West German Study G, Triple-negative high-risk breast cancer derives particular benefit from dose intensification of adjuvant chemotherapy: results of WSG AM-01 trial. *Ann Oncol* 2008, 19 (5), 861–70. [PubMed: 18174609]
10. Bendell JC; Domchek SM; Burstein HJ; Harris L; Younger J; Kuter I; Bunnell C; Rue M; Gelman R; Winer E, Central nervous system metastases in women who receive trastuzumab-based therapy for metastatic breast carcinoma. *Cancer* 2003, 97 (12), 2972–7. [PubMed: 12784331]
11. Leone JP; Leone BA, Breast cancer brain metastases: the last frontier. *Experimental Hematology & Oncology* 2015, 4 (1), 33. [PubMed: 26605131]
12. Adkins CE; Mohammad AS; Terrell-Hall TB; Dolan EL; Shah N; Sechrest E; Griffith J; Lockman PR, Characterization of passive permeability at the blood-tumor barrier in five preclinical models of brain metastases of breast cancer. *Clin Exp Metastasis* 2016, 33 (4), 373–83. [PubMed: 26944053]
13. Ranjan A; German N; Mikelis C; Srivenugopal K; Srivastava SK, Penfluridol induces endoplasmic reticulum stress leading to autophagy in pancreatic cancer. *Tumour Biol* 2017, 39 (6).

14. Ranjan A; Srivastava SK, Penfluridol suppresses glioblastoma tumor growth by Akt-mediated inhibition of GII1. *Oncotarget* 2017, 8 (20), 32960–32976. [PubMed: 28380428]
15. Wu L; Liu YY; Li ZX; Zhao Q; Wang X; Yu Y; Wang YY; Wang YQ; Luo F, Anti-tumor effects of penfluridol through dysregulation of cholesterol homeostasis. *Asian Pac J Cancer Prev* 2014, 15 (1), 489–94. [PubMed: 24528079]
16. Hedrick E; Li X; Safe S, Penfluridol Represses Integrin Expression in Breast Cancer through Induction of Reactive Oxygen Species and Downregulation of Sp Transcription Factors. *Mol Cancer Ther* 2017, 16 (1), 205–216. [PubMed: 27811009]
17. Ranjan A; Gupta P; Srivastava SK, Penfluridol: An Antipsychotic Agent Suppresses Metastatic Tumor Growth in Triple-Negative Breast Cancer by Inhibiting Integrin Signaling Axis. *Cancer Res* 2016, 76 (4), 877–90. [PubMed: 26627008]
18. Shaw V; Srivastava S; Srivastava SK, Repurposing antipsychotics of the diphenylbutylpiperidine class for cancer therapy. *Semin Cancer Biol* 2019.
19. Tuan NM; Lee CH, Penfluridol as a Candidate of Drug Repurposing for Anticancer Agent. *Molecules* 2019, 24 (20).
20. Ashraf-Uz-Zaman M; Sajib MS; Cucullo L; Mikelis CM; German NA, Analogs of penfluridol as chemotherapeutic agents with reduced central nervous system activity. *Bioorganic & Medicinal Chemistry Letters* 2018, 28 (23–24), 3652–3657. [PubMed: 30389290]
21. Nair AB; Jacob S, A simple practice guide for dose conversion between animals and human. *J Basic Clin Pharm* 2016, 7 (2), 27–31. [PubMed: 27057123]
22. Wang RI; Larson C; Treul SJ, Study of penfluridol and chlorpromazine in the treatment of chronic schizophrenia. *J Clin Pharmacol* 1982, 22 (5–6), 236–42. [PubMed: 7107969]
23. Chouinard G; Annable L, Penfluridol in the treatment of newly admitted schizophrenic patients in a brief therapy unit. *Am J Psychiatry* 1976, 133 (7), 850–3. [PubMed: 937582]
24. Jackson DM; Anden NE; Engel J; Liljequist S, The effect of long-term penfluridol treatment on the sensitivity of the dopamine receptors in the nucleus accumbens and in the corpus striatum. *Psychopharmacologia* 1975, 45 (2), 151–5. [PubMed: 1240636]
25. Ota KY; Kurland AA; Slotnick VB, Safety evaluation of penfluridol, a new long-acting oral antipsychotic agent. *J Clin Pharmacol* 1974, 14 (4), 202–9. [PubMed: 4595986]
26. Chen G; Xia H; Cai Y; Ma D; Yuan J; Yuan C, Synthesis and SAR study of diphenylbutylpiperidines as cell autophagy inducers. *Bioorg Med Chem Lett* 2011, 21 (1), 234–9. [PubMed: 21126871]
27. Ananda Kumar CS; Benaka Prasad SB; Vinaya K; Chandrappa S; Thimmegowda NR; Kumar YC; Swarup S; Rangappa KS, Synthesis and in vitro antiproliferative activity of novel 1benzhydrylpiperazine derivatives against human cancer cell lines. *Eur J Med Chem* 2009, 44 (3), 1223–9. [PubMed: 18973966]
28. Cramer RD; Jilek RJ; Guessregen S; Clark SJ; Wendt B; Clark RD, “Lead hopping”. Validation of topomer similarity as a superior predictor of similar biological activities. *J Med Chem* 2004, 47 (27), 6777–91. [PubMed: 15615527]
29. Cramer RD; Poss MA; Hermsmeier MA; Caulfield TJ; Kowala MC; Valentine MT, Prospective identification of biologically active structures by topomer shape similarity searching. *J Med Chem* 1999, 42 (19), 3919–33. [PubMed: 10508440]
30. Sun H; Tawa G; Wallqvist A, Classification of scaffold-hopping approaches. *Drug Discov Today* 2012, 17 (7–8), 310–24. [PubMed: 22056715]
31. Mauser H; Guba W, Recent developments in de novo design and scaffold hopping. *Curr Opin Drug Discov Devel* 2008, 11 (3), 365–74.
32. Penfluridol in the treatment of newly admitted schizophrenic patients in a brief therapy unit. *American Journal of Psychiatry* 1976, 133 (7), 850–853.
33. Ota KY; Kurland AA; Slotnick VB, Safety Evaluation of Penfluridol, a New Long-Acting Oral Antipsychotic Agent. *The Journal of Clinical Pharmacology* 1974, 14 (4), 202–209. [PubMed: 4595986]
34. Dale E; Pehrson AL; Jeyarajah T; Li Y; Leiser SC; Smagin G; Olsen CK; Sanchez C, Effects of serotonin in the hippocampus: how SSRIs and multimodal antidepressants might regulate pyramidal cell function. *CNS Spectr* 2016, 21 (2), 143–61. [PubMed: 26346726]

35. Al Shoyaib A; Archie SR; Karamyan VT, Intraperitoneal Route of Drug Administration: Should it Be Used in Experimental Animal Studies? *Pharmaceutical Research* 2019, 37 (1). [PubMed: 30623253]
36. Airoidi L; Marcucci F; Mussini E; Garattini S, Distribution of penfluridol in rats and mice. *Eur J Pharmacol* 1974, 25 (3), 291–5. [PubMed: 4857151]
37. Bouillot Anne Marie J; Dodic N; Gellibert Françoise J; Mirguet O. Thiazole Compounds As Activators Of Soluble Guanylate Cyclase. WO 2010/015652 A2, 2009/08/05, 2010.
38. Wang C; Yang G; Li J; Mele G; Slota R; Broda M; Duan M; Vasapollo G; Zhang X; Zhang F, Novel meso-substituted porphyrins: Synthesis, characterization and photocatalytic activity of their TiO<sub>2</sub>-based composites. *Dyes and Pigments* 2009, 80 (3), 321–328.
39. Chen T-HCPPD Synthetic epigallocatechin gallate (egcg) analogs. 2012.
40. Hassib ST; Hassan GS; El-Zaher AA; Fouad MA; Abd El-Ghafar OA; Taha EA, Synthesis and biological evaluation of new prodrugs of etodolac and tolfenamic acid with reduced ulcerogenic potential. *European Journal of Pharmaceutical Sciences* 2019, 140. [PubMed: 30630089]
41. Carlsen PHJ; Sørbye K; Ulven T; Aasbø K; Klinga M; Romerosa A, Synthesis of Benzylidene-Protected Dihydroxyacetone. *Acta Chemica Scandinavica* 1996, 50, 185–187.
42. Jurayi J. F. e. a. Preparation of trans-1,2-disubstituted cycloalkanes from 1,2-cycloalkanols and related compounds. 12/24/2003, 2003.
43. Dorel R; Grugel CP; Haydl AM, The Buchwald–Hartwig Amination After 25 Years. *Angewandte Chemie International Edition* 2019, 58 (48), 17118–17129. [PubMed: 31166642]
44. Cao J; Lever JR; Kopajtic T; Katz JL; Pham AT; Holmes ML; Justice JB; Newman AH, Novel azido and isothiocyanato analogues of [3-(4-phenylalkylpiperazin-1-yl)propyl]bis(4-fluorophenyl)amines as potential irreversible ligands for the dopamine transporter. *J Med Chem* 2004, 47 (25), 6128–36. [PubMed: 15566284]
45. Xiang J; Wan ZK; Li HQ; Ipek M; Binnun E; Nunez J; Chen L; McKew JC; Mansour TS; Xu X; Suri V; Tam M; Xing Y; Li X; Hahm S; Tobin J; Saiah E, Piperazine sulfonamides as potent, selective, and orally available 11beta-hydroxysteroid dehydrogenase type 1 inhibitors with efficacy in the rat cortisone-induced hyperinsulinemia model. *J Med Chem* 2008, 51 (14), 4068–71. [PubMed: 18578516]
46. Appel R, Tertiary Phosphane/Tetrachloromethane, a Versatile Reagent for Chlorination, Dehydration, and P?N Linkage. *Angewandte Chemie International Edition in English* 1975, 14 (12), 801–811.
47. Davis M; Deady LW; Paproth TG, The Nitration of alkylbenzenes: A lecture demonstration. *Journal of Chemical Education* 1978, 55 (1).
48. Esteves PM; de M. Carneiro JW; Cardoso SP; Barbosa AGH; Laali KK; Rasul G; Prakash GKS; Olah GA, Unified Mechanistic Concept of Electrophilic Aromatic Nitration: Convergence of Computational Results and Experimental Data. *Journal of the American Chemical Society* 2003, 125 (16), 4836–4849. [PubMed: 12696903]
49. Benati L; Bencivenni G; Leardini R; Minozzi M; Nanni D; Scialpi R; Spagnolo P; Zanardi G, Radical reduction of aromatic azides to amines with triethylsilane. *J Org Chem* 2006, 71 (15), 5822–5. [PubMed: 16839176]
50. Saito Y; Matsumoto K; Bag SS; Ogasawara S; Fujimoto K; Hanawa K; Saito I, C8-alkynyl- and alkylamino substituted 2'-deoxyguanosines: a universal linker for nucleic acids modification. *Tetrahedron* 2008, 64 (16), 3578–3588.
51. Liu D; Tian Z; Yan Z; Wu L; Ma Y; Wang Q; Liu W; Zhou H; Yang C, Design, synthesis and evaluation of 1,2-benzisothiazol-3-one derivatives as potent caspase-3 inhibitors. *Bioorg Med Chem* 2013, 21 (11), 2960–7. [PubMed: 23632366]
52. Chen J-N; Wang X-F; Li T; Wu D-W; Fu X-B; Zhang G-J; Shen X-C; Wang H-S, Design, synthesis, and biological evaluation of novel quinazolinyl-diaryl urea derivatives as potential anticancer agents. *European Journal of Medicinal Chemistry* 2016, 107, 12–25. [PubMed: 26560049]
53. Yadagiri B; Holagunda UD; Bantu R; Nagarapu L; Guguloth V; Polepally S; Jain N, Rational design, synthesis and anti-proliferative evaluation of novel benzosuberone tethered with hydrazide-hydrazones. *Bioorg Med Chem Lett* 2014, 24 (21), 5041–4. [PubMed: 25264072]

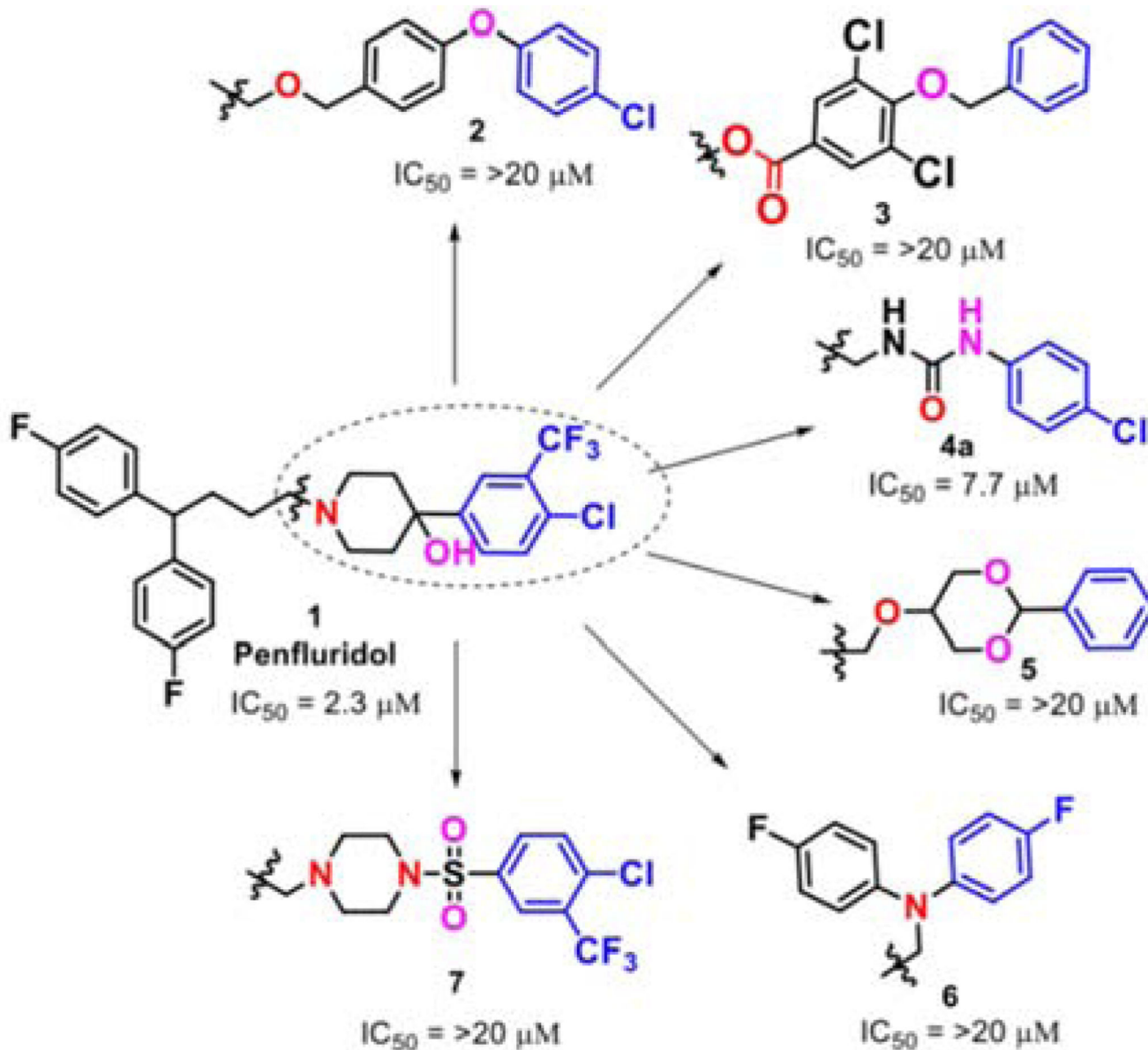
54. Brough PA; Baker L; Bedford S; Brown K; Chavda S; Chell V; D'Alessandro J; Davies NG; Davis B; Le Strat L; Macias AT; Maddox D; Mahon PC; Massey AJ; Matassova N; McKenna S; Meissner JW; Moore JD; Murray JB; Northfield CJ; Parry C; Parsons R; Roughley SD; Shaw T; Simmonite H; Stokes S; Surgenor A; Stefaniak E; Robertson A; Wang Y; Webb P; Whitehead N; Wood M, Application of Off-Rate Screening in the Identification of Novel Pan-Isoform Inhibitors of Pyruvate Dehydrogenase Kinase. *J Med Chem* 2017, 60 (6), 2271–2286. [PubMed: 28199108]
55. Chayah M; Camacho ME; Carrión MD; Gallo MA; Romero M; Duarte J, N,N'-Disubstituted thiourea and urea derivatives: design, synthesis, docking studies and biological evaluation against nitric oxide synthase. *MedChemComm* 2016, 7 (4), 667–678.
56. Ponzano S; Berteotti A; Petracca R; Vitale R; Mengatto L; Bandiera T; Cavalli A; Piomelli D; Bertozzi F; Bottegoni G, Synthesis, biological evaluation, and 3D QSAR study of 2-methyl-4-oxo-3-oxetanylcarbamic acid esters as N-acylethanolamine acid amidase (NAAA) inhibitors. *J Med Chem* 2014, 57 (23), 10101–11. [PubMed: 25380517]
57. Sumita A; Kurouchi H; Otani Y; Ohwada T, Acid-Promoted Chemoselective Introduction of Amide Functionality onto Aromatic Compounds Mediated by an Isocyanate Cation Generated from Carbamate. *Chemistry - An Asian Journal* 2014, 9 (10), 2995–3004.
58. Manickam M; Jalani HB; Pillaiyar T; Boggu PR; Sharma N; Venkateswararao E; Lee YJ; Jeon ES; Son MJ; Woo SH; Jung SH, Design and synthesis of sulfonamidophenylethylureas as novel cardiac myosin activator. *Eur J Med Chem* 2018, 143, 1869–1887. [PubMed: 29224951]
59. De Luca L; Giacomelli G; Masala S; Porcheddu A, Trichloroisocyanuric/TEMPO Oxidation of Alcohols under Mild Conditions: A Close Investigation. *The Journal of Organic Chemistry* 2003, 68 (12), 4999–5001. [PubMed: 12790622]
60. Winterton SE; Capota E; Wang X; Chen H; Mallipeddi PL; Williams NS; Posner BA; Nijhawan D; Ready JM, Discovery of Cytochrome P450 4F11 Activated Inhibitors of Stearoyl Coenzyme A Desaturase. *Journal of Medicinal Chemistry* 2018, 61 (12), 5199–5221. [PubMed: 29869888]
61. Walsh DA; Franzysen SK; Yanni JM, Synthesis and antiallergy activity of 4-(diarylhydroxymethyl)-1-[3-(aryloxy)propyl]piperidines and structurally related compounds. *Journal of Medicinal Chemistry* 1989, 32 (1), 105–118. [PubMed: 2562852]
62. Sander K; Galante E; Gendron T; Yiannaki E; Patel N; Kalber TL; Badar A; Robson M; Johnson SP; Bauer F; Mairinger S; Stanek J; Wanek T; Kuntner C; Kottke T; Weizel L; Dickens D; Erlandsson K; Hutton BF; Lythgoe MF; Stark H; Langer O; Koepf M; Årstad E, Development of Fluorine-18 Labeled Metabolically Activated Tracers for Imaging of Drug Efflux Transporters with Positron Emission Tomography. *Journal of Medicinal Chemistry* 2015, 58 (15), 6058–6080. [PubMed: 26161456]
63. Ghosh AK; Brindisi M, Urea Derivatives in Modern Drug Discovery and Medicinal Chemistry. *J Med Chem* 2020, 63 (6), 2751–2788. [PubMed: 31789518]
64. Perez-Garcia J; Muñoz-Couselo E; Soberino J; Racca F; Cortes J, Targeting FGFR pathway in breast cancer. *The Breast* 2018, 37, 126–133. [PubMed: 29156384]
65. Lehmann BD; Pietenpol JA, Identification and use of biomarkers in treatment strategies for triple-negative breast cancer subtypes. *The Journal of Pathology* 2014, 232 (2), 142–150. [PubMed: 24114677]
66. Lee HJ; Seo AN; Park SY; Kim JY; Park JY; Yu JH; Ahn J-H; Gong G, Low Prognostic Implication of Fibroblast Growth Factor Family Activation in Triple-negative Breast Cancer Subsets. *Annals of Surgical Oncology* 2014, 21 (5), 1561–1568. [PubMed: 24385208]
67. Sharpe R; Pearson A; Herrera-Abreu MT; Johnson D; Mackay A; Welti JC; Natrajan R; Reynolds AR; Reis-Filho JS; Ashworth A; Turner NC, FGFR Signaling Promotes the Growth of Triple-Negative and Basal-Like Breast Cancer Cell Lines Both In Vitro and In Vivo. *Clinical Cancer Research* 2011, 17 (16), 5275–5286. [PubMed: 21712446]
68. De Luca A; Frezzetti D; Gallo M; Normanno N, FGFR-targeted therapeutics for the treatment of breast cancer. *Expert Opinion on Investigational Drugs* 2017, 26 (3), 303–311. [PubMed: 28121208]
69. Tucker Julie A.; Klein T; Breed J; Breeze Alexander L.; Overman R; Phillips C; Norman Richard A., Structural Insights into FGFR Kinase Isoform Selectivity: Diverse Binding Modes of AZD4547 and Ponatinib in Complex with FGFR1 and FGFR4. *Structure* 2014, 22 (12), 1764–1774. [PubMed: 25465127]

70. Wang H; Huwaimel B; Verma K; Miller J; Germain TM; Kinarivala N; Pappas D; Brookes PS; Trippier PC, Synthesis and Antineoplastic Evaluation of Mitochondrial Complex II (Succinate Dehydrogenase) Inhibitors Derived from Atpenin A5. *ChemMedChem* 2017, 12 (13), 1033–1044. [PubMed: 28523727]
71. Slack RD; Ku TC; Cao J; Giancola JB; Bonifazi A; Loland CJ; Gadiano A; Lam J; Rais R; Slusher BS; Coggiano M; Tanda G; Newman AH, Structure-Activity Relationships for a Series of (Bis(4-fluorophenyl)methyl)sulfinyl Alkyl Alicyclic Amines at the Dopamine Transporter: Functionalizing the Terminal Nitrogen Affects Affinity, Selectivity, and Metabolic Stability. *J Med Chem* 2020, 63 (5), 2343–2357. [PubMed: 31661268]
72. Di L; Kerns EH; Hong Y; Kleintop TA; McConnell OJ; Hury DM, Optimization of a higher throughput microsomal stability screening assay for profiling drug discovery candidates. *J Biomol Screen* 2003, 8 (4), 453–62. [PubMed: 14567798]
73. Bera R; Kundu A; Sen T; Adhikari D; Karmakar S, In Vitro Metabolic Stability and Permeability of Gymnemagenin and Its In Vivo Pharmacokinetic Correlation in Rats - A Pilot Study. *Planta Med* 2016, 82 (6), 544–50. [PubMed: 26916641]
74. Alden D. S. a. P. Determination of Microsomal Stability by UPLC/MS/MS. [https://www.waters.com/waters/library.htm?locale=en\\_us&lid=10070741](https://www.waters.com/waters/library.htm?locale=en_us&lid=10070741) (accessed March 27).
75. Zahra FT; Sajib MS; Ichiyama Y; Akwii RG; Tullar PE; Cobos C; Minchew SA; Doçi CL; Zheng Y; Kubota Y; Gutkind JS; Mikelis CM, Endothelial RhoA GTPase is essential for in vitro endothelial functions but dispensable for physiological in vivo angiogenesis. *Scientific Reports* 2019, 9 (1).

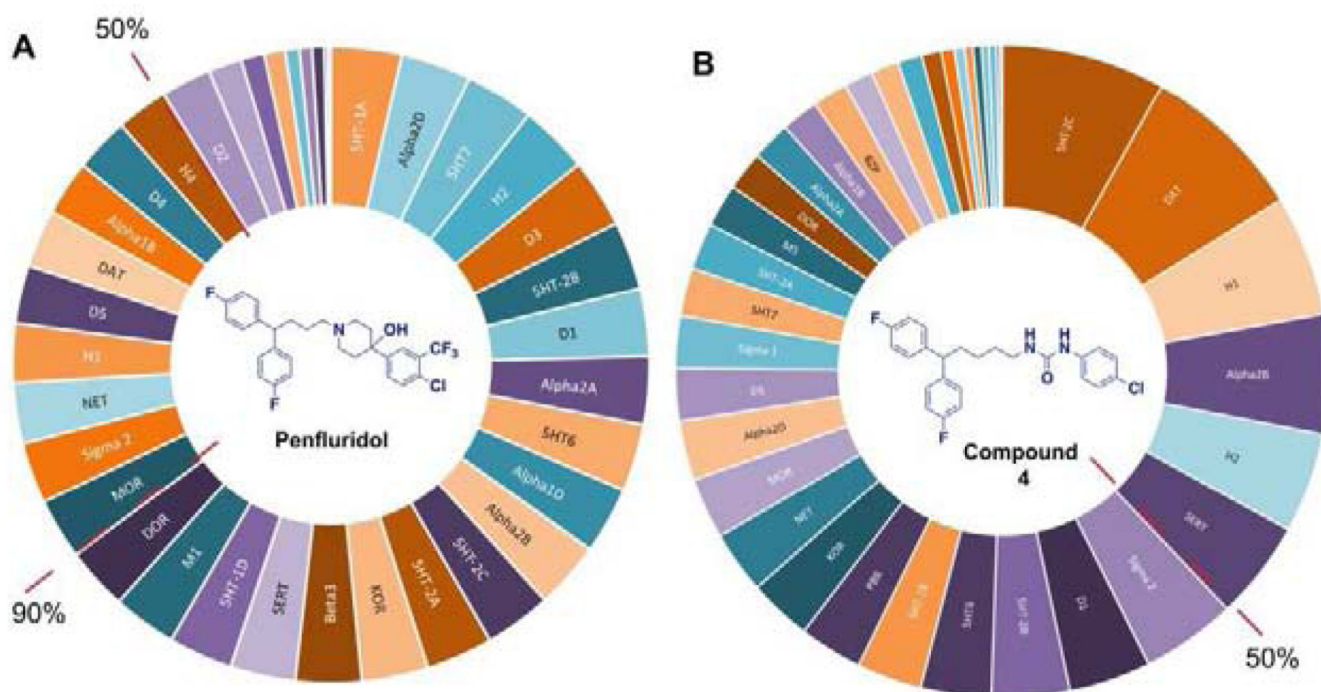
**HIGHLIGHTS**

- TNBC is a highly metastatic type of breast cancer with poor prognosis
- We have identified novel urea-based compounds with the activity against TNBC and ability to cross the BBB in vivo
- We identified potential off-target activity at DAT and structural requirements associated with this activity
- Our compounds induce apoptosis and modulate FGFR1 expression in MDA-MB-231 triple-negative breast cancer cell lines

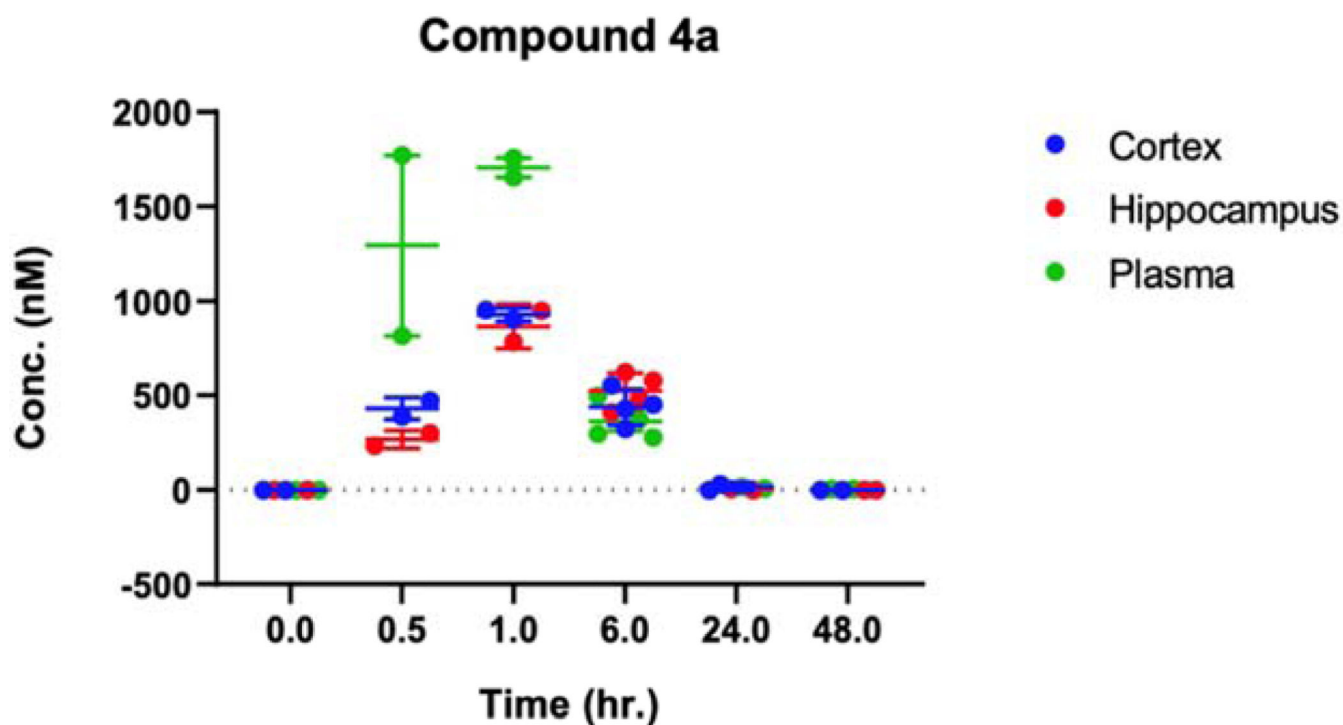




**Figure 1.** Search for a new hit molecule using scaffold hopping approach.  $IC_{50}$  indicates compound concentration required to inhibit viability of the MDA-MB-231 triple-negative breast cancer cells by 50%. Data are expressed as the mean of three independent experiments, each performed in sextet.

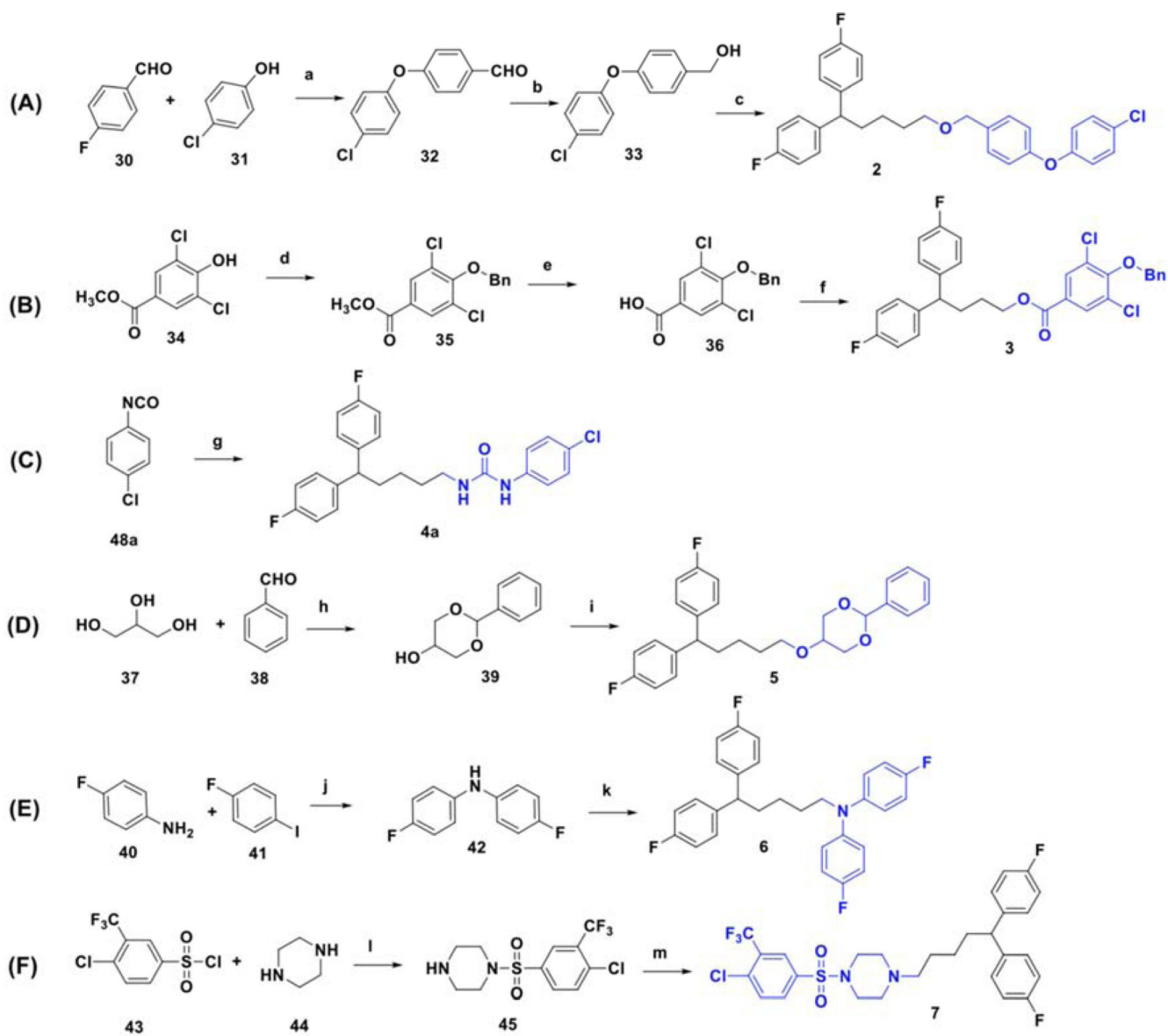


**Figure 2.** Inhibitory activity of penfluridol (**A**) and compound **4a** (**B**) at selected CNS receptors. Primary binding assay was performed at 10  $\mu$ M concentration and data are expressed as the mean  $\pm$  SEM of four independent experiments. The red dotted line identifies groups of the receptors being inhibited by >90% and by >50% in the presence of these compounds.



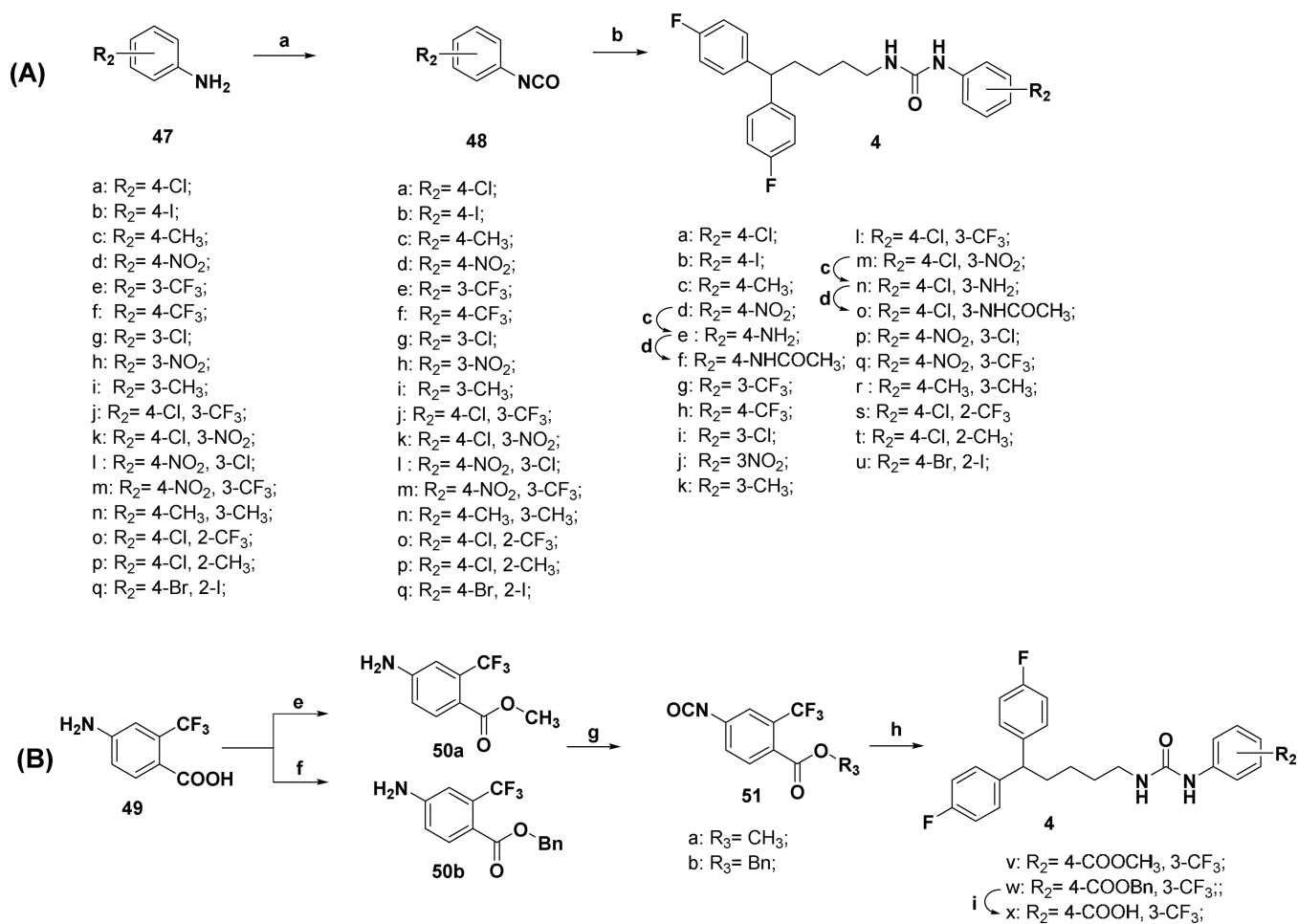
**Figure 3.**

Distribution of **4a** in plasma and brain. Concentration (nM) of compound **4a** in plasma and brain at 0, 0.5, 1, 6, 24, and 48 hours after single i.p. administration (10 mg/kg) was measured by liquid chromatography-tandem mass spectrometry. Data are expressed as the mean  $\pm$  SEM of 2–4 independent experiments.

**Scheme 1.**

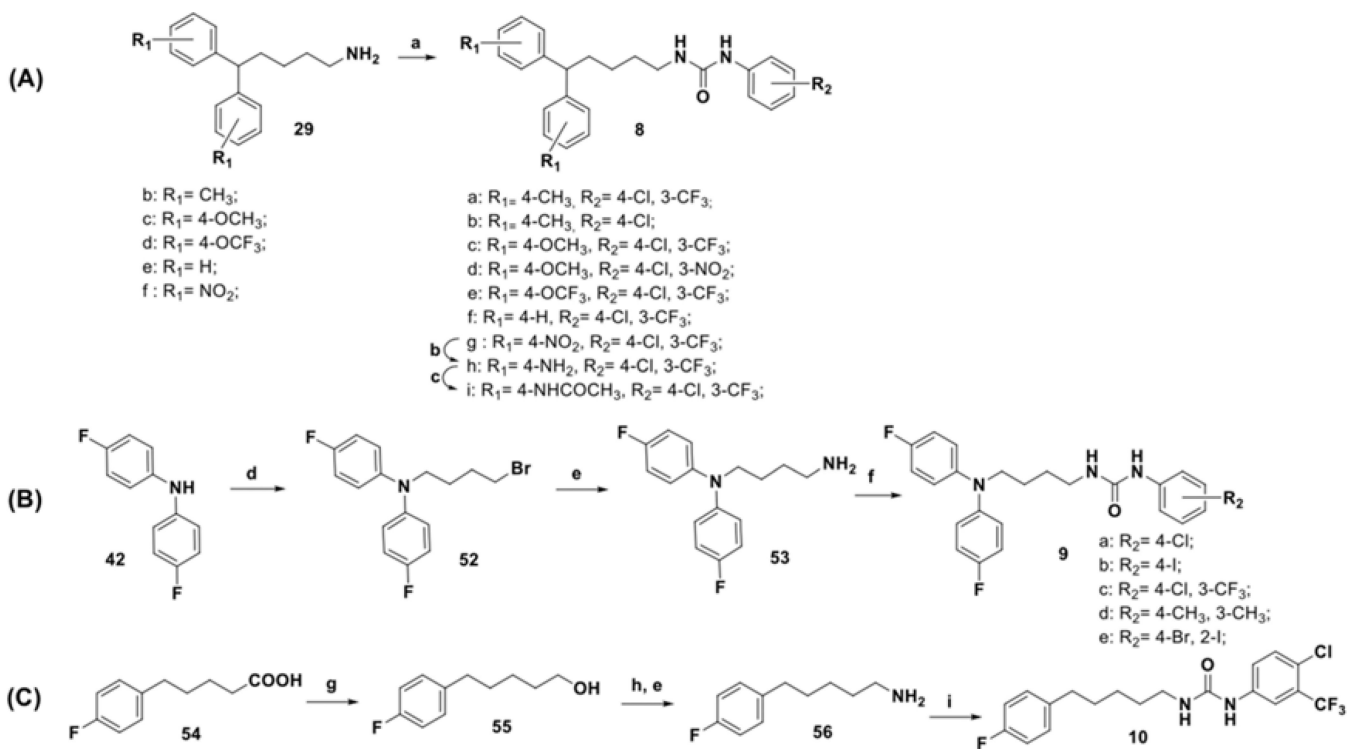
Synthesis of compounds selected for a scaffold-hopping study. Reagents and conditions: (a)  $\text{Cs}_2\text{CO}_3$ , DMF, 85 °C; (b)  $\text{LiAlH}_4$ , THF, rt; (c) **27a**, NaH, DMF, 80 °C; (d) Benzyl bromide,  $\text{K}_2\text{CO}_3$ , DMF, rt; (e) KOH, ethanol, reflux; (f) **25b**, DCC, DMAP, DCM, rt to 32 °C; (g) **29a**, DCM, 0 °C to 32 °C; (h) conc.  $\text{H}_2\text{SO}_4$ , 85 °C; (i) **27a**, NaH, DMF, rt; (j) dppf (cat.),  $\text{PdCl}_2(\text{dppf}) \cdot \text{CH}_2\text{Cl}_2$ , KOtBu, anhydrous THF, 100 °C; (k) **27a**, NaH, DMF, rt; (l) DIPEA, DCM, rt; (m) **27a**,  $\text{Na}_2\text{CO}_3$ , KI (cat.), acetonitrile, reflux.



**Scheme 3.**

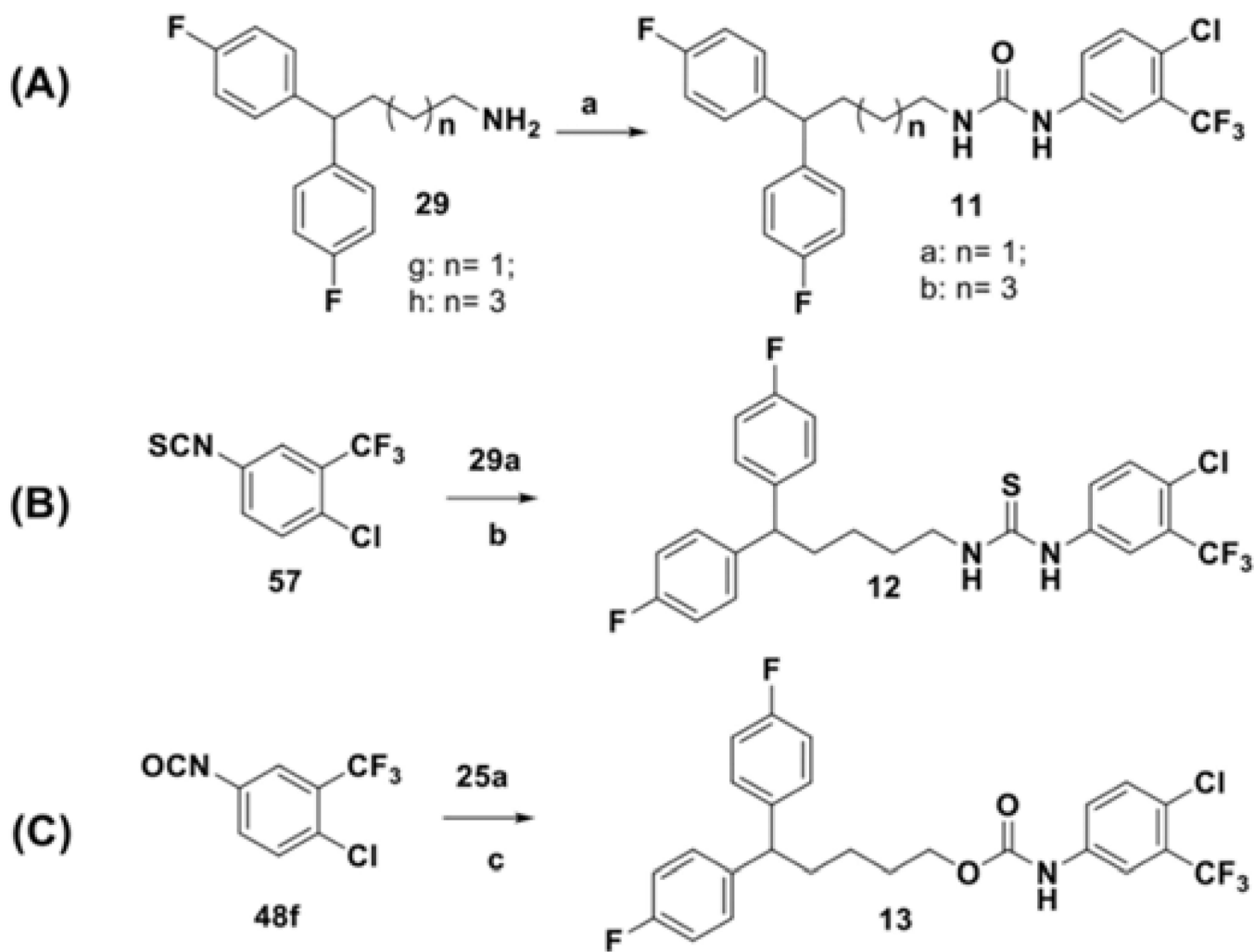
Synthesis of analogues with substitutions at monophenyl “head” moiety. Reagents and conditions: (a) triphosgene, DCM, rt; (b) **29a**, DCM, 0 °C to 32 °C; (c) H<sub>2</sub>N-NH<sub>2</sub>, Raney-nickel, ethanol, 50 °C; (d) acetic anhydride, DCM. (e) SOCl<sub>2</sub>, MeOH, reflux; (f) benzyl bromide, K<sub>2</sub>CO<sub>3</sub>, DMF, 100 °C; (g) triphosgene, DCM, r.t.; (h) **29a**, DCM, 0 °C to 32 °C; (i) Pd/C, NaBH<sub>4</sub>, MeOH.



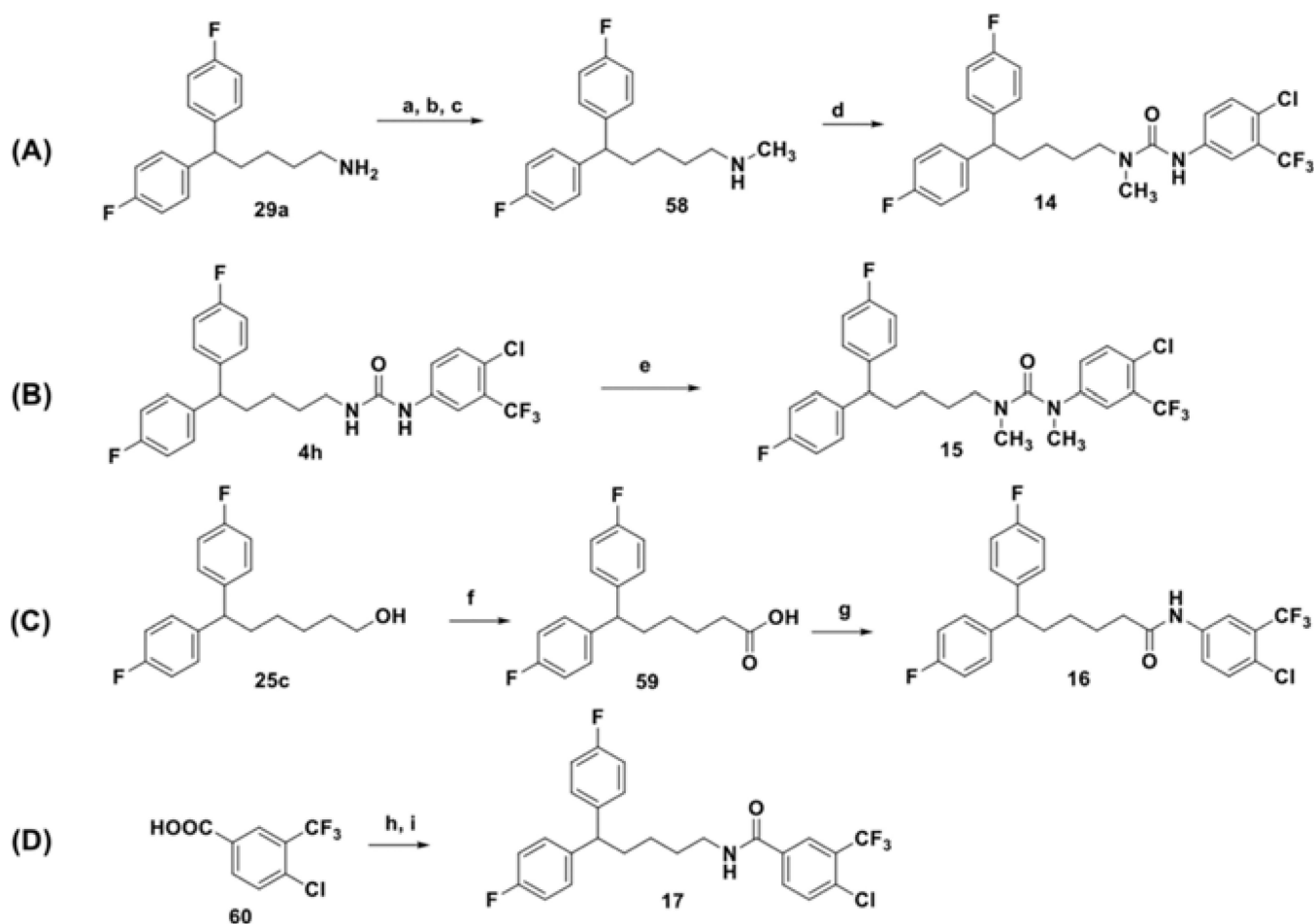
**Scheme 4.**

Synthesis of analogs with substitution at diphenyl (“tail”) moiety. Reagents and conditions:

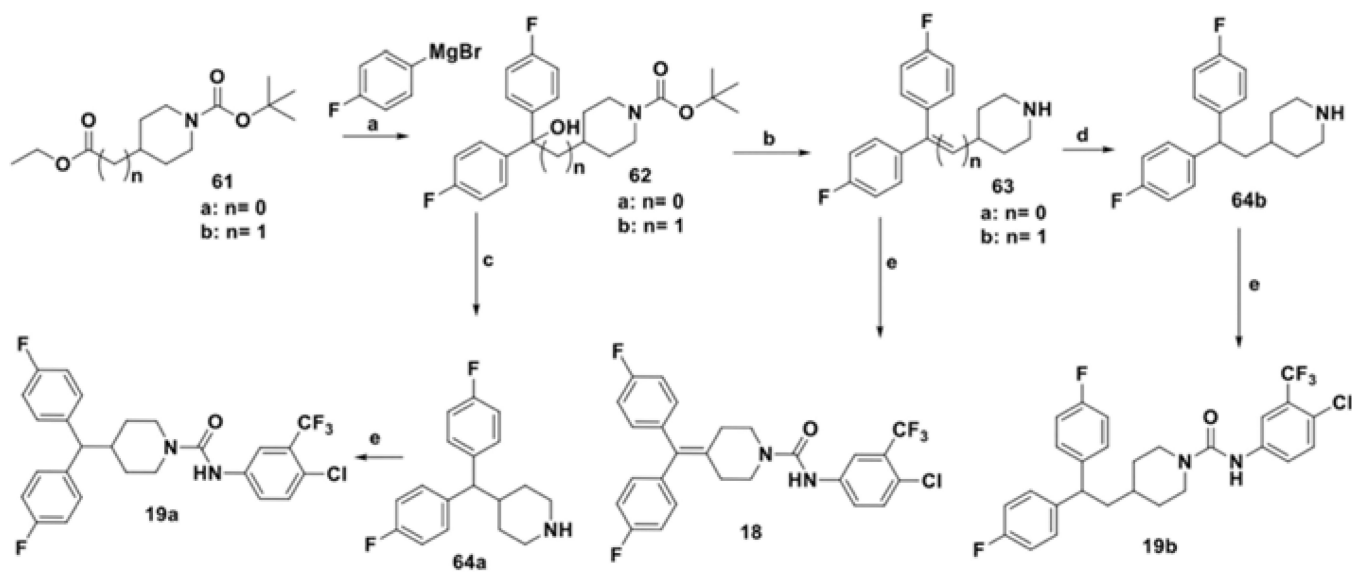
(a) **48a**, **48j-k**, DCM, 0 °C to 32 °C; (b) H<sub>2</sub>N-NH<sub>2</sub>, Raney nickel, ethanol, 50 °C; (c) acetic anhydride, DCM; (d) NaH, 1, 4-dibromobutane, THF, rt; (e) NH<sub>4</sub>OH, dioxane, 100 °C; (f) **48a**, **48b**, **48j**, **48n**, **48q**, DCM, 0 °C to 32 °C; (g) LiAlH<sub>4</sub>, 1N HCl, THF; (h) CBr<sub>4</sub>, Ph<sub>3</sub>P, DCM, 0 °C to rt; (i) **48j**, DCM, 0 °C to 32 °C.

**Scheme 5.**

Synthesis of analogs with structural modifications at the linker motif. Reagents and conditions: (a) **48j**, DCM, 0 °C to 32 °C; (b) DCM, 0 °C to 32 °C; (c) TEA, CCl<sub>4</sub>, rt.

**Scheme 6.**

Synthesis of analogs containing methylated urea functionality and analogs with the amide linker. Reagents and conditions: (a) Boc anhydride, TEA, DCM; (b) NaH, CH<sub>3</sub>I, DMF; (c) TFA, DCM; (d) **48j**, DCM, 0 °C to 32 °C; (e) NaH, CH<sub>3</sub>I, DMF; (f) NaHCO<sub>3</sub>, isocyanuric chloride, TEMPO (cat.), NaBr (cat.), water: acetone (1:3.5), 0 °C to 25 °C; (g) i) oxalyl chloride, DMF, ii) **47j**, TEA, DCM; (h) oxalyl chloride, DMF (cat.), DCM, rt, 1 hr; (i) **29a**, TEA, DCM, rt, 12 hrs.

**Scheme 7.**

Synthesis analogues with cyclic alkyl chain. Reagents and conditions: (a) THF, reflux; (b)  $\text{HCl}_{\text{conc}}$ , EtOH, reflux; (c)  $\text{NaBH}_4$ , TFA, DCM, 0 °C to rt; (d)  $\text{H}_2$  (80 psi), Pd/C (cat.), EtOH; (e) **48j**, DCM, rt

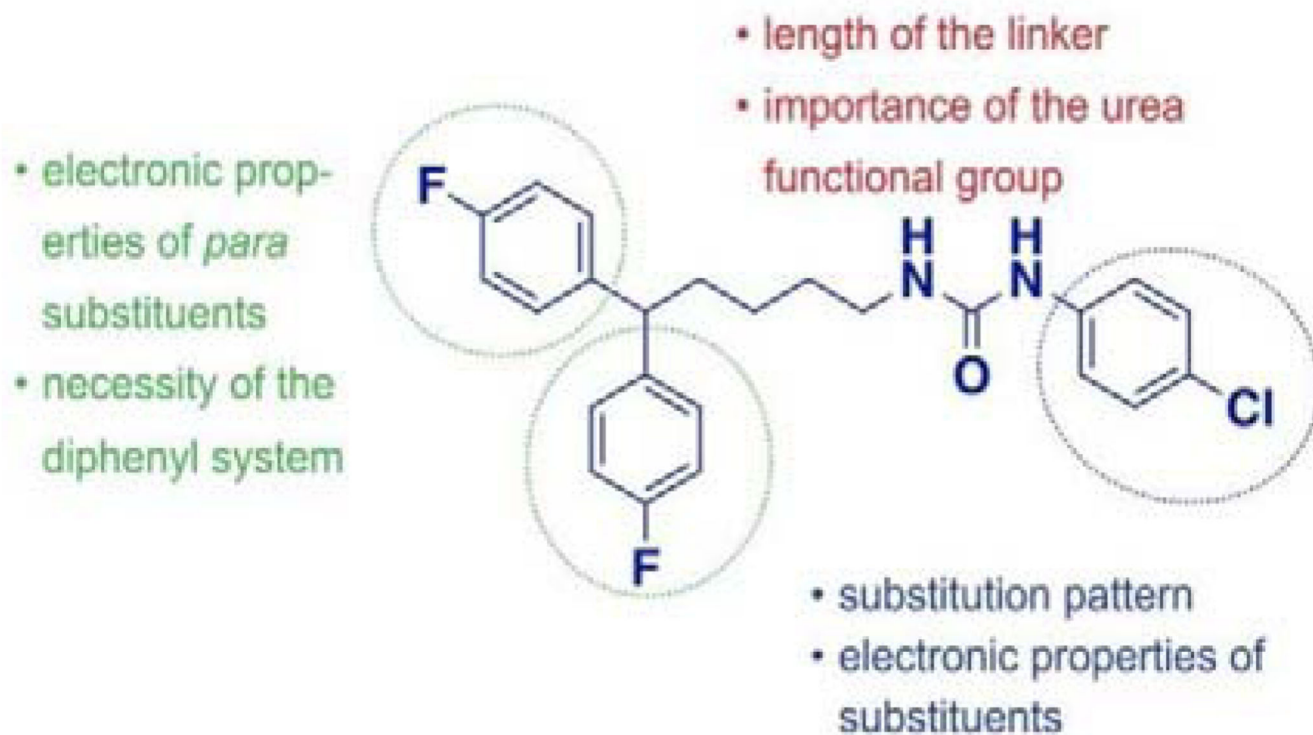


**Figure 4.**  
Areas of the proposed structural modifications.

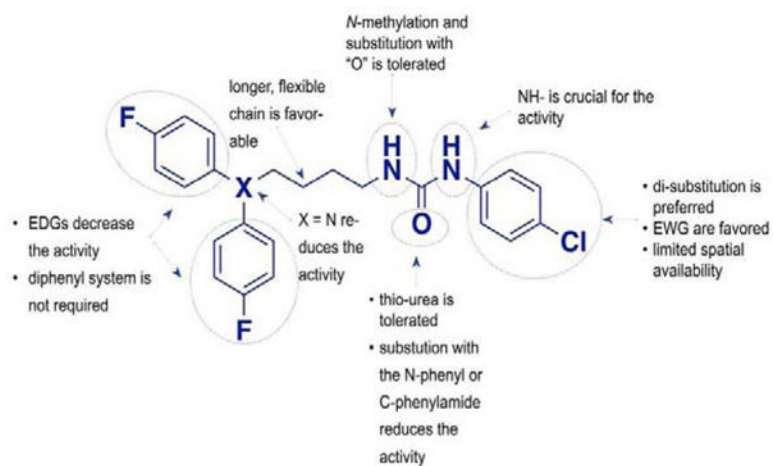


**Figure 5.** Summary of the SAR data for the anticancer activity of studied urea analogs



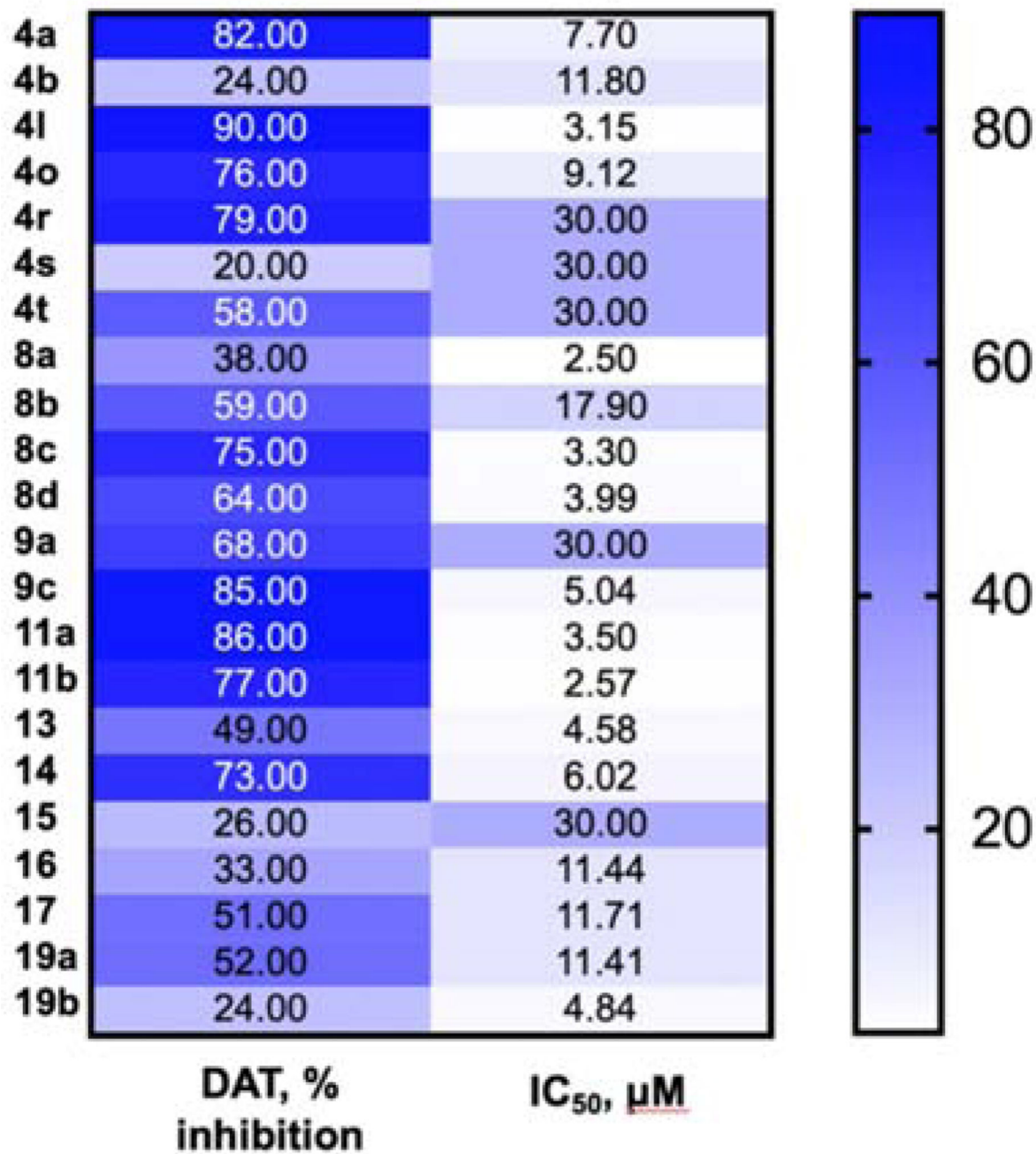


**Figure 6.**

Heat map of the observed trends in the cytotoxic activity of selected compounds and their ability to inhibit DAT (% inhibition was measured at 10  $\mu\text{M}$  level). Compounds with IC<sub>50</sub> >20  $\mu\text{M}$  (tables 1–5) were ascribed IC<sub>50</sub> value of 30  $\mu\text{M}$ .

## Liver microsome (rat) stability

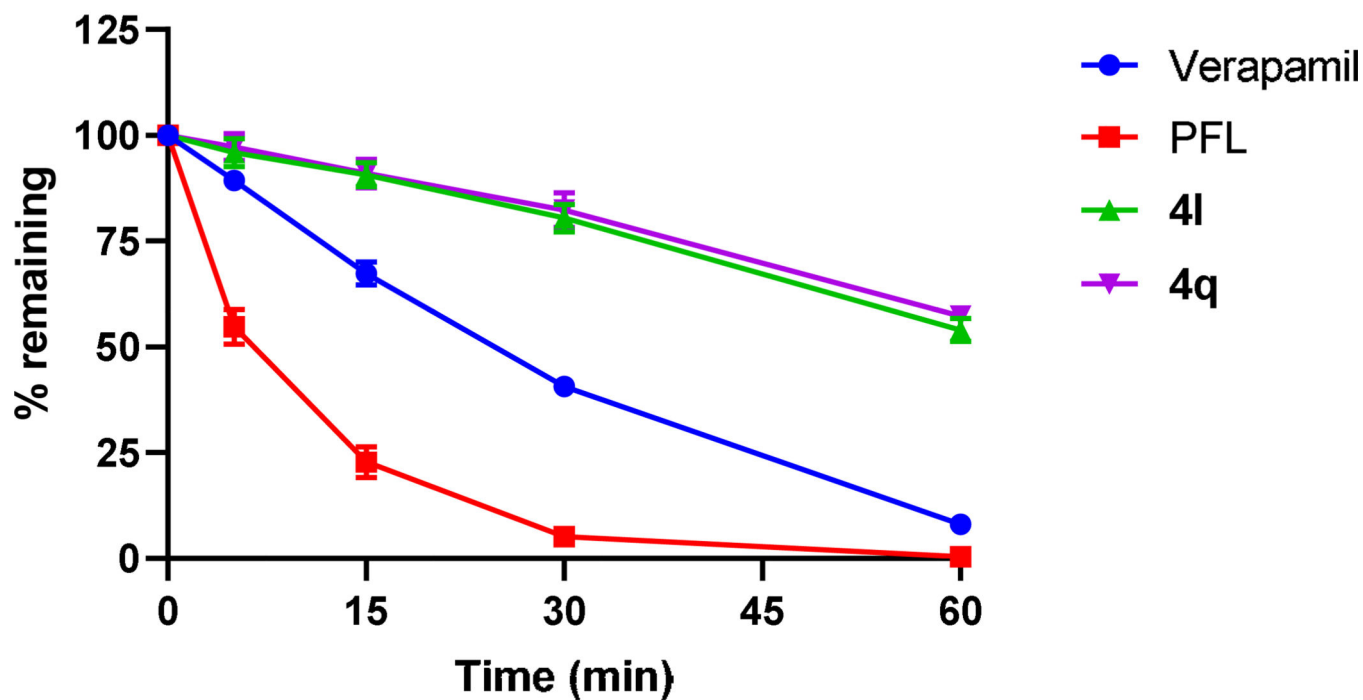


**Figure 7.** Stability of verapamil, PFL, **4l**, and **4q** in liver microsomes following 60-min incubation was measured by liquid chromatography-tandem mass spectrometry. Data are expressed as the mean  $\pm$  SEM of three independent experiments, each performed in triplicate.

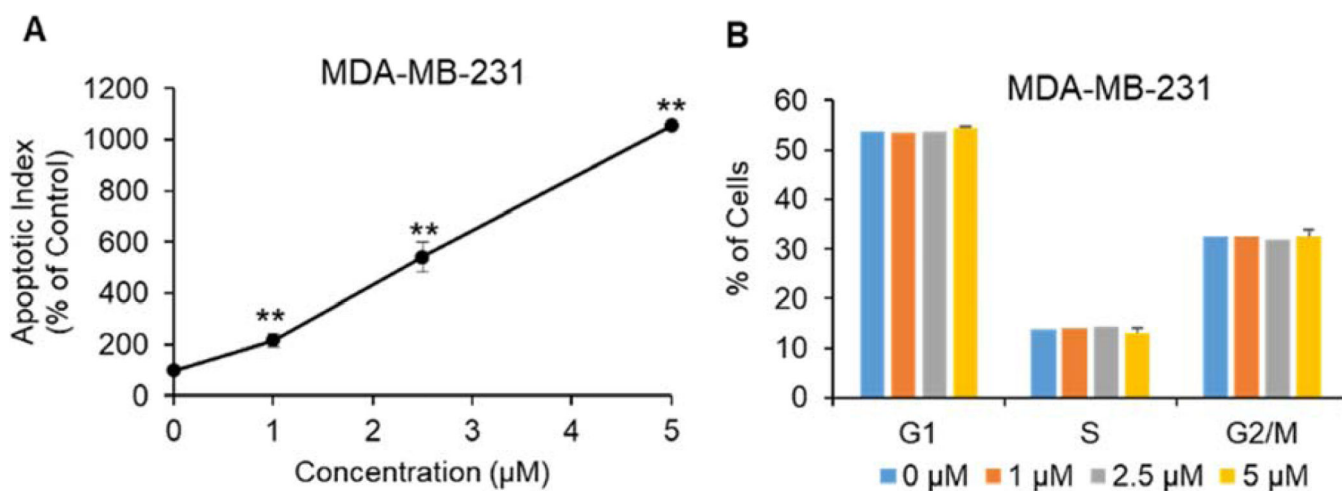


**Figure 8.** Effect of **4q** on the induction of apoptosis (A) and cell cycle (B) in MDA-MB-231 triple-negative breast cancer cells. Data are expressed as the mean  $\pm$  SEM of three independent experiments, each performed in triplicate. \*\*P<0.01

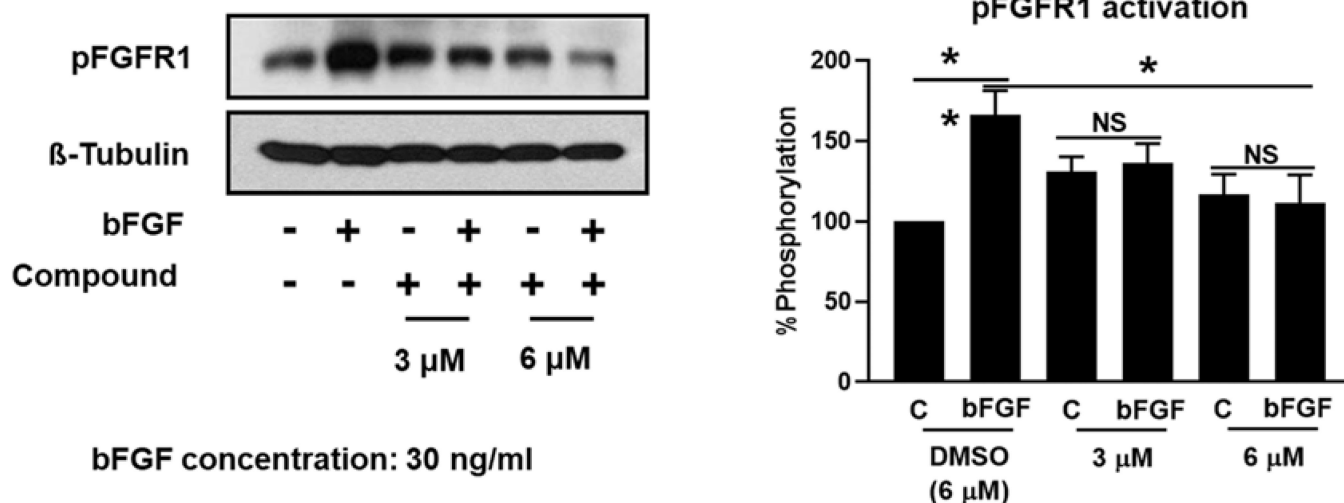


**Figure 9.**

The expression of FGFR1 was significantly reduced by compound **4q**. Representative images (left panel) and quantification (right panel) of pFGFR1 expression in MDA-MB-231 cells after 48 hours of treatment with compound **4q** at the concentrations depicted in the presence and absence of natural ligand bFGF (n = 3). NS: no significance; \*P < 0.05; \*\*P < 0.01.

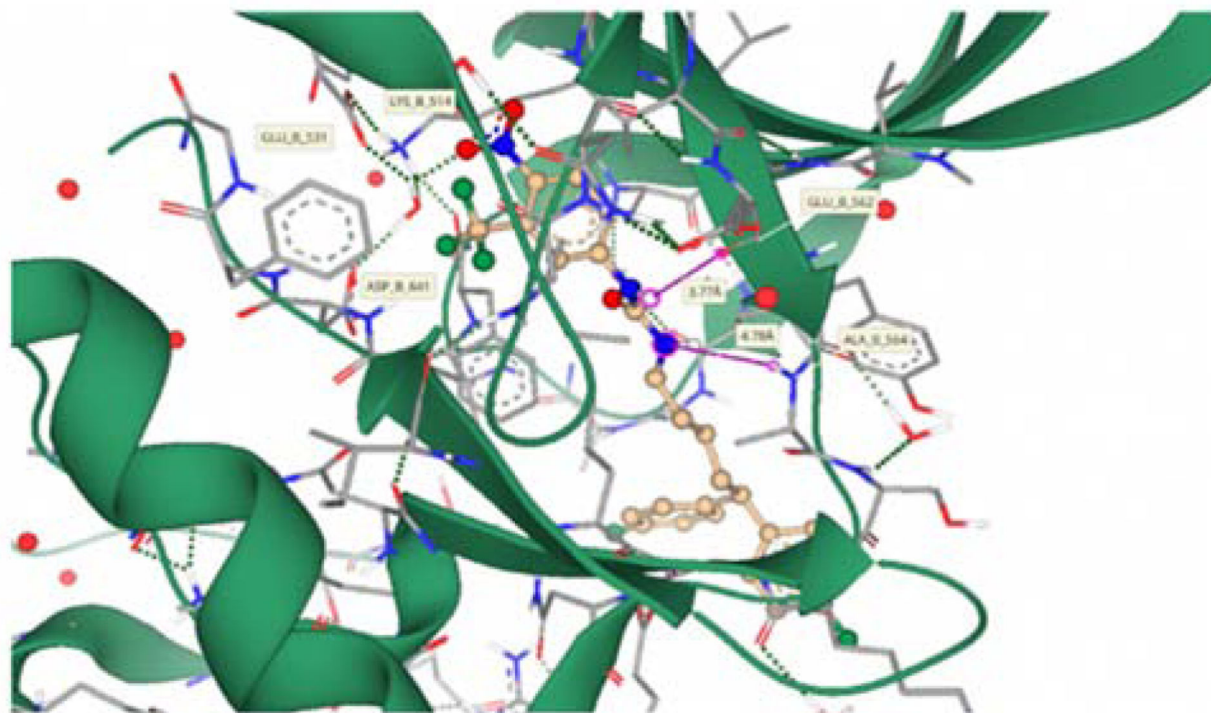


**Figure 10.** Compound **4q** (Gold) docked into the ATP-binding cleft of FGFR1 (Grey/Green). The green dashed lines depict putative binding interactions indicating strong hydrogen bonding. Pink lines represent predicted distance between hydrogen bond acceptors and donors..

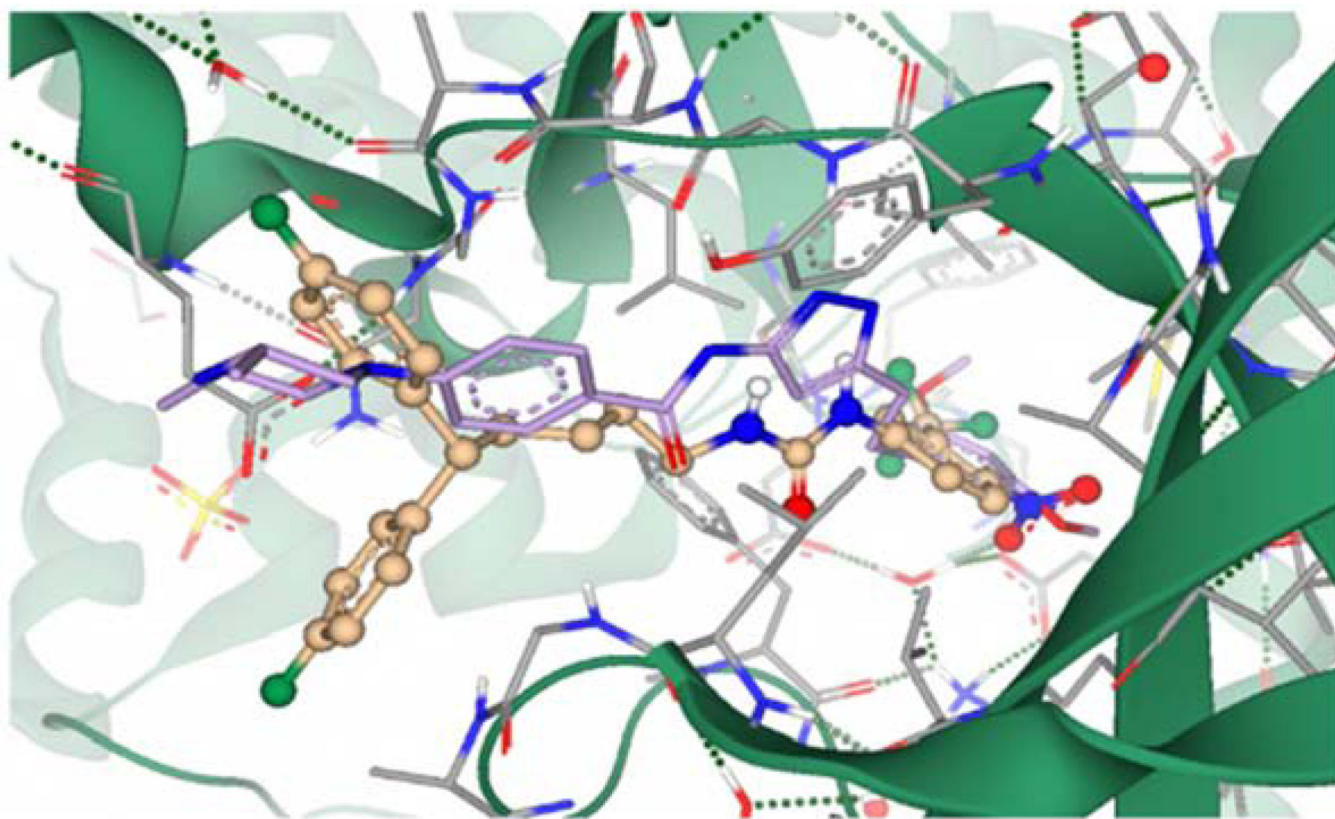
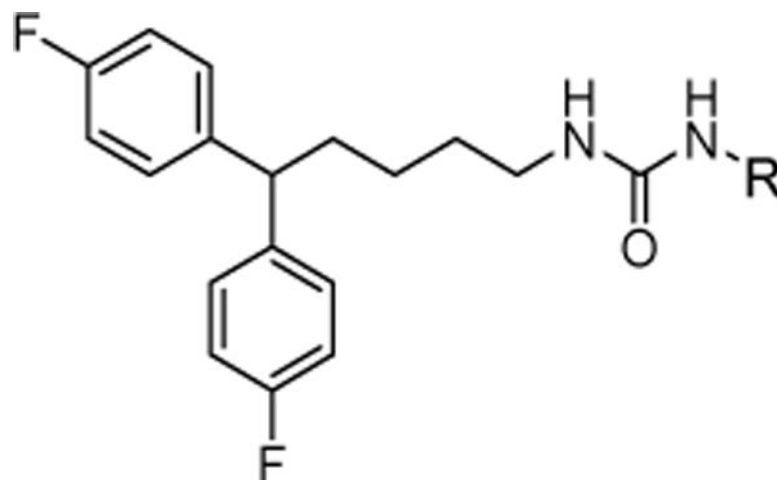


**Figure 11.**  
Overlay of compound **4q** (Gold) and the known inhibitor AZD4547 (Magenta) in the ATP-binding site of FGFR1



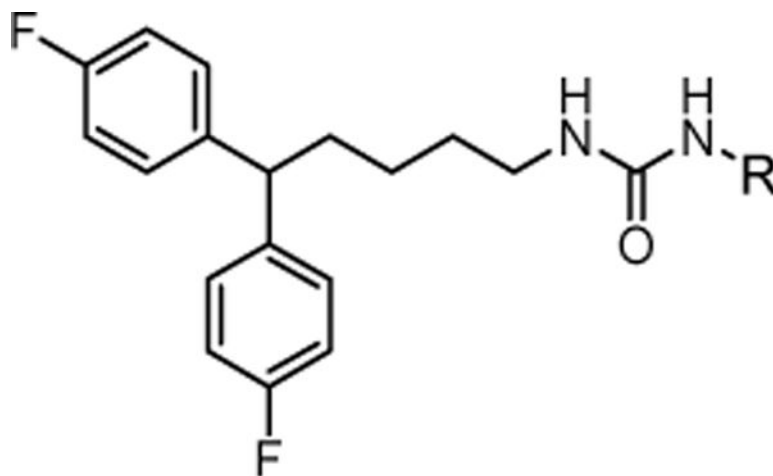
Table 1.

*In vitro* cytotoxic activity of analogs with the mono-substitution at the “head” moiety.

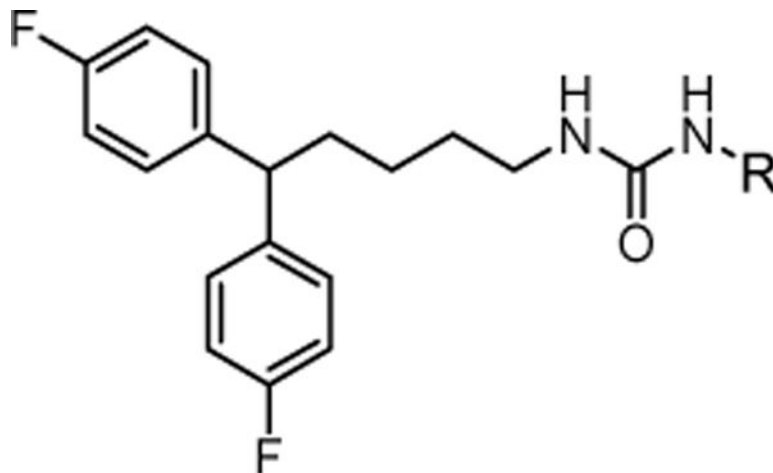


	R	MDA-MB-231 <sup>a</sup> IC <sub>50</sub> (μM)	R	MDA-MB-231 <sup>a</sup> IC <sub>50</sub> (μM)	
4a		7.68 ± 0.21	4g		3.38 ± 0.08
4b		11.79 ± 0.40	4h		2.78 ± 0.09
4c		>20.00	4i		5.07 ± 0.33
4d		6.47 ± 0.84	4j		3.79 ± 0.22
4e		>20.0	4k		>20.0
4f		>20.0			

<sup>a</sup>Data are expressed as the mean ± SEM of three independent experiments, each performed in a quartet.

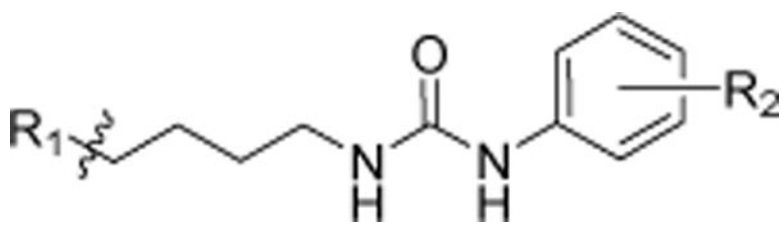
**Table 2.***In vitro* cytotoxic activity of analogs with the di-substitution at the “head” moiety.

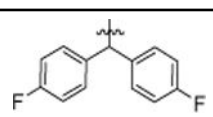
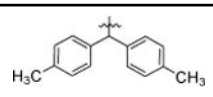
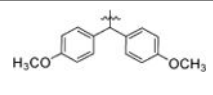
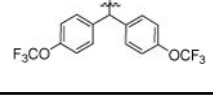
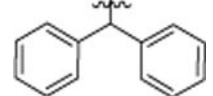
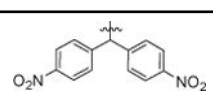
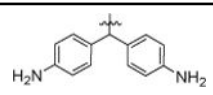
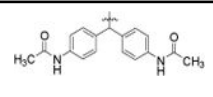
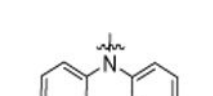
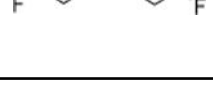
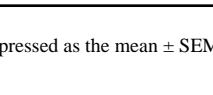
	R	MDA-MB-231 <sup>a</sup> IC <sub>50</sub> (μM)	R	MDA-MB-231 <sup>a</sup> IC <sub>50</sub> (μM)	
4l		3.15 ± 0.11	4r		>20.0
4m		4.06 ± 0.74	4s		>20.0
4n		9.24 ± 0.29	4t		>20.0
4o		9.12 ± 0.43	4u		>20.0
4p		3.47 ± 0.14	4v		4.43 ± 0.23



	R	MDA-MB-231 <sup>a</sup> IC <sub>50</sub> (μM)	R	MDA-MB-231 <sup>a</sup> IC <sub>50</sub> (μM)	
4q		4.55 ± 0.12	4x		>20.0

<sup>a</sup>Data are expressed as the mean ± SEM of three independent experiments, each performed in a quartet.

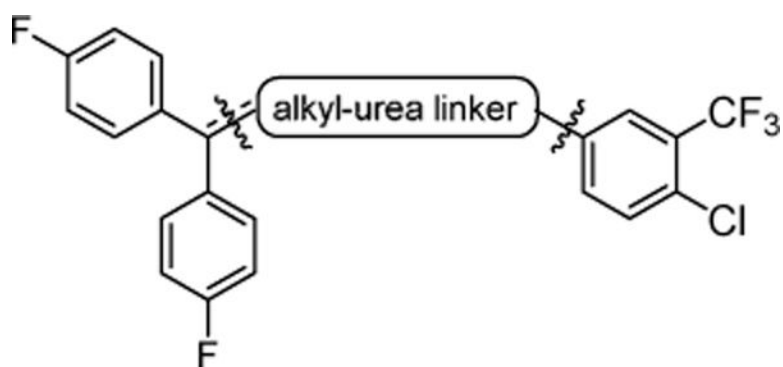
**Table 3.***In vitro* cytotoxic activity of analogs with the modifications at the “tail” di-phenyl moiety.



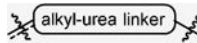
	R <sub>1</sub>	R <sub>2</sub>	MDA-MB-231 <sup>a</sup> IC <sub>50</sub> (μM)
4l		4-Cl, 3-CF <sub>3</sub>	3.15 ± 0.11
8a		4-Cl, 3-CF <sub>3</sub>	2.51 ± 0.09
8b		4-Cl	17.93 ± 0.37
8c		4-Cl, 3-CF <sub>3</sub>	3.30 ± 0.32
8d		4-Cl, 3-NO <sub>2</sub>	3.99 ± 0.44
8e		4-Cl, 3-CF <sub>3</sub>	1.69 ± 0.11
8f		4-Cl, 3-CF <sub>3</sub>	5.72 ± 0.26
8g		4-Cl, 3-CF <sub>3</sub>	1.23 ± 0.20
8h		4-Cl, 3-CF <sub>3</sub>	12.20 ± 0.59
8i		4-Cl, 3-CF <sub>3</sub>	>20.0
9a		4-Cl	>20.0
9b		4-I	> 20.0
9c		4-Cl, 3-CF <sub>3</sub>	5.04 ± 0.14
9d		4-CH <sub>3</sub> , 3-CH <sub>3</sub>	>20.0
9e		4-Br, 2-I	> 20.0
10		4-Cl, 3-CF <sub>3</sub>	5.44 ± 0.59

<sup>a</sup>Data are expressed as the mean ± SEM of three independent experiments, each performed in a quartet.

Table 4.

*In vitro* inhibitory activity of analogs with modifications in the linker part.

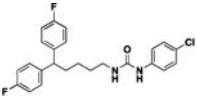
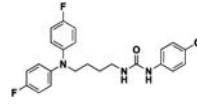
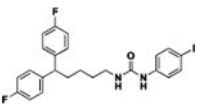
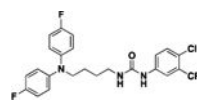
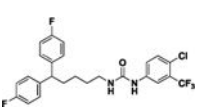
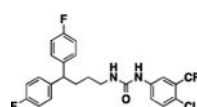
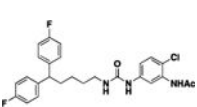
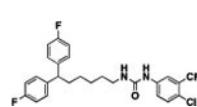
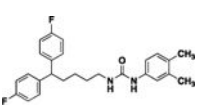
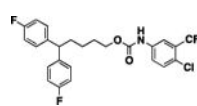
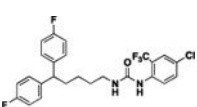
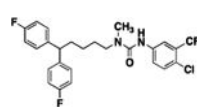
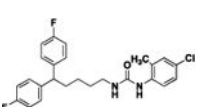
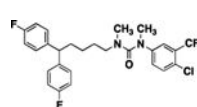
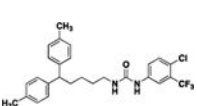
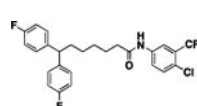
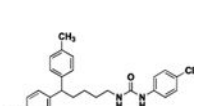
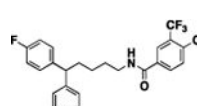
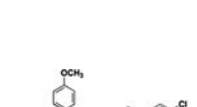
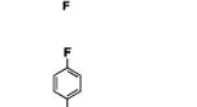


	 MDA-MB-231 <sup>a</sup> IC <sub>50</sub> (μM)		 MDA-MB-231 <sup>a</sup> IC <sub>50</sub> (μM)
4l	3.15 ± 0.11	15	> 20.0
11a	3.50 ± 0.08	16	11.44 ± 0.40
11b	2.57 ± 0.07	17	11.71 ± 0.38
12	3.66 ± 0.12	18	5.65 ± 0.43
13	4.58 ± 0.25	19a	11.41 ± 0.32
14	6.02 ± 0.09	19b	4.84 ± 0.17

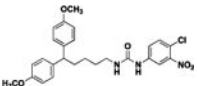
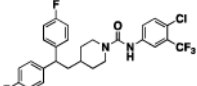
<sup>a</sup>Data are expressed as the mean ± SEM of three independent experiments, each performed in quartet.

**Table 5.**

Inhibitory activity of selected analogs at dopamine transporter\*.

Structure	% inhibition at 10 $\mu$ M	Ki, nM	Structure	% inhibition at 10 $\mu$ M	Ki, nM
	82	15		68	405
	24	ND		85	43
	90	6.5		86	141
	76	609		77	399
	79	80		49	ND
	20	ND		73	998
	58	118		26	ND
	38	ND		33	ND
	59	535		51	603
	75	40		52	1589



	Structure	% inhibition at 10 $\mu$ M	Ki, nM		Structure	% inhibition at 10 $\mu$ M	Ki, nM
<b>8d</b>		<b>64</b>	<b>144</b>	<b>19b</b>		<b>24</b>	<b>ND</b>

In primary screening assays, compounds were tested in triplicate or quadruplicate at a final concentration of 10  $\mu$ M. Compounds with a minimum of 50% antagonist activity were subjected to secondary screening (dose-response) assays.

\* Receptor binding profiles were generously provided by the National Institute of Mental Health's Psychoactive Drug Screening Program, Contract # HHSN-271-2013-00017-C (NIMH PDSP). The NIMH PDSP is Directed by Bryan L. Roth MD, Ph.D. at the University of North Carolina at Chapel Hill and Project Officer Jamie Driscoll at NIMH, Bethesda MD, USA. **ND**– not determined (Ki was not evaluated due to the less than 50% antagonist activity of a compound).

Author Manuscript

Author Manuscript

Author Manuscript

Author Manuscript